12-2018

Interactions Between Fire Severity and Forest Biota in the Central Sierra Nevada: Formation and Impact of Small-Scale Fire Refugia and the Effect of Fire on Forest Structure Predictive of Fisher (Pekania pennanti) Den Habitat

Erika M. Blomdahl
Utah State University

Utah State University
MERRILL-CAZIER LIBRARY

INTERACTIONS BETWEEN FIRE SEVERITY AND FOREST BIOTA IN THE

CENTRAL SIERRA NEVADA: FORMATION AND IMPACT OF

SMALL-SCALE FIRE REFUGIA AND THE EFFECT OF

FIRE ON FOREST STRUCTURE PREDICTIVE OF

FISHER (*PEKANIA PENNANTI*) DEN HABITAT

by

Erika M. Blomdahl

A thesis submitted in partial fulfillment
of the requirements for the degree

of

MASTER OF SCIENCE

in

Ecology

Approved:

_____   _____

James A. Lutz, Ph.D.   Julia I. Burton, Ph.D.
Major Professor   Committee Member

_____   _____

Craig M. Thompson, Ph.D.   Richard S. Inouye, Ph.D.
Committee Member   School of Graduate Studies

UTAH STATE UNIVERSITY
Logan, Utah

2018

ABSTRACT

Interactions Between Fire Severity and Forest Biota in the Central Sierra Nevada:

Formation and Impact of Small-Scale Fire Refugia and the Effect of Fire on

Forest Structure Predictive of Fisher (*Pekania pennanti*) Den Habitat

by

Erika M. Blomdahl, Master of Science

Utah State University, 2018

Major Professor: Dr. James A. Lutz
Department: Wildland Resources

Fire is an essential forest component that has been altered in western North America. Widespread fire exclusion is incongruous with the critical objectives of preserving forest function, conserving biodiversity, and increasing resilience to high-severity disturbance. To manage for fire reintroduction in historically frequent-fire forests, it is critical that we understand the interactions between fire and forest biota in forests where fire has been excluded since European settlement.

In Chapter 2, I examined the importance of small-scale fire refugia in the Yosemite Forest Dynamics Plot (YFDP). Fire refugia are unburned areas within fire perimeters where forest biota can retreat to during and after the disturbance. Following the 2014 Rim Fire, I mapped all unburned areas ≥ 1 m^2 in relation to known locations of the 34,061 live trees in the YFDP. Within the 25.6 ha plot, I found small fire refugia within burned areas with dNBR values ranging from 7 to 428, and a total unburned

proportion of 4.9%. Using random forest models I found the unburned proportion was predicted by pre-fire stem density, basal area, distance of the refuge to stream, and fire severity. Vegetation located with small fire refugia had increased survival (stems ≥ 1 cm DBH, $P<0.001$) and species richness of understory communities. My results suggest that burn heterogeneity in mixed-conifer forests exists at all scales and small refugia contribute to diversity of forest species and structures.

In Chapter 3, I assessed whether forest structural characteristics associated with fisher dens were maintained in recently burned areas. Fishers are a species of high conservation concern due to the perceived threat of fire to essential habitat. I used lidar-derived forest structure metrics to differentiate fisher den sites from randomly-generated points. The random forest model correctly predicted 74.3% of observations and the logistic regression model correctly predicted 69.5%. The parsimonious model I selected included cover >2 m, 95th percentile height, and 25th percentile height. I found suitable thresholds of these structural characteristics in recently burned areas in Yosemite, particularly after low-severity fire. My results suggest that burned areas may offer suitable habitat for intermediate-scale selection of den sites by fishers.

(120 pages)

PUBLIC ABSTRACT

Interactions Between Fire Severity and Forest Biota in the Central Sierra Nevada:

Formation and Impact of Small-Scale Fire Refugia and the Effect of Fire on Forest

Structure Predictive of Fisher (*Pekania pennanti*) Den Habitat

Erika M. Blomdahl

Fire is a natural and essential component of forests in western North America.

Fire maintains biodiversity through the creation of different habitat types, and regular fire

rotations reduce the accumulation of woody fuels and thick understory plant densities that

give rise to catastrophic fire. The practice of fire exclusion has altered western forests and

increased the risk of widespread change under rising temperatures projected for the 21st

century. To manage for the reintroduction of fire it is critical that we understand the

interactions between fire and forest biota in recently fire-suppressed forests.

In Chapter 2, I studied the formation and impact of small-scale fire refugia. Fire

refugia are areas within burned forest that experienced relatively little change, and are

recognized as important places that offer protection for forest biota (vegetation, wildlife)

during and after the fire. Very few studies, however, have examined small-scale fire

refugia despite their importance to many organisms (e.g., small mammals, understory

plants). In a long-term forest monitoring plot in Yosemite National Park, I mapped all

unburned areas ≥ 1 m^2 the first year after fire. I found small fire refugia were abundant,

somewhat predictable, and fostered increased survival and diversity of nearby plant life.

My results suggest that small fire refugia are an important component of burned forests

that should be included in management considerations.

In Chapter 3, I examined possible fisher habitat in burned areas. Fishers are forest carnivores of high conservation concern due to widespread declines since European settlement and the risk of habitat loss due to fire. An isolated population remains in the Sierra National Forest, where managers are weighing the need to reintroduce fire against possible detrimental impacts to current habitat. My research examined the forest structural characteristics (vegetative cover, heights of different forest layers) surrounding fisher dens. I found suitable thresholds of these structural characteristics in recently burned areas in Yosemite, particularly after low-severity fire. My results suggest that burned areas may offer suitable denning habitat for fishers, though more research is needed to determine if this conclusion holds for all fisher activities (e.g., foraging, resting) and scales of selection.

ACKNOWLEDGMENTS

conducted all trapping and telemetry field work to obtain fisher locations, and Jonathan Kane and the University of Washington team that conducted parallel research and wrote the final NPS Cooperative Agreement report.

I am sincerely grateful for my community of family and friends that have supported me throughout the ups and downs of this process. My mother, Linda, I thank for teaching me to have strength. My father, Daryl, I thank for instilling a love of the natural world. My brother, Nick, I thank for inspiring perseverance. My partner and dearest friend, David Soderberg, receives my deepest gratitude. David, your positive spirit is my antidote to chaos, thank you for always helping me return to center.

Erika M. Blomdahl

CONTENTS

LIST OF TABLES

LIST OF FIGURES

CHAPTER 1

INTRODUCTION

Fire is an integral forest ecosystem component that has been altered in western North America. In the Sierra Nevada, the policy of fire suppression that has dominated since late 19th century European settlement has led to altered fire regimes (McKelvey and Busse 1996, Skinner and Chang 1996), high understory stem densities (Parsons and DeBendetti 1979), compositional shifts to less fire-resistant species (Vankat and Major 1978, Scholl and Taylor 2010), and uncharacteristic accumulations of woody fuels (Covington and Moore 1994, van Wagtendonk and Fites-Kaufman 2006). As a result, forests with historically frequent fire regimes (characterized by low- to moderate-severity fire) are at increased risk of high-severity fire (McKelvey et al. 1996, Noss et al. 2006), particularly under projected warming temperatures and drought conditions over the next century (Dale et al. 2001). The reintroduction of fire to the dry, fire-prone forests of the west is critical to achieve the management objectives of maintaining forest function, biodiversity, and resilience to high-severity disturbance (e.g. wildfire, drought, insect outbreak). In order to inform management action, especially objectives concerning the conservation of species, it is important to understand the interactions between fire and forest biota in forests where fire has been excluded since European settlement.

In the absence of fire suppression, forest ecosystems exist in a feedback between fire and vegetation (Fites-Kaufman et al. 2006). Fire influences vegetation patterns across the landscape, resulting in a patchwork of stands with different successional stages, compositional mixtures, and structural attributes (Heinselman 1981). Plant species in the west have adaptations that cause variable responses to fire, from stimulated regrowth

following the death of the main stem (e.g., *Quecus* spp; Keeley and Zedler 1978), to thick, plated bark attained by large-diameter trees (e.g., *Pinus* spp; Pausas 2015). In turn, vegetation impacts fire behavior and severity (Hély et al. 2001). The spatial pattern, composition, and density of woody species affects the loading and continuity of fuels consumed by fire (Agee 1996, Ryan 2002). Fire severity is a function of the pre-fire live vegetation, and estimates the degree to which the vegetation has changed (Key and Benson 2006).

A chief source of interaction between fire and wildlife is through subsequent changes to habitat. Fire can cause the immediate destruction of habitat, by removing forest cover, food sources (Cook 1959), and previously inhabited structures (Horton and Mannan 1988). In the long-term, however, fire causes the proliferation of new habitat types, including edge habitats and areas of early succession that are associated with increased forage and diversity (Thomas et al. 1979, Roberts et al. 2008). Fire also creates dead wood components such as snags and logs, which are used and inhabited by many species (Shaffer and Laudenslayer 2006). Native wildlife species are adapted to persist in frequent-fire environments, often by retreating to refugia or adjacent unburned forest during and after a fire, and then recolonizing burned areas after a period of recovery (Robinson et al. 2013). Anthropogenic habitat fragmentation, however, poses a considerable threat to species with reduced population sizes, eliminating available unburned habitat that species may use while burned habitat becomes more hospitable.

While our understanding of fire as an essential ecological process has expanded in recent decades, more research is needed to meet critical management objectives under global change. Interactions between forest biota and fire are complex, and not easily

subject to generalization—what is true for one study organism or forest type does not necessarily hold for another species or ecoregion. My research fills knowledge gaps in mixed-conifer forests of the central and south Sierra Nevada mountains.

My research objectives are in two parts, corresponding with the different aspects of interactions between fire and forest biota I addressed between my two chapters. Chapter 2 is a study of small-scale fire refugia—fire components recognized as important for the persistence of forest organisms that have not yet been systematically studied. My objectives for Chapter 2 were first to characterize the spatial pattern and formation of small fire refugia in a long-term forest monitoring plot in Yosemite National Park. Second, I examined the impact of small refugia on the survival of woody species and the diversity of understory species. Chapter 3 concerns the fisher (*Pekania pennanti*), a forest mustelid with a small isolated population in the southern Sierra Nevada where the need to reintroduce fire is high. My objectives were to determine forest structural characteristics predictive of fisher den habitat, and to relate those characteristics to fire metrics.

LITERATURE CITED

Agee, J. K. 1996. The influence of forest structure on fire behavior. Pages 52-68 in: Proceedings of the 17th Annual Forest Vegetation Management Conference. Redding, California.

Cook, S. F. 1959. The effects of fire on a population of small rodents. Ecology 40(1): 102-108.

Covington, W. W., and M. M. Moore. 1994. Southwestern ponderosa pine forest structure: changes since Euro-American settlement. Journal of Forestry 92: 39-47.

Dale, V. H., L. A. Joyce, S. McNulty, R. P. Neilson, M. P. Ayres, M. D. Flannigan, P. J. Hanson, L. C. Irland, A. E. Lugo, C. J. Peterson, D. Simberloff, F. J. Swanson, B. J. Stocks, and B. M. Wotton. 2001. Climate change and forest disturbances. BioScience 52: 723-734.

Heinselman, M. L. 1981. Fire and Succession in the Conifer Forests of Northern North America. Pages 374-405 in: D. C. West, H. H. Shugart, D. B. Botkin, editors. Forest Succession. Springer Advanced Texts in Life Sciences. Springer, New York, NY.

Hély, C., M. Flannigan, Y. Bergeron, and D. McRae. 2001. Role of vegetation and weather on fire behavior in the Canadian mixedwood boreal forest using two fire behavior prediction systems. Canadian Journal of Forest Research 31(3): 430-441.

Fites-Kaufman, J., A. F. Bradley, and A. G. Merrill. 2006. Fire and plant interactions. Pages 94-117 in: N. G. Sugihara, J. W. van Wagtendonk, J. Fites-Kaufman, K. E. Shaffer, and A. E. Thode, editors. Fire in California's ecosystems. University of California Press, Berkeley, USA.

Horton, S. P., and R. W. Mannan. 1988. Effects of prescribed fire on snags and cavity-nesting birds in southeastern Arizona pine forests. Wildlife Society Bulletin 16(1): 37-44.

Keeley, J. E., and P. H. Zedler. 1978. Reproduction of chaparral shrubs after fire: A comparison of sprouting and seeding. The American Midland Naturalist 99(1): 142-161.

Key, C. H., and N. C. Benson. 2006. Landscape assessment: Sampling and analysis methods. General Technical Report RMRS-GTR-164-CD. USDA Forest Service,

Rocky Mountain Research Station, Fort Collins, Colorado.

McKelvey, K. S., and K. L. Busse. 1996. Twentieth century fire patterns on Forest Service lands. In Sierra Nevada Ecosystem Project: Final report to Congress, Volume II, Chapter 41. University of California, Davis, Wildland Resources Center Report 37.

McKelvey, K.S., C. N. Skinner, C. R. Chang, D. C. Erman, S. J. Husari, D. J. Parsons, J. W. van Wagtendonk, and C. W. Weatherspoon. 1996. Pages 1033-1040 in: D.C. Erman, editor. Sierra Nevada ecosystem project: Final report to Congress, Volume II. University of California, Davis, Wildland Resources Center Report 37.

Noss R. F., J. F. Franklin, W. L. Baker, T. Schoennagel, and P. B. Moyle. 2006. Managing fire-prone forests in the western United States. Frontiers of Ecology and the Environment 4: 481-7.

Parsons, D.J., and S.H. DeBenedetti. 1979. Impact of fire suppression on a mixed-conifer forest. Forest Ecology and Management 2: 21-33.

Pausas J. G. 2015. Evolutionary fire ecology: lessons learned from pines. Trends in Plant Science 20: 318-324.

Roberts, S. L., J. W. van Wagtendonk, D. A. Kelt, A. K. Miles, and J. A. Lutz. 2008. Modeling the effects of fire severity and spatial complexity on small mammals in Yosemite National Park, California. Fire Ecology 4(2): 83-104.

Robinson, N. M., S. W. J. Leonard, E. G. Ritchie, M. Bassett, E. K. Chia, S. Buckingham, H. Gibb, A. F. Bennett, and M. F. Clarke. 2013. Refuges for fauna in fire-prone landscapes: Their ecological function and importance. Journal of

Applied Ecology 50: 1321-1329.

Ryan K. C. 2002. Dynamic interactions between forest structure and fire behavior in boreal ecosystems. Silva Fennica 36: 13-39

Scholl, A. E., and A. H. Taylor. 2010. Fire regimes, forest change, and self-organization in an old-growth mixed-conifer forest, Yosemite National Park, USA. Ecological Applications 20(2): 362-380.

Shaffer, K. E., and W. F. Laudenslayer. 2006. Fire and animal interactions. Pages 118-144 in: N. G. Sugihara, J. W. van Wagtendonk, J. Fites-Kaufman, K. E. Shaffer, and A. E. Thode, editors. Fire in California's ecosystems. University of California Press, Berkeley, USA.

Skinner, C.N., and C. Chang. 1996. Fire regimes: past and present. Pages 1041-1067 in: D.C. Erman, editor. Sierra Nevada ecosystem project: Final report to Congress, Volume II. University of California, Davis, Wildland Resources Center Report 37.

Thomas, J. W., C. Maser, and J. E. Rodiek. 1979. Edges. Pages 48–59 in J. W. Thomas, editor. Wildlife habitats in managed forests: the Blue Mountains of Oregon and Washington. U.S. Department of Agriculture Forest Service, Portland , Oregon.

Vankat, J.L., and J. Major. 1978. Vegetation changes in Sequoia National Park, California. Journal of Biogeography 5: 377-402.

Van Wagtendonk, J.W., and J. Fites-Kaufman. 2006. Sierra Nevada bioregion. Pages
264-294 in: N. G. Sugihara, J. W. van Wagtendonk, J. Fites-Kaufman, K. E.
Shaffer, and A. E. Thode, editors. Fire in California's ecosystems. University of
California Press, Berkeley, USA.

CHAPTER 2

THE IMPORTANCE OF SMALL FIRE REFUGIA IN THE CENTRAL

SIERRA NEVADA, CALIFORNIA, USA

ABSTRACT

Fire refugia – which includes most unburned areas within fire perimeters – are

recognized as significant to the survival of many taxa through fire events and the

revegetation of post-fire landscapes. Previous work has shown that specific species use

and benefit from small-scale fire refugia (1 m^2 to 1000 m^2), but our understanding of

where and how fire refugia form is largely limited to the scale of remotely-sensed data

(i.e., 900 m^2 Landsat pixels). To examine the causes and consequences of small fire

refugia, I field-mapped all unburned patches ≥ 1 m^2 within a contiguous 25.6 ha forest

plot that burned at low-to-moderate severity in the 2013 Yosemite Rim Fire, California,

USA. Within the Yosemite Forest Dynamics Plot (YFDP), there were 685 unburned

patches ≥ 1 m^2, covering a total unburned area of 12,597 m^2 (4.9%). I found small fire

refugia within Landsat pixels with dNBR values ranging from 7 to 428. Random forest

models showed that the proportion of unburned area of 10 m^2 grid cells corresponded to

pre-fire density and basal area of trees, distance to the nearest stream, and immediate fire

mortality, but the relationships were complex and model accuracy was variable. From a

pre-fire population of 34,061 total trees ≥ 1 cm diameter at breast height (1.37 m; DBH)

within the plot (1,330 trees ha^{-1}), trees of all five of the most common species and those

DBH <30 cm in had higher immediate survival rates if their boles were wholly or

partially within an unburned patch ($P \leq 0.001$). Trees 1 cm $\leq$ DBH <10 that survived were

located closer to the center of the unburned patch than the edge (mean 1.1 m versus 0.6 m; ANOVA; $P \leq 0.001$). Four-year survival rates for trees 1 cm $\leq$ DBH <10 cm were 58.8% within small refugia and 2.7% in burned areas ($P \leq 0.001$). NMDS ordinations of understory plant indicated unburned areas were correlated with species richness and the Shannon Diversity Index, suggesting small fire refugia are areas with more diverse understory communities. Burn heterogeneity in mixed-conifer forests likely exists at all scales and small refugia contribute to diversity of forest species and structures, thus managers may wish to consider scales from 1-m^2 to the landscape when designing fuel reduction prescriptions. The partial predictability of refugia location suggests that further research may lead to predictive models of refugial presence that have considerable potential to preserve ecological function or human habitation in fire-frequent forests.

1. Introduction

Fire is a principal disturbance process in the dry forests of western North America, and there is widespread evidence that fire activity is increasing (Westerling et al., 2006; Miller and Safford 2012; Dennison et al., 2014). High severity fires and the total area burned have received considerable media attention, depicting an overly simplistic view of fire activity that omits natural variability in fire effects. Within fire perimeters, the distribution of burn severity (i.e., the degree of environmental change following a fire; Key and Benson 2006; Keeley, 2009) is heterogeneous. Fire mosaics consist of myriad burn severities, including areas that experienced little or no burning. A critical outcome of this heterogeneity is the formation of fire refugia—unburned or lightly burned areas in the burned matrix that are functionally unaltered by fire. Fire

refugia are important but largely understudied landscape components that preserve

ecological function in the immediate aftermath of the fire, and may reduce vulnerability

to future disturbance (Meddens et al., 2018b). Scientific understanding is particularly

limited in the study of small-scale fire refugia (<0.1 ha), which are known to benefit

forest organisms (Robinson et al., 2013), but cannot be detected with remote-sensing.

Fire refugia influence forest recovery and succession. By buffering lethal

temperatures, refugia facilitate the survival and persistence of many taxa during and after

a fire event (Gasaway and DuBois 1985; Robinson et al., 2013). Remnant vegetation

provides immediate post-fire habitat for faunal species, expediting recolonization of

burned areas (e.g., Banks et al., 2011). Islands of unburned forest preserve patches of

different successional stages (Turner et al., 1997; Kane et al., 2010), thus increasing

overall diversity of habitats and forest structure. Patches of surviving mature vegetation

act as barriers to erosion and influence immediate successional processes by providing

seed sources to repopulate gaps created by the disturbance (Turner et al., 1998). Fire

refugia, therefore, are associated with both immediate and long-term benefits to forest

organisms.

The study of large-scale fire refugia (≥1 ha) has increased in recent decades with

the aid of remote sensing (e.g. Meddens et al., 2016; 2018a). Most recent studies have

utilized satellite-derived indices based on 30 m × 30 m Landsat pixels; the resolution of

the Landsat instrument is well-suited for analysis of landscape-scale patterns and trends

in burn severity and fire size. Fire refugia in this type of study are identified as pixels

with an unchanged surface reflectance between pre- and post-fire scenes, which could

include several surface conditions (e.g., unburned forest, a sub-canopy burn not reflected

in the overstory, or a burn followed by rapid vegetative regrowth; Kolden et al., 2012).

Previous work has described the spatial characteristics and environmental predictors of

large fire refugia, as well as differences between remnant vegetation and the surrounding

forest. Kolden et al., (2012) found that characteristics such as patch size, density, and

shape complexity vary with forest type. Other studies have successfully predicted the

presence of large fire refugia based on environmental factors such as terrain ruggedness,

soil moisture, aspect, and slope (Román-Cuesta et al., 2009; Krawchuk et al.; 2016, Haire

et al., 2017). Patches of remnant forest and the surrounding matrix of young forest have

exhibited differences in structure, composition, and regeneration (Delong and Kessler,

2000).

Although large fire refugia have been the subject of much interest, fire refugia

smaller than a Landsat pixel have been less studied. Small fire refugia are often obscured

by the forest canopy and may not be reliably quantified with remote sensing techniques.

Fire refugia of this size have been exclusively studied in the context of a specific study

organism, involving ground-based measurements of unburned forest floor. Small fire

refugia have been shown to be important mechanisms of survival for individual species

(Brennan et al., 2011; Robinson et al., 2013; Meddens et al., 2018b) and plant

communities (Schwilk and Keeley, 2006; Hylander and Johnson, 2010). Rodent

populations have been shown to shift to use small unburned drainages, possibly to avoid

predation (Banks et al., 2011) or to use post-fire areas with higher levels of burn

heterogeneity, including unburned areas (Roberts et al., 2008). Other studies have shown

that forest-floor-dwelling invertebrates survive fire in unburned patches (Zaitsev et al.,

2014) and that unburned microhabitats near residual trees and other vegetation correlate

positively with beetle diversity (Gandhi et al., 2001). Tree seedlings and saplings can survive in unburned patches, creating structural diversity that provides more habitat for forest fauna and increases overall forest resilience to disturbances (North et al., 2009).

There is a considerable knowledge gap in our spatial and predictive understanding of small fire refugia. It is unknown how the distribution and formation of small fire refugia compare with studies conducted at a coarser scale, a question relevant to managing forests with fire refugia—of all scales—in mind. It is important, additionally, to understand the relationship between small fire refugia and satellite-derived burn severity. Although, satellite-based remote sensing techniques are unlikely to identify all unburned areas relevant to biota, these methods may help estimate spatial attributes of small refugia in relation to burn severity.

To examine the causes and consequences of small refugia, I field mapped all unburned areas ≥ 1 m^2 within a 25.6 ha study area. Our objectives were to: 1) characterize the fine-scale spatial distribution of unburned patches, including their sizes, distributions, and relationship with Landsat-derived burn severity; 2) determine the environmental variables predictive of small fire refugia; and 3) compare vegetation in unburned patches and burned areas. I expected the spatial distribution of small unburned patches to be aggregated in areas that inhibit fire spread; for example, riparian areas may be less likely to burn due to the high soil moisture content (Dwire and Kauffman, 2003). If the same processes that drive large fire refugia formation also apply to small fire refugia, then abiotic factors such as topography and aspect may be predictive of patch presence (Krawchuk et al.; 2016, Haire et al., 2017). I expected that small unburned patches would increase tree survival and have distinct understory communities relative to burned areas.

2. Methods

2.1 Study area

I conducted this study in the Yosemite Forest Dynamics Plot (YFDP, 37.77°N, 119.92°W; Lutz et al., 2012), a 25.6 ha plot in the lower-montane forest zone (1774 m to 1911 m) of Yosemite National Park (Yosemite). The climate at the YFDP is Mediterranean, characterized by hot, dry summers and cool, wet winters. Between 1981 and 2010 the annual mean monthly minimum and maximum temperatures were 6 °C and 16 °C respectively; annual precipitation was 1070 mm with most precipitation falling as snow between December and March (Lutz et al., 2010; Prism Climate Group, 2017). The YFDP is located in primary *Abies concolor-Pinus lambertiana* (white fir-sugar pine) forest of the White Fir Superassociation (Keeler-Wolf et al., 2012), with trees older than 500 years. The five most abundant tree species are (in decreasing abundance): *Abies concolor* (white fir), *Pinus lambertiana* (sugar pine), *Cornus nuttallii* (Pacific dogwood,) *Calocedrus decurrens* (incense-cedar), and *Quercus kelloggii* (California black oak). Plant nomenclature follows Flora of North America (1993+).

2.2 Fire regime

The fire regime in dry mixed-conifer forests of the Sierra Nevada prior to European settlement was characterized by a mean fire return interval of 11 years (van de Water and Safford, 2011), consistent with an interval of 10 to 13 years found by Scholl and Taylor (2010) approximately 10 km north of the YFDP. However, the mean fire return interval in the YFDP itself was 29.5 years (Barth et al., 2015), possibly due to the northerly aspect of the plot (Lutz et al., 2017). The last widespread fire in the YFDP

occurred in 1899, followed by a period of fire exclusion from 1900 to 2012 (Scholl and Taylor, 2010, Barth et al., 2015). In Yosemite as a whole, the reintroduction of fire since the 1970s has resulted in mixed- and high-severity fires (van Wagtendonk, 2007; van Wagtendonk and Lutz, 2007; Lutz et al., 2009).

The Rim Fire burned 104,131 ha of mostly forested land in August-September 2013 (Kane et al., 2015a; Stavros et al., 2016), including 32,079 ha within Yosemite. The YFDP was contained entirely within the fire perimeter (Fig. 2.1). The YFDP burned on September 1st and 2nd in a management-ignited backfire intended to control the spread of the Rim Fire. The fire was started 1 km away from the YFDP and unmanaged thereafter, with portions of the plot burning in a backing fire at night and the rest burning upslope the following day (Lutz et al., 2017). Unlike portions of the Rim Fire in the Stanislaus National Forest that burned at high severity in plume-dominated fire behavior (Lydersen et al., 2014), the YFDP burned at low- to moderate-severity (Fig. 2.1). Pre-fire surface fuel loading was 334.8 Mg ha^{-1} (Larson et al., 2016), with high values for litter (63.9 Mg ha^{-1}) and duff (188.8 Mg ha^{-1}). Surface fuel consumption was 95% for litter, 93% for duff, and 90% for 1-hour fuels (Larson et al., 2016).

2.3 Field methods

The YFDP is a contiguous, rectangular plot comprised of 640 permanent 20 m × 20 m quadrats, within which all trees ≥1 cm DBH were identified, tagged, and mapped in 2009 and 2010 following the methods of the Smithsonian ForestGEO network (Lutz et al., 2012; Anderson-Teixeira et al., 2015, Lutz, 2015). Each tree was revisited annually between 2011 and 2017 and its status tracked (e.g., live or dead). In June 2014 (eight
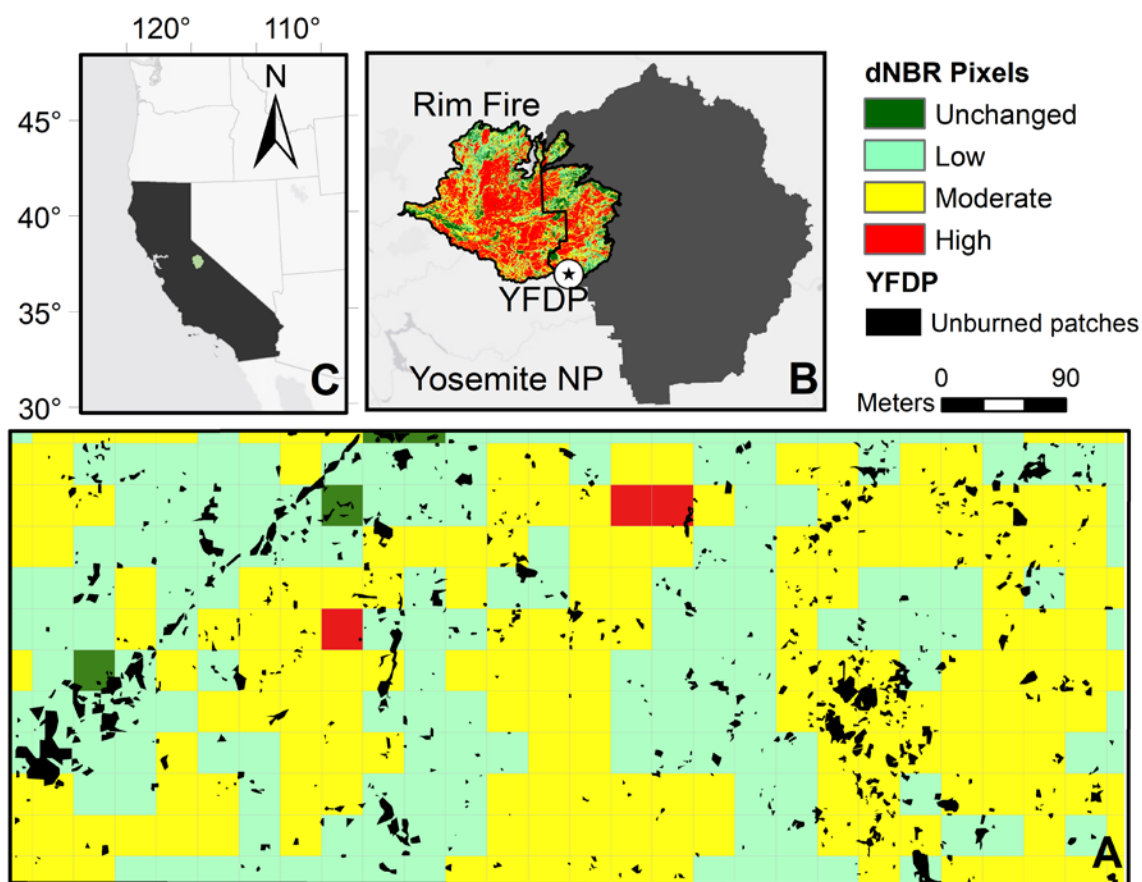
Fig. 2.1. Location of the Yosemite Forest Dynamics Plot (A) within Yosemite National Park (B), California (C). The footprint of the Rim Fire of 2013 had portions that burned at high-severity, but within the YFDP, the Rim Fire burned at low- to moderate-severity (A). There were 260 Landsat pixels completely within the YFDP and 336 pixels that intersected the YFDP (A). Small fire refugia (≥ 1 m^2) were present in all burn severity classes. Differenced Normalized Burn Ratio (dNBR) classifications are from Miller and Thode (2007): unchanged, < 41; low, 41-176; moderate, 176-366; high, ≥ 367.

months post-fire), I mapped unburned patches ≥ 1 m^2 in the YFDP. Unburned patches

were defined at the surface by an intact litter and duff layer (i.e. canopy conditions were

not evaluated in patch delineation). I mapped the unburned patches as polygons following

the methods of North et al., (2002), by traversing each quadrat to identify patches. I used

ocular estimation to delineate patch vertices in relation to features on field maps (e.g.,

trees and quadrat grid corners; Figs. A.1 and A.2). The unburned patch edges were

measured using meter tapes, and the datasheets included a representation of a 1-m grid to increase mapping accuracy. Field technicians recorded spatial references to nearby features which were individually verified during digitization (ArcMap 10.3 georeferencing toolbar; Fig. A.1). The position of nearby trees was recorded as outside, intersecting, or within an unburned patch.

I established 63, 1-m^2 square subplots on a defined grid, 54 of which were burned (>95% surface fuel consumption). Percent cover of understory vegetation was measured in the early summer (May, June) in 2015 through 2017. In order to compare vegetation in both burned and unburned areas, in 2016 I installed 40 additional 1-m^2 subplots within unburned patches that ranged in size from 16 m^2 to 40 m^2. In 2016, I measured litter cover and litter and duff depth in the center of each of the four sides of the 103 1-m^2 subplots.

2.4 Ancillary data

To calculate burn severity of the Rim Fire, I used Landsat 8/OLI Level 1T surface reflectance pre-fire (July 14, 2013) and post-fire (July 1, 2014) scenes (path 43 row 34) downloaded from the Earth Resources Observation and Science (EROS) Center Science Processing Architecture (ESPA) web portal. The scene pair was selected from all available scenes from the growing seasons of 2013 and 2014 for consistent sun angle, phenology, and low cloud cover (Key, 2006). I calculated the differenced normalized burn ratio (dNBR) according to Key and Benson (2006). I calculated the dNBR offset (following Meddens et al., 2016) from 780 pixels of unburned forest of the same type located approximately 2 km south of the YFDP. Categorical burn severity classification

was based on dNBR thresholds from Miller and Thode (2007): unchanged, <41; low, 41-176; moderate, 177-366; high, ≥367. There were 260 contiguous Landsat pixels completely within the boundaries of the YFDP and 336 Landsat pixels that intersected at least a portion of the area of the YFDP.

2.5 Patch summary statistics

Patch metrics (Table 2.2) were calculated for the total area occupied by each dNBR burn severity category (unchanged, low, moderate, high), and for the entire plot. To calculate distance to nearest patch neighbor the digitized unburned polygons were rasterized using the raster package version 2.6-7 (Hijmans, 2016) in R version 3.4.3 (R Core Team, 2017). I selected a raster cell size of 0.25-m to ensure no measured unburned polygons were dropped from the analysis. The nearest patch neighbor was determined as Euclidean distance from the cell center of the focal patch to the cell center of the neighboring patch.

2.6 Random forest modeling of the unburned fraction

I used a random forest model (randomForest package version 4.6-12; Liaw and Wiener, 2002) to determine the environmental variables most predictive of unburned patch presence. The response variable was calculated as the proportion of unburned area for each 10 m × 10 m cell. The predictor variables (Table 2.1) were a combination of abiotic and biotic factors hypothesized to influence fire behavior based on previous studies at larger spatial scales (Kane et al., 2013; 2014; 2015b). Abiotic variables included the distance to water, local surface roughness, slope, insolation, topographic position, and topographic ruggedness. Distance to water was the minimum Euclidean

distance from each unburned patch center to a water source (all water courses were vernal streams).

Topographic indices were calculated using the 2013 USGS 1/3 arc second (10 m) digital elevation model (DEM). From the DEM, I calculated the topographic position index (TPI), terrain ruggedness index (TRI), roughness, and slope using the terrain function in the raster package (Hijmans, 2016; Wilson et al., 2007). I calculated insolation using the solar radiation toolset in ArcGIS version 10.3 (ESRI, 2011). Potential biotic predictor variables included dNBR, the local density and basal area of pre-fire trees (by diameter class), the local density and basal are of trees that died (by diameter class), and the proximity to shrub patches (divided by guild; riparian, montane, or generalist; Lutz et al., 2014; 2017). Mortality-based metrics were defined as pre-fire live trees that died in the first year following the fire.

The majority of the plot surface burned, so the proportion unburned response variable was heavily weighted with zero values. I therefore used a zero-inflated model approach in which I first built a classification model with a binary response of unburned patch presence/absence, and second I examined the response as a continuous variable, the proportion unburned, of the non-zero observations. I first included all variables hypothesized to influence fire behavior (Table 2.1, Fig. A.3), and then developed a final model with the ten variables with highest importance by iteratively removing variables of lowest importance (Fig. A.4). I calculated accuracy measures for individual cells (observed vs. predicted) and in aggregate (binned observed values vs. mean predicted values).

Table 2.1

 Small fire refugia formation model predictors. The predictor variables were derived from the US Geological Survey 1/3 arc-second (10 m) digital elevation model (DEM), the National Hydrological Database (NHD), Landsat 8, and the Yosemite Forest Dynamics Plot (YFDP) tree and mortality data. The satellite-derived burn severity index used was the differenced normalized burn ratio (dNBR). Shrub cover was separated by species into three guilds: montane, generalist, and riparian according to the classifications of Lutz et al., (2017).

Variable Name	Variable description	Units	Source
Abiotic factors			
distance to water	Minimum distance from patch perimeter to water source	Meters	NHD
roughness	Surface complexity	Relative index	DEM
slope	Steepness of landscape	Degrees	DEM
solar incidence	Total amount of solar energy hitting a pixel surface on the day of the fire	Degrees	DEM
topographic position	Position of focal cell relative to surrounding cells	Relative index	DEM
topographic ruggedness	Local variation surrounding a focal pixel	Relative index	DEM
Biotic factors			
burn severity (dNBR)	Satellite-derived index of environmental change caused by fire	Relative index	Landsat
burn severity (tree mortality)	Proportion of live trees that experienced immediate fire-related mortality	Percent	YFDP
burn severity (BA mortality)	Proportion of basal area that experienced immediate fire-related mortality	Percent	YFDP
shrub cover	Cover occupied by shrub species (all guilds)	m^2	Lutz et al., 2017
shrub cover by guild	Shrub cover separated into guilds: generalist, montane, and riparian	m^2	Lutz et al., 2017
tree basal area	Area occupied by tree stems	$m^2\,ha^{-1}$	YFDP
tree density	Number of tree stems	stems ha^{-1}	YFDP
tree density (1 to 10 cm)	Number of tree stems 1 cm $\leq$ DBH < 10 cm	stems ha^{-1}	YFDP
tree density (10 to 30 cm)	Number of tree stems 10 cm $\leq$ DBH < 30 cm	stems ha^{-1}	YFDP
tree density (30 to 60 cm)	Number of tree stems 30 cm $\leq$ DBH < 60 cm	stems ha^{-1}	YFDP
tree density (60 to 90 cm)	Stems 60 cm $\leq$ DBH < 90 cm	stems ha^{-1}	YFDP
tree density ($\geq$ 90 cm)	Number of tree stems with DBH $\geq$ 90 cm per hectare	stems ha^{-1}	YFDP

2.7 Tree mortality

To analyze the effect of unburned patches on tree survival, I calculated mortality

rates in burned and unburned areas by species and diameter class. Trees were considered

to be in an unburned patch if they were completely within the unburned patch or if their

boles intersected the perimeter of a patch. I tested for significance (α=0.05) using χ^2 tests

under the null hypothesis of equal proportion of mortality in burned and unburned areas

and used a Bonferroni correction to account for multiple tests. I assessed the relationship

of immediate post-fire tree mortality and tree location relative to unburned patch edge. I

analyzed trees in unburned patches and trees within burned areas for both burned and

unburned trees. I used ANOVA (α=0.05) to test the response of distance to patch edge

and the two predictors, diameter class and post-fire status (live, dead). The distance to

patch edge was calculated using the gDistance function in the rgeos package version 0.3-

26 (Bivand et al., 2017). I used logistic regression to predict post-fire status and validated

model accuracy using ten-fold cross-validation.

2.8 Understory vegetation

I used non-metric multidimensional scaling (NMDS) to compare understory plant

communities in burned and unburned 1-m^2 quadrats in the YFDP. I examined only the

species occurring in greater than 5% of the quadrats, and each species was relativized by

the column total. To build the ordinations I used the metaMDS function in R (vegan

package version 2.4-6; Oksanen et al., 2013), which performed a double Wisconsin

standardization and square root transformation on the community matrix. The final

solutions were assembled in two-dimensions using the Bray-Curtis dissimilarity index,

wherein all species centroids were displayed and the species with the 5 largest correlation

coefficients were labeled. To examine the correlation between environmental variables

and measures of species diversity, I used the env.fit function in R (Oksanen et al., 2013)

to plot the significant vectors ($\alpha = 0.05$) on to the ordination space.

3. Results

3.1 Unburned patch metrics

In the YFDP (25.6 ha), there were 685 unburned patches ≥ 1 m^2, with a total

unburned area of 12,597 m^2 (4.9%; Table 2.2; Fig. 2.1). Mean unburned patch size was

18.4 m^2 (SD: 49.4 m^2, min: 1 m^2, max: 895.6 m^2). Patch density varied with burn severity

class, with the highest concentration of actual unburned patches in Landsat pixels

calculated as unburned by dNBR (48.8 patches ha^{-1}). Unburned patch densities were

similar in low- and moderate-severity pixels (27.5 and 26.0 patches ha^{-1}, respectively),

with the lowest number of unburned patches in high-severity pixels (11.1 patches ha^{-1}).

Table 2.2
Spatial attributes of small fire refugia in the Yosemite Forest Dynamics Plot (YFDP),
categorized by differenced Normalized Burn Ratio (dNBR) severity classes. Burn
severity classifications are from Miller and Thode (2007): unchanged, < 41; low, 41-176;
moderate, 176-366; high, $\geq$ 367. The nearest neighbor metric is the mean of the nearest
neighbor distances for each burn severity class.

Burn severity (dNBR)	Unburned area (m^2)	Prop. YFDP (%)	Prop. unburned (%)	Unburned patches (n)	Density (patches ha^{-1})	Mean size (m^2)	Patch SD (m^2)	Nearest neighbor (m)
Unchanged	339.1	0.9	15.0	11	48.8	30.8	39.0	1.6
Low	6,756.3	44.8	5.9	316	27.5	21.4	61.0	4.4
Moderate	5,419.9	53.2	4.0	355	26.0	15.3	36.7	4.3
High	81.3	1.1	3.0	3	11.1	27.1	41.1	6.2
Total YFDP	12,596.6	100.0	4.9	685	26.7	18.4	49.5	4.3
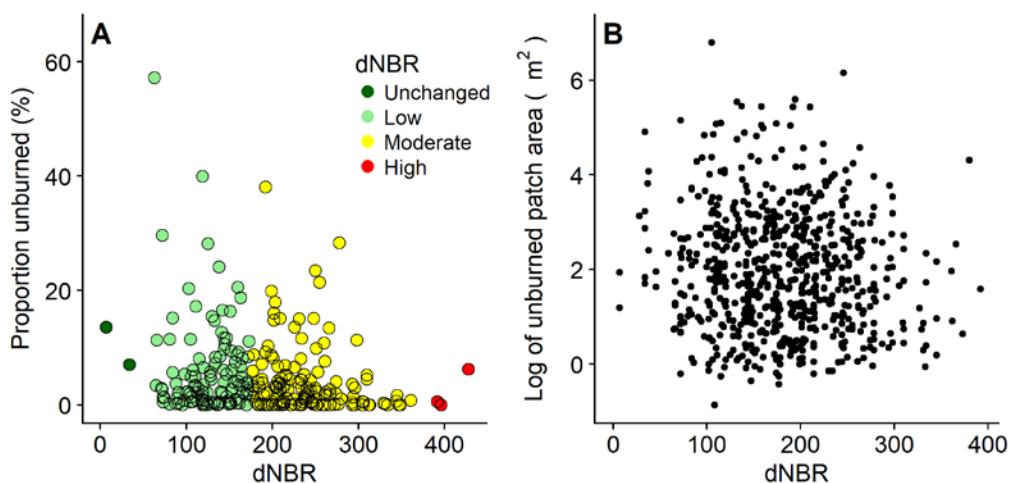
Fig. 2.2. Differenced Normalized Burn Ratio (dNBR) pixel values for the Yosemite Forest Dynamics Plot and the proportion of each pixel that was observed as unburned (A). There was no relationship between the log-transformed unburned patch area and the associated dNBR values (B), suggesting factors other than satellite-derived burn severity control the size of small refugia. The dNBR severity classifications are from Miller and Thode (2007): unchanged, < 41; low, 41-176; moderate, 176-366; high, ≥ 367.

The average nearest neighbor distance between unburned patches was 4.3 m for the whole plot, with the shortest nearest neighbor distances occurring between unchanged pixels (mean: 1.6 m) and the longest nearest neighbor distances occurring between high-severity pixels (mean: 6.2 m; Table 2.2). The actual unburned area within individual dNBR pixels had a weak negative relationship with dNBR burn severity, whether considered categorically (Table 2.2) or continuously (Fig. 2.2).

3.2 Random forest model

The presence-absence random forest model correctly predicted observed values 73.6% of the time. The model correctly predicted unburned patch absence (i.e. completely burned areas) 88.7% of the time, compared to 46.3% for unburned patch presence. Of the rows incorrectly classified by the model (25.6%), 72.2% of these errors were unburned presence observations incorrectly predicted as absence.

Table 2.3
Accuracy statistics for random forest classification models predicting the presence of
unburned patches: out of bag (OOB) error rate (a measure of overall percent correctly
classified), sensitivity (the true positive rate), specificity (the true negative rate), and area
under curve (AUC; a threshold-independent metric that combines sensitivity and
specificity). Accuracy measures for the random forest regression model predicting the
non-zero unburned proportion: Variation explained (%), mean difference between
predicted and observed values, root mean square error (RMSE), mean absolute error
(MAE), and the difference between RMSE and MAE.

Presence-absence model with binary response			
OOB Error	**Sensitivity**	**Specificity**	**AUC**
25.7	0.85	0.47	0.76
Presence-only model with continuous response			
Var. explained	**Mean difference**	**RMSE**	**MAE**
30.4	0.63	17.3	13.1

The presence-only random forest model with a continuous response of proportion
unburned had a mean difference between predicted and observed values of 0.63 (Table
2.3). The predictors that contributed the most to increase in mean square error (MSE), a
measure of variable importance to model accuracy, were (in order of importance):
distance to stream (m), mortality basal area (m^2 ha^{-1}), basal area (m^2 ha^{-1}), density (stems
ha^{-1}), mortality density (stems ha^{-1}) and the Topographic Position Index. The mean of the
predicted values plotted against the observed values demonstrated the model was best at
predicting unburned proportion from 0 m^2 to 30 m^2, and less accurate for predicting
larger patches (Fig. 2.3). However, the model consistently underpredicted the proportion
unburned for grid cells that were >30% unburned (Fig. 2.3).

3.3 Understory tree mortality

Total pre-fire tree density in the unburned areas of the plot was 871 stems ha^{-1}
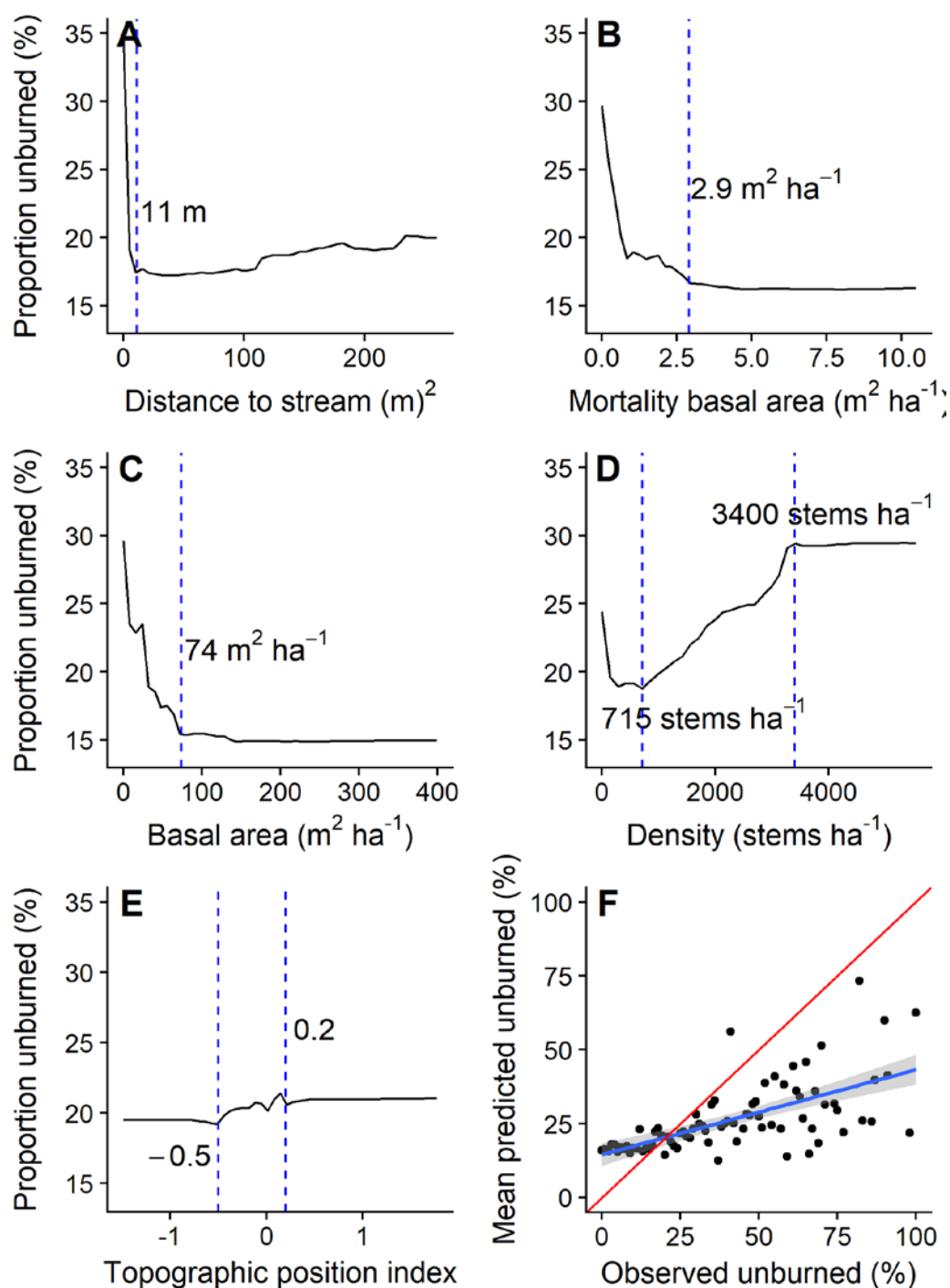
Fig. 2.3. Partial dependence plots of random forest model variables, listed in order of variable importance: distance to stream (A), mortality basal area (B), basal area (C), tree density (D), and topographic position index (E). Panel F depicts a measure of model accuracy in aggregate: the mean of the predicted dependence variable plotted against the observed response in bins (rounded to the nearest whole number). Dashed vertical lines indicate inflection points.

compared to 1,359 stems ha^{-1} in burned areas. Immediate tree mortality rate was 26.7%

within unburned patches and 72.5% in burned areas (Table 2.4). The greatest difference

in tree mortality was in the 1 cm ≤ DBH < 10 cm diameter class, with mortality in burned

and unburned areas of 90.5% and 30.6% respectively (χ^2 tests, P <0.001). There was no

mortality for trees ≥30 cm DBH located within unburned patches, compared to 11.5%

mortality for trees 30 cm ≤ DBH < 60 cm in burned areas (Table 2.4). *Cornus nuttallii*

was the tree species with the highest proportion of its population located within unburned

patches (15.8%) and consequently had the greatest reduction in mortality relative to other

species. The species with the lowest proportion of individuals located within unburned

patches was *Pinus lambertiana* (1.5%).

Table 2.4
Abundances and immediate (2014) mortality rates of all trees in the Yosemite Forest
Dynamics Plot during the Rim fire (2013). Trees were categorized based on whether their
bole was wholly or partially in an unburned patch ≥1 m^2 (unburned) or not (burned).
Mortality rates for trees within unburned patches were lower for the five most abundant
species and the two smallest diameter classes (χ^2 tests with a Bonferroni correction,
modified α=0.01; P <0.001 for all). Significant differences indicated in bold.

	Pre-fire live tree abundance			Post-fire mortality rates		
	Entire plot (*n*)	Unburned areas (*n*)	Burned areas (*n*)	Entire plot (%)	Unburned areas (%)	Burned areas (%)
Species						
Abies concolor	23999	473	23526	72.5	**29.2**	**73.3**
Pinus lambertiana	4616	67	4549	63.7	**35.8**	**64.1**
Cornus nuttallii	2701	428	2273	77.1	**23.4**	**87.2**
Calocedrus decurrens	1635	49	1586	63.9	**24.5**	**65.1**
Quercus kelloggii	1110	63	1047	63.2	**14.3**	**66.1**
Diameter class						
1 cm ≤ DBH < 10 cm	21226	890	20336	90.5	**30.6**	**93.1**
10 cm ≤ DBH < 30 cm	9415	195	9220	50.9	**10.8**	**51.8**
30 cm ≤ DBH < 60 cm	2293	10	2283	11.5	0.0	11.5
60 cm ≤ DBH < 90 cm	690	3	687	3.3	0.0	3.3
DBH ≥ 90 cm	621	0	621	4.0	*NA*	4.0
Total	34061	1080	32981	71.0	**26.7**	**72.5**

Four years after the fire, trees had markedly higher survival rates in unburned patches for all species and diameter classes ≤60 cm DBH (Fig. 2.4). The greatest difference in survival was for trees 1 cm ≤ DBH <10 cm, where 58.8% survived in unburned patches and 2.7% survived in burned areas (χ^2 tests, $P<0.001$). Survival rates
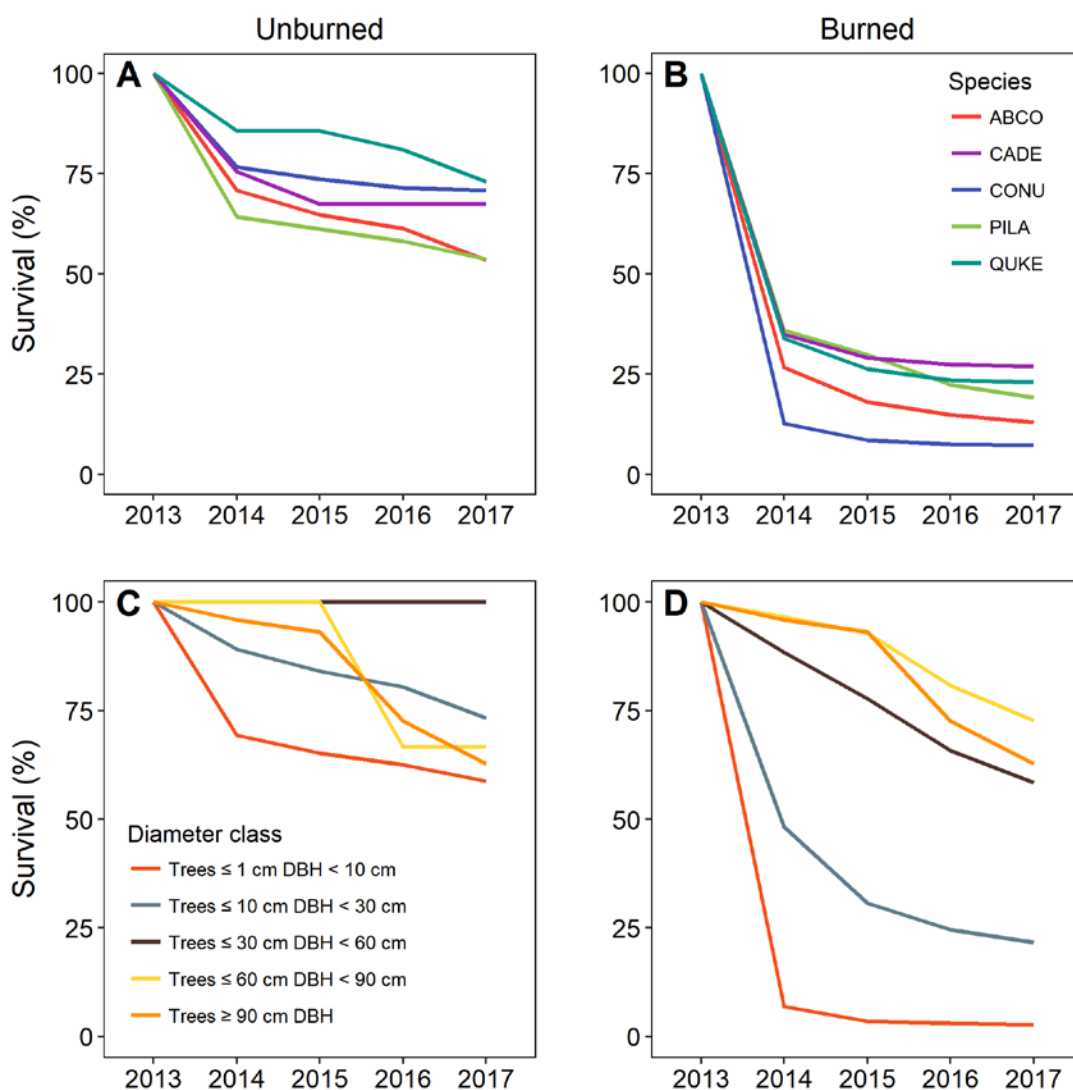
Fig. 2.4. Tree survival rates in the Yosemite Forest Dynamics Plot from 2014 – 2017. Trees of the five most abundant species (*Abies concolor, Calocedrus decurrens, Cornus serecia, Pinus lambertiana, Quercus kelloggii*) had higher survival rates if their boles were in unburned patches (A) compared to areas with burned substrate (B). Trees ≤ 30 cm DBH had higher survival rates in unburned (C) versus burned (D) patches.

for trees 60 cm $\leq$ DBH < 90 cm did not differ between unburned and burned areas

(66.7% and 62.9%; χ^2 tests, P=0.901).

Trees in unburned patches that survived were positioned further from the patch

edge (mean: 1.1 m, min: 0 m, max: 5.7 m), while trees in unburned patches that died were

closer to the patch edge (mean: 0.6 m, min: 0 m, max: 2.9 m). The position within

unburned patches of trees 1 cm $\leq$ DBH < 10 cm that survived was further from the edge

than trees that died (ANOVA, $P < 0.001$), indicating that buffering from radiant and

convective heat was critical to survival of small-diameter trees. Distance to patch edge

did not predict survival for trees 10 cm $\leq$ DBH < 30 cm (ANOVA, P=0.204) or larger.

Trees in burned areas that survived were closer to unburned patches (mean: 8.6 m, min: 0

m, max: 44.3 m) than trees that died (mean: 11.0 m, min: 0 m, max: 47.6 m), with

significant differences (ANOVA, P<0.05) for all diameter classes except for trees $\geq$ 90

cm DBH (ANOVA, P=0.643).

3.4 Understory vegetation

The NMDS ordinations showed a clear separation between burned and unburned

quadrats for both years, suggesting these areas contain distinct understory communities

(Fig. 2.5). The final solutions had a stress of 17.5 for the 2016 data, and 17.6 for the 2017

data. Six vectors had significant associations ($\alpha = 0.05$) with the ordination configuration:

percent burned, litter depth, seedling abundance, percent cover, species richness, and the

Shannon Diversity Index (SDI). Most notably, plant communities in small refugia appear

to be more diverse than those of burned areas, both in terms of diversity indices and the

position of species centroids in ordination space (Fig. 2.5). Species richness and SDI
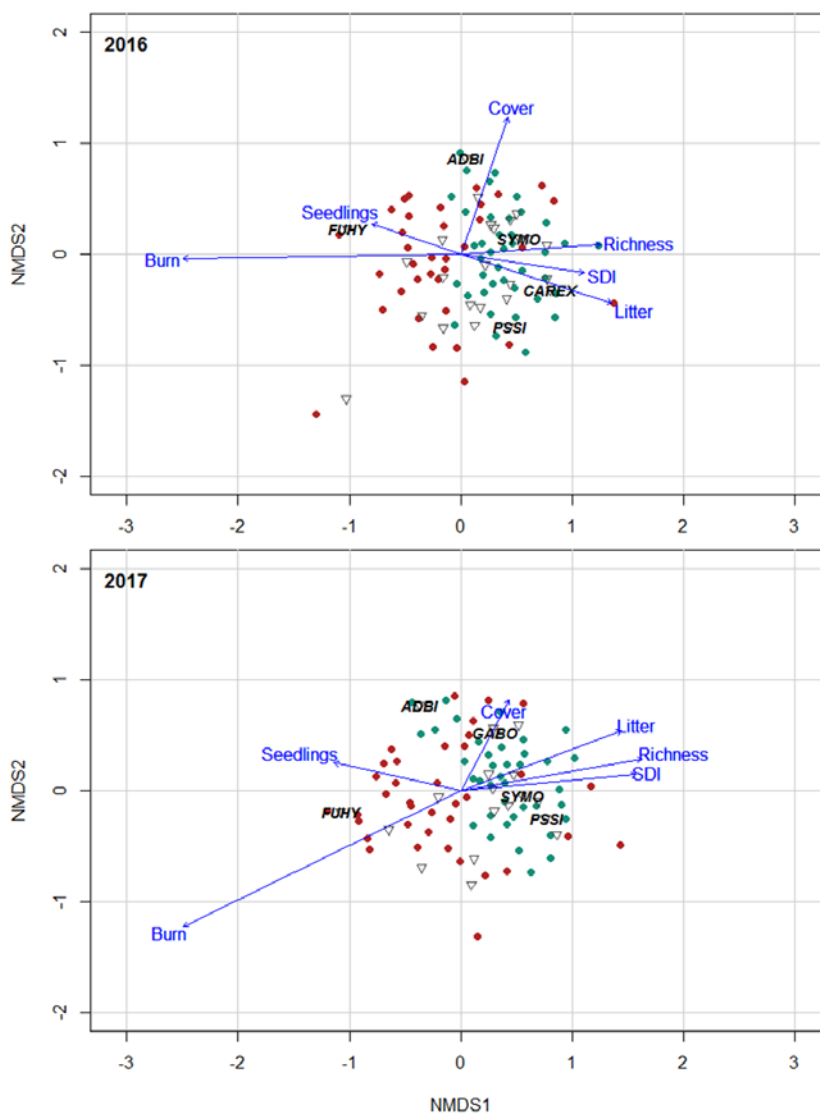
Fig. 2.5. Non-metric multidimensional scaling (NMDS) ordination showing understory vegetation community differences in the Yosemite Forest Dynamics Plot (YFDP) 3 and 4 years following the 2013 Yosemite Rim fire. Vegetation was measured in 1-m^2 quadrats in burned (represented by red circles) and unburned (represented by green circles) areas. Species centroids are represented by black triangles, wherein the species with the 5 largest correlation coefficients are labeled. ADBI= *Adenocaulon bicolor;* CAREX= *Carex spp.;* FUHY= *Funaria hygrometrica*; GABO= *Galium bolanderi*; PSSI= *Pseudostellaria sierra;* SYMO= *Symphoricarpos mollis*. Environmental variables with significant associations ($P \leq 0.05$) are represented by blue arrows. Burn= percent of 1-m^2 quadrat that burned; Cover= percent vegetative cover; Litter= depth (cm) of the litter layer; Richness= number of species observed at a quadrat; SDI= the Shannon Diversity Index; Seedlings= seedling abundance.

were associated with unburned quadrats (richness: $r_{2016}= 0.10$, $r_{2017}=0.11$; SDI: $r_{2016}=$ 0.09, $r_{2017}= 0.10$). In addition to the diversity indices, percent cover and litter depth were correlated with unburned areas (cover: $r_{2016}= 0.10$, $r_{2017}=0.04$; litter depth: $r_{2016}= 0.09$, $r_{2017}=0.10$), suggesting either that small fire refugia are places with high vegetative cover, or that recolonization of burned areas 3 to 4 years after fire does not match the cover observed in unburned areas. Seedling abundance was negatively correlated with unburned plots in 2017 ($r= 0.06$), likely because the litter layer acts as a barrier for the anchoring of seedling roots. Species composition in the burned plots was more similar to that of the unburned plots in 2017 relative to 2016, suggesting that understory recolonization four years post-fire homogenizes these two areas.

Despite community differences visible in the NMDS ordinations, mean quadrat summary metrics for all understory species (including rare species) were the same in burned and unburned areas (Table A.1). Mean cover in unburned quadrats was 21.8% (SD: 22.2%, min: 0%, max: 150.8%); compared to 13.1% in burned quadrats (SD: 22.4%, min: 0%, max: 104.5%; Table A.1; $P=0.121$). Average seedling abundance was 6 m^{-2} in burned quadrats and 2 m^{-2} in unburned quadrats ($P= 0.180$). Species richness in unburned quadrats was 6.4 m^{-2} (min: 0 m^{-2}, max: 15 m^{-2}) and 3.2 m^{-2} in burned quadrats (min: 0 m^{-2}, max: 12 m^{-2}), but the differences were not significant ($P=0.266$).

4. Discussion

4.1 Characteristics of small fire refugia

Small fire refugia (<0.1 ha) were present throughout the study area in this low- to moderate-severity fire (Fig. 2.1). The fire traversed the entire plot, with the exception of

approximately 5% of the forest surface (Table 2.2). Refugia were abundant, and occurred in all landscape positions and dNBR burn severity classes. The distribution of dNBR pixels in the YFDP is consistent with the severity of recent fires in Yosemite (van Wagtendonk and Lutz, 2007; Lutz et al., 2011; Thode et al., 2011), suggesting that the density of refugia (26.7 patches ha-1) is representative fire effects from other contemporary fires in the white fir-sugar pine forest type in the Sierra Nevada.

While small fire refugia were present within dNBR pixels of all severities, unburned patches tended to have lower densities and greater dispersion (higher nearest neighbor distances; Table 2.2) with increasing burn severity. I posit that this pattern is influenced by soil, fuel continuity, and litter moisture (Wohlgemuth et al., 2006). Environments that tend to burn at moderate or high severity, such as steep, rocky areas, may exhibit reduced fuel continuity because of the rocky matrix and low productivity (Kolden et al., 2017). Low fuel continuity could lead some areas to remain unburned despite high flame heights associated with steep slopes. In low burn severity environments, such as drainages and riparian areas, high litter moisture and cold air pooling inhibit fire spread, possibly leading to more abundant and less dispersed unburned patches (Dwire and Kauffman, 2003).

Individual unburned patch area showed no relationship with dNBR as a continuous metric (Fig. 2.2), suggesting that burn severity does not control small patch size and that many conditions associated with both high and low dNBR can give rise to large and small patches. Stochasticity in fire behavior, such as a change in wind direction, may give rise to small skips (<20 m^2) in the burning of surface fuels (irrespective of burn severity).

4.2 Patch detection limitations with dNBR

These results show that dNBR cannot detect small, ground-mapped refugia. Pixels with an unchanged surface reflectance occupied 0.9% of the YFDP, much lower than the 4.9% unburned fraction determined by field observations (Table 2.2). This is not surprising—dNBR values primarily exhibit overstory changes because differenced Landsat scenes cannot detect surface burning when masked by the canopy (Kolden et al., 2012). Furthermore, most refugia in this study occurred at a scale unlikely to be reflected by dNBR, as Landsat-derived pixels represent an average of spectral changes over a 900 m^2 area. Continuous dNBR values, however, can help estimate the proportion of unburned surface within a 30 m $\times$ 30 m pixel (Fig. 2.2), and to a lesser extent predict reductions in mean patch size by severity class (Table 2.2). In future research commercial high-resolution satellite and/or multi-temporal lidar (McCarley et al., 2017) remote sensing methods could potentially improve detection of small fire refugia.

4.3 Predicting small refugia

Inaccuracies in our presence-absence random forest model may be due to the presence of different types of small fire refugia in our dataset. Fire refugia include those that are permanent or ephemeral (*sensu* Meddens et al., 2018b). Predictive models might reach a high level of accuracy for permanent refugia that are controlled primarily by their landscape position or surrounding vegetation, but it may be difficult to model ephemeral refugia, where the locations are controlled by the vagaries of fire progression, in anything other than a probabilistic sense. The relative proportion of permanent and ephemeral refugia on the landscape remains an open area of research.

In a separate analysis of the cells our presence-absence model could accurately predict, I found that the proportion of permanent refugia (*sensu* Meddens et al., 2018b) is considerable, and can be modeled with physiologically plausible predictors (i.e., distance to streams, proximate tree density and basal area, proximate tree mortality, and topographic position; Fig. 2.3). Both minimum and maximum distances from streams were associated with high unburned proportion, showing that the distribution of refugia responds to multiple factors (Fig. 2.3A). The unburned proportion was highest in areas with the lowest mortality by basal area, a measure of burn severity (Fig. 2.3B). Low basal area, which is often associated with low productivity areas, was also correlated with high unburned proportion (Fig. 2.3C). Refugia occurred in areas of both high and low stem densities (Fig. 2.3D), likely a reflection of high stem densities of riparian species (i.e., *Cornus sericea* and *Cornus nuttallii*) and low-productivity rocky outcroppings (Fig. 2.3D). Topographic Position Index had less explanatory power, but indicated unburned proportion was slightly higher in concave lower slopes and convex upper slopes (Fig. 2.3E)

Data limitations likely contributed to model inaccuracies in predicting small fire refugia presence. Following the abstraction of the fire behavior triangle (fuels, weather, topography), our set of predictors was incomplete. Topography was the only component I was thoroughly able to include in the model and its predictive ability was less than vegetation-related predictors (Fig. 2.3). Our measures of fuel loading and consumption were indirect, as I used proxies known to contribute to the litter and duff layer (e.g., nearby tree density and basal area) or to represent fire intensity (e.g., local tree mortality). I had no measurements of fine-scale fire weather (but see Lutz et al., 2017). There was

also a scale problem, wherein our predictive data did not necessarily match the spatial scale of the refugia I delineated, which influences model predictive power (Birch et al., 2015).

4.4 Impact of small refugia on tree mortality and survival

Despite our definition of refugia as entirely unburned at the surface, tree mortality still occurred in unburned areas. Our field measurements of unburned patches considered only the forest floor and root crowns when classifying an area as either burned or unburned. Radiant and convective heat from the flames, however, was often lethal for sub-canopy foliage, and many trees located within unburned patches experienced crown scorch despite having an intact litter layer. Overall, however, small refugia were a significant source of tree survival for all species and diameter classes <60 cm DBH (Table 2.4) and these higher survival rates persisted for at least four years (Fig. 2.4). The deciduous species *Quercus kelloggii* and *Cornus nuttallii* were more susceptible to bole scorch mortality due to their thinner bark, and consequently these species experienced the greatest increases in survival when located in small refugia. Trees positioned deeper within unburned patches had higher survival rates, likely due to heat buffering resulting in sub-lethal fire heating (i.e., Smith et al., 2016b; 2017).

Small-diameter trees disproportionally benefited from the heat buffering effects of small refugia. After a century of fire suppression, which resulted in increased tree densities and high ground fuel accumulations, even low- to moderate-severity surface fires are fatal to most sub-canopy trees. Small refugia may be important determinants of the trees that eventually recruit into the canopy; trees <10 cm DBH that escape fire by

virtue of being in refugia may be large enough to survive the next fire, even if that subsequent fire burns near them (Becker and Lutz, 2016). By preserving a population of advanced regeneration, small refugia may be a means through which forests maintain structural diversity.

4.5 Understory vegetation in burned and unburned areas

Small fire refugia appear to host more diverse understory plant communities relative to burned areas 3 and 4 years post-fire (Fig. 2.5). Burned areas were dominated by colonizing species or in some cases, lacked any vegetative regrowth, while unburned areas likely maintained pre-fire species composition. I draw two conclusions from the higher understory plant diversity found in unburned areas. First, places where small fire refugia form may host different and/or more diverse understory communities than areas that burned. Alternatively, the same understory communities may have been prevalent throughout burned and unburned areas, and those surviving in small fire refugia represent starting points for post-fire recolonization of burned areas. In either case, refugial areas may be a mechanism by which forests maintain biodiversity across periods of disturbance.

4.6 Scale

The fine-scale resolution and spatial extent of this dataset allows us to address whether spatial patterns of fire refugia are maintained across scales (i.e., Lutz et al., 2018). Previous work has examined fire refugia primarily at the landscape scale, for which the smallest unit of measure is a 900 m^2 Landsat pixel. Kolden et al., (2012) and Kolden et al., (2015) reported the average unburned proportion in Yosemite National

Park at 20% to 25%, much higher than the 5% unburned area found in this study.

Moreover, the fire in the YFDP had a substantial low-severity component (44.8%); based

on the results of Kolden et al., (2012) I would expect a higher proportion of unburned

area following lower severity fire. Several conditions could explain these incongruities.

First, these results suggest that—at least for low- to moderate-severity fire—landscape-

scale factors that give rise to large fire refugia (e.g. aspect, topography, burn history) may

not apply at fine scales. Second, the methods associated with measuring small vs. large

fire refugia are based on different definitions of unburned refugia. Whereas I delineated

unburned patches based on the presence of an intact litter and duff layer, unchanged

dNBR pixels could represent several ground conditions, including unburned forest; an

undetectable low-severity burn; or regrown vegetation with an identical spectral signal to

that of the pre-fire scene (Kolden et al., 2012). Given the possible surface conditions that

large fire refugia could represent, it is not surprising that the unburned proportion differs

between large and small scales.

5. Conclusion

5.1 Management implications

Frequent-fire forests of the Sierra Nevada are renowned for their vascular plant

species diversity and their structural heterogeneity, which is at least partially due to fire

heterogeneity (Kane et al., 2015a). I show that the small fire refugia observed after a low-

to moderate-severity fire were associated with more diverse understory plant

communities and may contribute to structural diversity through increased survival of

small-diameter trees relative to burned areas. To preserve these outcomes, managers

conducting prescribed fires as fuel reduction treatments may wish to consider allowing some unburned patches to remain within treatment areas. Uniformly burning all surface area within a treatment block is uncharacteristic of the contemporary, unmanaged fire regime in these forests, and may stall elements of post-fire development. Fire heterogeneity in Sierra Nevada forests is likely present at all spatial scales, and therefore managers may wish to consider all scales from 1-m^2 to the landscape.

Better knowledge of refugia may also help create fire-resilient communities (*sensu* Smith et al., 2016a). The predictability of refugia location (albeit with limited skill) suggests that further research may lead to predictive models of refugial presence that have considerable potential to preserve ecological function or human habitation in frequent-fire forests. If characteristics associated with refugia can be better identified, these characteristics (to the extent that they are biotic in nature) can be modified by planting or thinning to help protect areas of ecological or anthropogenic importance.

References

Anderson-Teixeira, K. J., S. J. Davies, A. C. Bennett, E. B. Gonzalez-Akre, H. C. Muller-Landau, S. Joseph Wright, K. Abu Salim, A. M. Almeyda Zambrano, A. Alonso, J. L. Baltzer, Y. Basset, N. A. Bourg, E. N. Broadbent, W. Y. Brockelman, S. Bunyavejchewin, D. F. R. P. Burslem, N. Butt, M. Cao, D. Cardenas, G. B. Chuyong, K. Clay, S. Cordell, H. S. Dattaraja, X. Deng, M. Detto, X. Du, A. Duque, D. L. Erikson, C. E. N. Ewango, G. A. Fischer, C. Fletcher, R. B. Foster, C. P. Giardina, G. S. Gilbert, N. Gunatilleke, S. Gunatilleke, Z. Hao, W. W. Hargrove, T. B. Hart, B. C. H. Hau, F. He, F. M. Hoffman, R. W. Howe, S. P.

Hubbell, F. M. Inman-Narahari, P. A. Jansen, M. Jiang, D. J. Johnson, M. Kanzaki, A. R. Kassim, D. Kenfack, S. Kibet, M. F. Kinnaird, L. Korte, K. Kral, J. Kumar, A. J. Larson, Y. Li, X. Li, S. Liu, S. K. Y. Lum, J. A. Lutz, K. Ma, D. M. Maddalena, J. R. Makana, Y. Malhi, T. Marthews, R. Mat Serudin, S. M. Mcmahon, W. J. McShea, H. R. Memiaghe, X. Mi, T. Mizuno, M. Morecroft, J. A. Myers, V. Novotny, A. A. de Oliveira, P. S. Ong, D. A. Orwig, R. Ostertag, J. den Ouden, G. G. Parker, R. P. Phillips, L. Sack, M. N. Sainge, W. Sang, K. Sringernyuang, R. Sukumar, I. F. Sun, W. Sungpalee, H. S. Suresh, S. Tan, S. C. Thomas, D. W. Thomas, J. Thompson, B. L. Turner, M. Uriarte, R. Valencia, M. I. Vallejo, A. Vicentini, T. Vrška, X. Wang, X. Wang, G. Weiblen, A. Wolf, H. Xu, S. Yap, and J. Zimmerman. 2015. CTFS-ForestGEO: A worldwide network monitoring forests in an era of global change. Global Change Biology 21: 528-549.

Banks, S. C., M. Dujardin, L. McBurney, D. Blair, M. Barker, and D. B. Lindenmayer. 2011. Starting points for small mammal population recovery after wildfire: Recolonisation or residual populations? Oikos 120: 26-37.

Barth, M. A. F., A. J. Larson, and J. A. Lutz. 2015. A forest reconstruction model to assess changes to Sierra Nevada mixed-conifer forest during the fire suppression era. Forest Ecology and Management 354: 104-118.

Becker, K., and J. A. Lutz. 2016. Low-severity fire fails to reverse overstory compositional change in montane forests of the Sierra Nevada. Ecosphere 7(12): e01484.

Birch, D. S., P. Morgan, C. A. Kolden, J. T. Abatzoglou, G. K. Dillon, A. T. Hudak, and

A. M. S. Smith. 2015. Vegetation, topography and daily weather influenced burn severity in central Idaho and western Montana forests. Ecosphere 6: art17.

Bivand, R., C. Rundel, E. Pebesma, R. Stuetz, and K. O. Hufthammer. 2017. Interface to geometry engine - open source ('GEOS'). Version 0.3-26. http://cran.r-project.org/package=rgeos. Downloaded 23 March 2018.

Brennan, K. E. C., M. L. Moir, and R. S. Wittkuhn. 2011. Fire refugia: The mechanism governing animal survivorship within a highly flammable plant. Austral Ecology 36:131-141.

Delong, S. C., and W. B. Kessler. 2000. Ecological characteristics of mature forest remnants left by wildfire. Forest Ecology and Management 131: 93-106.

Dennison, P. E., S. C. Brewer, J. D. Arnold, and M. A. Moritz. 2014. Large wildfire trends in the western United States, 1984-2011. Geophysical Research Letters 41: 2928-2933.

Dwire, K. A., and J. B. Kauffman. 2003. Fire and riparian ecosystems in landscapes of the western USA. Forest Ecology and Management 178(1-2): 61-74.

ESRI. 2011. ArcGIS Desktop: Release 10.3. Environmental Systems Research Institute, Redlands, California, USA.

Gandhi, K. J. K., J. R. Spence, D. W. Langor, and L. E. Morgantini. 2001. Fire residuals as habitat reserves for epigaeic beetles (Coleoptera: Carabidae and Staphylinidae). Biological Conservation 102: 131-141.

Gasaway, W. C., and S. D. DuBois. 1985. Initial response of moose, *Alces alces*, to a wildfire in Interior Alaska. Canadian Field-Naturalist 99: 135-140.

Haire, S., J. Coop, and C. Miller. 2017. Characterizing spatial neighborhoods of refugia

following large fires in northern New Mexico USA. Land 6: 19.

Hijmans, R. J. 2016. raster: Geographic Data Analysis and Modeling. R package version 2.6-7. https://CRAN.R-project.org/package=raster. Downloaded 23 March 2018.

Hylander, K., and S. Johnson. 2010. In situ survival of forest bryophytes in small-scale refugia after an intense forest fire. Journal of Vegetation Science 21: 1099-1109.

Kane, V. R., J. D. Bakker, R. J. McGaughey, J. A. Lutz, R. F. Gersonde, and J. F. Franklin. 2010. Examining conifer canopy structural complexity across forest ages and elevations with LiDAR data. Canadian Journal of Forest Research 40: 774-787.

Kane, V. R., C. A. Cansler, N. A. Povak, J. T. Kane, R. J. McGaughey, J. A. Lutz, D. J. Churchill, and M. P. North. 2015a. Mixed severity fire effects within the Rim fire: Relative importance of local climate, fire weather, topography, and forest structure. Forest Ecology and Management 358: 62-79.

Kane, V. R., J. A. Lutz, C. Alina Cansler, N. A. Povak, D. J. Churchill, D. F. Smith, J. T. Kane, and M. P. North. 2015b. Water balance and topography predict fire and forest structure patterns. Forest Ecology and Management 338: 1-13.

Kane, V. R., J. A. Lutz, S. L. Roberts, D. F. Smith, R. J. McGaughey, N. A. Povak, and M. L. Brooks. 2013. Landscape-scale effects of fire severity on mixed-conifer and red fir forest structure in Yosemite National Park. Forest Ecology and Management 287: 17-31.

Kane, V. R., M. P. North, J. A. Lutz, D. J. Churchill, S. L. Roberts, D. F. Smith, R. J.

McGaughey, J. T. Kane, and M. L. Brooks. 2014. Assessing fire effects on forest spatial structure using a fusion of landsat and airborne LiDAR data in Yosemite national park. Remote Sensing of Environment 151: 89-101.

Keeler-Wolf, T., P. E. Moore, E. T. Reyes, J. M. Menke, D. N. Johnson, and D. L. Karavidas. 2012. Yosemite National Park Vegetation Classification and Mapping Project Report. Natural Resource Report NPS/YOSE/NRTR-2012/598. National Park Service, Fort Collins, Colorado.

Keeley, J. E. 2009. Fire intensity, fire severity and burn severity: A brief review and suggested usage. International Journal of Wildland Fire 18: 116-126.

Key, C. H. 2006. Ecological and sampling constraints on defining landscape fire severity. Fire Ecology 2: 34-59.

Key, C. H., and N. C. Benson. 2006. Landscape assessment: Sampling and analysis methods. General Technical Report RMRS-GTR-164-CD. USDA Forest Service, Rocky Mountain Research Station, Fort Collins, Colorado.

Kolden, C. A., J. A. Lutz, C. H. Key, J. T. Kane, and J. W. van Wagtendonk. 2012. Mapped versus actual burned area within wildfire perimeters: characterizing the unburned. Forest Ecology and Management 286: 38-47.

Kolden, C. A., J. T. Abatzoglou, J. A. Lutz, C. A. Cansler, J. T. Kane, J. W. van Wagtendonk, and C. H. Key. 2015. Climate contributors to forest mosaics: ecological persistence following wildfire. Northwest Science 89(3): 219-238.

Kolden, C. A., T. M. Bleeker, A. M. S. Smith, H. M. Poulos, and A. E. Camp. 2017. Fire effects on historical wildfire refugia in contemporary wildfires. Forests 8: f8100400.

Krawchuk, M. A., S. L. Haire, J. D. Coop, M.-A. Parisien, E. Whitman, G. W. Chong, and C. Miller. 2016. Topographic and fire weather controls of fire refugia in forested ecosystems of northwestern North America. Ecosphere 7(12): e01632.

Larson, A. J., C. A. Cansler, S. G. Cowdery, S. Hiebert, T. J. Furniss, M. E. Swanson, and J. A. Lutz. 2016. Post-fire morel (*Morchella*) mushroom abundance, spatial structure, and harvest sustainability. Forest Ecology and Management 377: 16-25.

Liaw, A., and M. Wiener. 2002. Classification and Regression by randomForest. R News 2:18-22.

Lutz, J. A., J. W. Van Wagtendonk, A. E. Thode, J. D. Miller, and J. F. Franklin. 2009. Climate, lightning ignitions, and fire severity in Yosemite National Park, California, USA. International Journal of Wildland Fire 18(7): 765-774.

Lutz, J. A., J. W. van Wagtendonk, and J. F. Franklin. 2010. Climatic water deficit, tree species ranges, and climate change in Yosemite National Park. Journal of Biogeography 37: 936-950.

Lutz, J. A., C. H. Key, C. A. Kolden, J. T. Kane, and J. W. van Wagtendonk. 2011. Fire frequency, area burned, and severity: A quantitative approach to defining a normal fire year. Fire Ecology 7(2): 51-65.

Lutz, J. A., A. J. Larson, M. E. Swanson, and J. A. Freund. 2012. Ecological importance of large-diameter trees in a temperate mixed-conifer forest. PLoS ONE 7(5): e36131.

Lutz, J. A., K. A. Schwindt, T. J. Furniss, J. A. Freund, M. E. Swanson, K. I. Hogan, G.

E. Kenagy, and A. J. Larson. 2014. Community composition and allometry of *Leucothoe davisiae*, *Cornus sericea*, and *Chrysolepis sempervirens*. Canadian Journal of Forestry Research 44(6): 677-683.

Lutz, J. A. 2015. The evolution of long-term data for forestry: large temperate research plots in an era of global change. Northwest Science 89:255-269.

Lutz, J. A., T. J. Furniss, S. J. Germain, K. M. L. Becker, E. M. Blomdahl, S. A. Jeronimo, C. A. Cansler, J. A. Freund, M. E. Swanson, and A. J. Larson. 2017. Shrub communities, spatial patterns, and shrub-mediated tree mortality following reintroduced fire in Yosemite National Park, California, USA. Fire Ecology 13(1): 104-126.

Lutz, J. A., A. J. Larson, and M. E. Swanson. 2018. Advancing fire science with large forest plots and a long-term multidisciplinary approach. Fire 1(1): 5.

Lydersen, J. M., M. P. North, and B. M. Collins. 2014. Severity of an uncharacteristically large wildfire, the Rim Fire, in forests with relatively restored frequent fire regimes. Forest Ecology and Management 328: 326-334.

McCarley, T. R., C. A. Kolden, N. M. Vaillant, A. T. Hudak, A. M. S. Smith, B. M. Wing, B. S. Kellogg, and J. Kreitler. 2017. Multi-temporal LiDAR and Landsat quantification of fire-induced changes to forest structure. Remote Sensing of Environment 191: 419-432.

Meddens, A. J. H., C. A. Kolden, and J. A. Lutz. 2016. Detecting unburned areas within wildfire perimeters using Landsat and ancillary data across the northwestern United States. Remote Sensing of Environment 186: 275-285.

Meddens, A. J. H., C. A. Kolden, J. A. Lutz, J. T. Abatzoglou, and A. T. Hudak. 2018a.

Spatiotemporal patterns of unburned areas within fire perimeters in the
northwestern United States from 1984 to 2014. Ecosphere 9(2): e02029.

Meddens, A. J. H., C. A. Kolden, J. A. Lutz, A. M. S. Smith, C. A. Cansler, J. T.
Abatzoglou, G. W. Meigs, W. M. Downing, and M. A. Krawchuk. 2018b. Fire
refugia: What are they and why do they matter for global change? BioScience.

Miller, J. D., and A. E. Thode. 2007. Quantifying burn severity in a heterogeneous
landscape with a relative version of the delta Normalized Burn Ration (dNBR).
Remote Sensing of Environment 109: 66-80.

Miller, J. D., and H. Safford. 2012. Trends in wildfire severity: 1984 to 2010 in the Sierra
Nevada, Modoc Plateau, and southern Cascades, California, USA. Fire Ecology 8:
41-57.

North, M., B. Oakley, J. Chen, H. Erickson, A. Gray, A. Izzo, D. Johnson, S. Ma, J.
Marra, M. Meyer, K. Purcell, T. Rambo, D. Rizzo, B. Roath, and T. Schowalter.
2002. Vegetation and Ecological Characteristics of Mixed Conifer and Red Fir
Forests at The Teakettle Experimental Forest. General Technical Report PSW-
GTR-186. Page General Technical Report PSW-GTR-186. U.S. Department of
Agriculture, Forest Service, Pacific Southwest Research Station, Davis,
California, USA.

North, M., P. Stine, K. O. Hara, W. Zielinski, and S. Stephens. 2009. An Ecosystem
Management Strategy for Sierran Mixed- Conifer Forests. PSW-GTR-220. U.S.
Department of Agriculture, Forest Service, Pacific Southwest Research Station,
Davis, California, USA.

Oksanen, J., F. G. Blanchet, R. Kindt, P. Legendre, P. R. Minchin, R. B. O'Hara, G. L.

Simpson, P. Solymos, M. H. H. Stevens, and H. Wagner. 2013. Vegan: community ecology package. Version 2.4-6. http://cran.r-project.org/package=vegan. Downloaded 23 March 2018.

Prism Climate Group. 2017. Climatological normals, 1981-2010. The PRISM Group, Oregon State University, Oregon, USA. http://prism.oregonstate.edu.

R Core Team. 2017. R: A language and environment for statistical computing. Version 3.4.3. R Core Team, R Foundation for Statistical Computing, Vienna, Austria.

Roberts, S. L., J. W. van Wagtendonk, D. A. Kelt, A. K. Miles, and J. A. Lutz. 2008. Modeling the effects of fire severity and spatial complexity on small mammals in Yosemite National Park, California. Fire Ecology 4(2): 83-104.

Robinson, N. M., S. W. J. Leonard, E. G. Ritchie, M. Bassett, E. K. Chia, S. Buckingham, H. Gibb, A. F. Bennett, and M. F. Clarke. 2013. Refuges for fauna in fire-prone landscapes: Their ecological function and importance. Journal of Applied Ecology 50: 1321-1329.

Román-Cuesta, R. M., M. Gracia, and J. Retana. 2009. Factors influencing the formation of unburned forest islands within the perimeter of a large forest fire. Forest Ecology and Management 258: 71-80.

Scholl, A. E., and A. H. Taylor. 2010. Fire regimes, forest change, and self-organization in an old-growth mixed-conifer forest, Yosemite National Park, USA. Ecological Applications 20: 362-380.

Schwilk, D. W., and J. E. Keeley. 2006. The role of fire refugia in the distribution of *Pinus sabiniana* (Pinaceae) in the southern Sierra Nevada. Madroño 53(4): 364-372.

Smith, A. M. S., C. A. Kolden, T. B. Paveglio, M. A. Cochrane, D. M. J. S. Bowman, M. A. Moritz, A. D. Kliskey, L. Alessa, A. T. Hudak, C. M. Hoffman, J. A. Lutz, L. P. Queen, S. J. Goetz, P. E. Higuera, L. Boschetti, M. Flannigan, K. M. Yedinak, A. C. Watts, E. K. Strand, J. W. Van Wagtendonk, J. W. Anderson, B. J. Stocks, and J. T. Abatzoglou. 2016a. The science of firescapes: achieving fire-resilient communities. BioScience 66: 130-146.

Smith, A. M. S., A. M. Sparks, C. A. Kolden, J. T. Abatzoglou, A. F. Talhelm, D. M. Johnson, L. Boschetti, J. A. Lutz, K. G. Apostol, K. M. Yedinak, W. T. Tinkham, and R. J. Kremens. 2016b. Towards a new paradigm in fire severity research using dose-response experiments. International Journal of Wildland Fire 25: 158-166.

Smith, A. M. S., A. F. Talhelm, D. M. Johnson, A. M. Sparks, C. A. Kolden, K. M. Yedinak, K. G. Apostol, W. T. Tinkham, J. T. Abatzoglou, J. A. Lutz, A. S. Davis, K. S. Pregitzer, H. D. Adams, and R. L. Kremens. 2017. Effects of fire radiative energy density dose on *Pinus contorta* and *Larix occidentalis* seedling physiology and mortality. International Journal of Wildland Fire 26: 82-94.

Stavros, E. N., Z. Tane, V. R. Kane, S. Veraverbeke, R. J. McGaughey, J. A. Lutz, and C. Ramirez. 2016. Unprecedented remote sensing data over the King and Rim Megafires in the Sierra Nevada Mountains of California. Ecology 97(11): 3244.

Thode, A. E., J. W. van Wagtendonk, J. D. Miller, and J. F. Quinn. 2011. Quantifying the fire regime distributions for severity in Yosemite National Park, California, USA. International Journal of Wildland Fire 20: 223-239.

Turner, M. G., W. L. Baker, C. J. Peterson, and R. K. Peet. 1998. Factors Influencing

Succession: Lessons from Large, Infrequent Natural Disturbances. Ecosystems 1: 511-523.

Turner, M. G., W. H. Romme, R. H. Gardner, and W. W. Hargrove. 1997. Effects of fire size and pattern on early succession in Yellowstone National Park. Ecological Monographs 67: 411-433.

Van Wagtendonk, J. W. 2007. The history and evolution of wildland fire use. Fire Ecology 3(2): 3-17.

Van Wagtendonk, J. W., and J. A. Lutz. 2007. Fire regime attributes of wildland fires in Yosemite National Park, USA. Fire Ecology 3(2): 34-52.

Van de Water, K. M., and H. D. Safford. 2011. A summary of fire frequency estimates for California vegetation before Euro-American settlement. Fire Ecology 7(3): 26-58.

Westerling, A. L., H. G. Hidalgo, D. R. Cayan, and T. W. Swetnam. 2006. Warming and earlier spring increase western U.S. forest wildfire activity. Science 313: 940-3.

Wilson, M. F. J., B. O'Connell, C. Brown, J. C. Guinan, and A. J. Grehan. 2007. Multiscale terrain analysis of multibeam bathymetry data for habitat mapping on the continental slope. Marine Geodesy 30(1-2): 3-35.

Wohlgemuth, P. M., K. Hubbert, and M. J. Arbaugh. 2006. Fire and Physical Environment Interactions. Pages 75-93 in N. G. Sugihara, J. W. van Wagtendonk, K. E. Shaffer, J. Fites-Kaufman, A. E. Thode, editors. Fire in California's Ecosystems. University of California Press, Berkeley, California.

Zaitsev, A. S., K. B. Gongalsky, T. Persson, and J. Bengtsson. 2014. Connectivity of

litter islands remaining after a fire and unburnt forest determines the recovery of

soil fauna. Applied Soil Ecology 83: 101-108.

CHAPTER 3

FOREST STRUCTURE PREDICTIVE OF FISHER (*PEKANIA PENNANTI*) DENS

EXISTS IN RECENTLY BURNED FOREST IN YOSEMITE, CALIFORNIA

ABSTRACT

A challenge that managers face is how to balance conservation of fisher (*Pekania pennanti*) habitat with the reintroduction of fire in the Sierra Nevada. The fisher population in the south Sierra is of high conservation priority, due to its small population size, genetic isolation, and the risk of habitat loss due to burning and fuel reduction activities. To examine the effect of fire on fisher habitat, I modeled habitat requirements surrounding den sites in the Sierra National Forest, and then assessed whether those characteristics existed in nearby forests (in Yosemite National Park) that had recently burned (after 1984). I developed random forest and logistic regression models using lidar-derived forest structure metrics to distinguish fisher den presence (*n=261*) from randomly-generated "available" points (*n=261*) within an estimate of the female population home range. The full logistic regression model correctly classified (under cross-validation) 69.5% of observations and the random forest model correctly classified 74.3%. The parsimonious logistic regression model I selected had comparable accuracy to the full model (correctly classified 68.8% of observations) and included the following variables: cover >2 m, 95th percentile height, and 25th percentile height. Partial dependence plots suggest thresholds at which predicted probability exceeds 50%: cover >2 m greater than 60%, 95th percentile height of at least 32 m, and 25th percentile height between 4m and 14 m. I found that suitable thresholds of forest cover and tree height

exist in burned areas in Yosemite; 43.0% of burned pixels had a high predicted

probability of den presence (probability ≥0.5). Areas with a high predicted probability of

den presence occurred within a range of fire severities and years since the most recent

fire, and particularly in low-severity fire conditions (mean differenced normalized burn

ratio [dNBR] value: 128.4). These results are promising for land managers that face the

challenge of reducing the risk of high-severity fire and conserving fisher habitat, however

more research is needed to conclude whether suitable fisher habitat can exist in burned

areas at all scales of selection and for all activities and demographics of the fisher

population.

1. Introduction

Understanding habitat requirements is essential for the conservation of wildlife

species, particularly for threatened populations that face extirpation. In the dry, fire-prone

forests of California, maintaining suitable habitat for threatened wildlife is complicated

by the need to simultaneously manage for the reintroduction of fire. The period of fire

suppression that took place throughout the 20th century (van Wagtendonk, 2007) has

caused increased woody fuel accumulations in the Sierra Nevada (Parsons and

DeBenedetti, 1979) that increase the risk of high-severity fire. The fisher (*Pekania*

pennanti) population in the south Sierra Nevada is of special concern to land managers

because of the potential for habitat loss due to fire (California Department of Fish and

Wildlife, 2015). In order to manage the forests in the Sierra Nevada for both a restored

fire regime and the preservation of the fisher population, we need to understand how fire

changes forest structure over time and when or how post-fire landscapes are suitable

habitat for fishers.

The fisher is a medium-sized mustelid with a historical range throughout the mixed-coniferous forests of the Sierra Nevada and Cascade mountains, the northern Rockies, the northeastern Unites States, and the boreal forests of Canada (Williams et al., 2007). Since European settlement, fisher populations in North America have declined due to human causes including trapping, logging, and habitat fragmentation (Aubry and Lewis, 2003). In California there are two remaining, native geographically separate fisher populations, one in the state's northern extent and one in the southern Sierra Nevada mountains. The southern Sierra Nevada population is estimated at only a few hundred individuals (Spencer et al., 2011), and is therefore of high conservation priority.

Fishers are associated with late-successional, mixed-conifer forests with high canopy cover and complex forest structure (Ruggiero et al., 1994; Purcell et al., 2009; Raley et al., 2012). Structurally complex forests include a variety of dead woody components (e.g. snags, logs, live trees with dead leaders), which fishers use as denning cavities and rest structures (Purcell et al., 2009; Zhao et al., 2012; Aubry et al., 2003). Three-dimensional complexity in forests creates light gaps and variation in understory vegetation, which creates microhabitats for a variety of species that fishers prey on. The home range of the fisher is large relative to its body size (Buskirk and Powell, 1994), and they occupy areas with spatially connected forest (Raley et al., 2012; Sauder and Rachlow, 2014; Sauder and Rachlow, 2015).

The impact of fire on fisher habitat is complex, with the potential for both positive and negative outcomes (U.S. Fish and Wildlife Service, 2016). The maintenance or destruction of fisher habitat components is tied to fire severity, spatial pattern, and time.

High-severity fire can significantly alter forest structure and poses a threat to fisher habitat by consuming critical dead woody components, reducing vegetative cover, and decreasing habitat connectivity (Spencer et al., 2011). Mixed-severity fire may destroy habitat elements in high-severity patches, but can also increase hardwood regeneration (commonly used as den structures; Halofsky et al., 2011) and may contribute to increased prey abundance where burn heterogeneity creates canopy openings and habitat edges (Franklin et al., 2000, Roberts et al., 2015). Low-severity fire can scorch understory vegetation and decrease habitat quality in the short term, while creating more snags, fire scars, and dead leaders on live trees that fishers could inhabit in the future (Weir et al., 2012). Further, Truex and Zielinski (2013) found that seasonal timing of a burn has implications for preservation of predicted rest habitat, with no difference between early season prescribed burns and untreated sites. Hanson (2013) found that fishers use burned areas after a decade of vegetative recovery, highlighting that time since fire is another important factor in post-fire habitat quality.

In this study, I explored the use of lidar-derived metrics to characterize forest structure surrounding fisher dens in the Sierra National Forest and predicted den habitat in burned areas in Yosemite National Park. Lidar data products estimate horizontal (e.g., cover at different forest strata) and vertical (e.g., heights of tree clusters) aspects of forest structure, and many have utilized lidar-derived metrics to characterize habitat of species with structural requirements (Vierling et al., 2008; Zhao et al., 2012; North et al., 2017). I chose to analyze the forest surrounding den sites, as fishers are highly selective when choosing dens and these structures are one of the most limiting habitat elements necessary for maintaining the population (Zielinski et al., 2004a). Our research objectives

were to: 1) identify variables most predictive of fisher dens, and 2) relate those variables to fire severity and time since fire.

2. Methods

2.1 Study area

The study area has two components: the Dinkey study area (Dinkey) in Sierra National Forest, California, and the Yosemite study area (Yosemite) in Yosemite National Park, California. Dinkey includes contemporaneous lidar and extensive fisher presence data, but has remained largely fire-suppressed, with few fires since 1984. Yosemite has been structurally characterized with lidar (Kane et al., 2013), has experienced approximately 170 fires $\geq$ 40 ha since 1984 (Lutz et al., 2011), but is not currently inhabited by fishers. The study areas are spatially defined by the extent of the lidar acquisitions (Fig. 3.1).

Dinkey is located in the Dinkey watershed of the Sierra National Forest in California (Fig. 3.1). The study area consists of approximately 43,093 ha of forested land, ranging in elevation from 390 m to 2962 m. The dominant forest types (from low to high elevation) are ponderosa pine-mixed conifer, white fir-mixed conifer, red fir, and lodgepole pine (Fites-Kaufman et al., 2007). The dominant California Wildlife Habitat Relationships (CWHR) habitat types are Sierran mixed conifer, ponderosa pine, red fir, and montane hardwood-conifer (Mayer and Laudenslayer, 1988). The climate is Mediterranean with hot, dry summers and cool, wet winters. Between 1971 and 2010 the annual mean minimum and maximum temperatures were 5° C and 17° C, respectively;
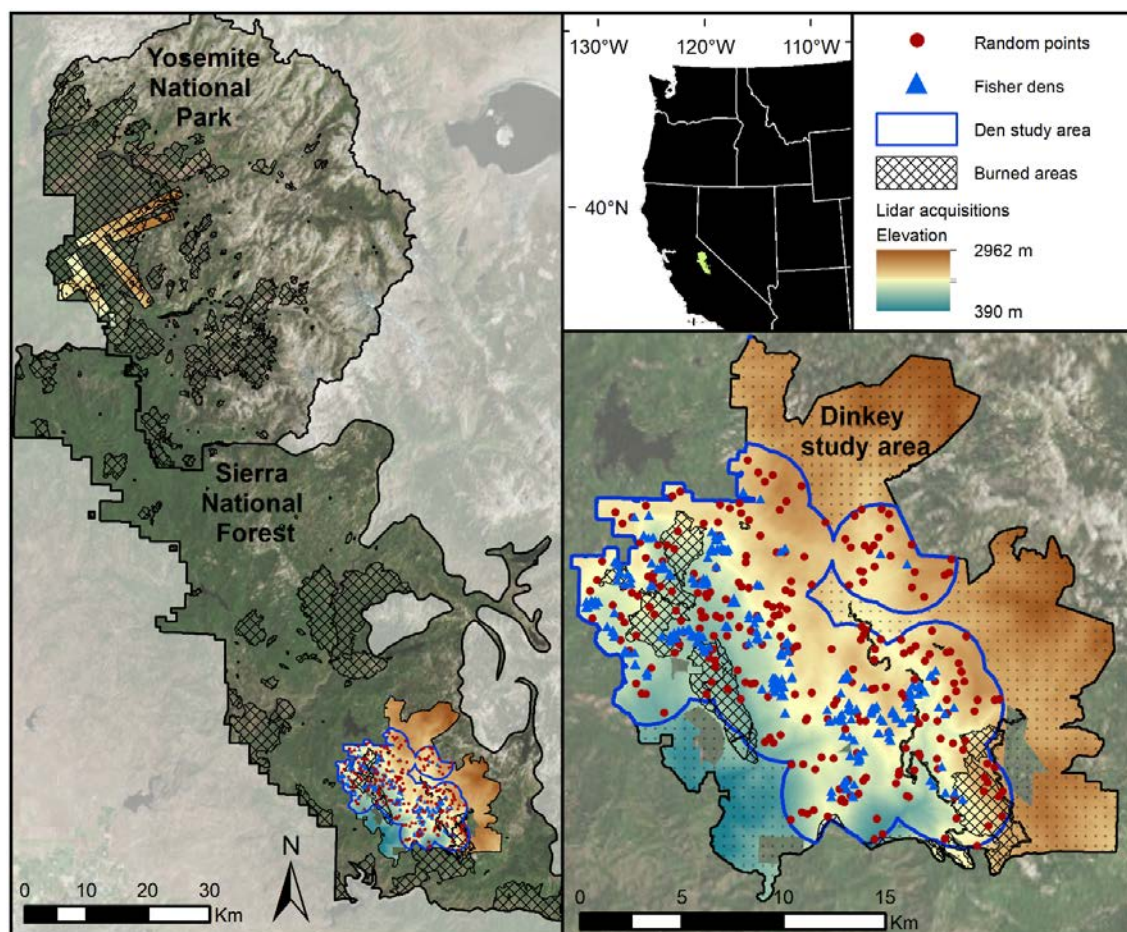
Fig. 3.1. Location of Yosemite National Park and Sierra National Forest within California (inset). The Yosemite study area is within the lidar acquisition footprint in Yosemite National Park. The Dinkey study area is within the lidar acquisition footprint in the Sierra National Forest and includes all fisher den locations. Burned areas include all fires ≥400 ha that have occurred since 1984, as well all prescribed burns (typically <400 ha) that occurred in the Dinkey study area during that period. The fisher dens that overlap with the Dinkey lidar footprint are displayed, as well as the corresponding randomly generated 'available' points used to build the predictive models. The den study area is an estimation of the areas available to the female population based on kernel utilization distributions (KUD); all random points were generated within the den study area.

annual precipitation was 1038 mm with most precipitation falling as snow between

January and March (Prism Climate Group, 2018).

Yosemite National Park borders the northern extent of the Sierra National Forest

in the central Sierra Nevada mountains of California (Fig. 3.1). The study area includes

approximately 11,186 ha of predominantly white fir-mixed conifer to red fir forest
(Keeler-Wolf et al., 2012) and ranges in elevation from 1277 m to 2543 m. The principal
CWHR habitat types are Sierran mixed conifer, Jeffery pine, red fir, and montane
hardwood-conifer. Between 1971 and 2010 the annual mean minimum and maximum
temperatures were 3° C and 16° C; annual precipitation was 1135 mm, primarily
occurring between January and March (Prism Climate Group, 2018).

2.2 Field methods

The Kings River Fisher Project conducted extensive trapping and telemetry-based
monitoring of male and female fishers from 2007 to 2016 (methods detailed in Thompson
et al., 2010). Traps were installed in the most suitable habitat along a 1-km^2 grid. Fishers
that were captured were given a radio collar, released, and monitored with remote
triangulation, walk-ins, and aerial telemetry (Thompson et al., 2010). During denning
season (March through July) female fishers were heavily monitored to identify den trees
and structures (e.g. snags, logs, cavities). Any tree or structure used by a female ≥3 times
was designated as a den. Structures identified as natal dens (place of birth) were used by
females for three consecutive days. Motion-sensor digital cameras were placed around
the natal dens to monitor continued occupancy or evidence of relocation to a maternal
den, defined as structures used by females and dependent kits subsequent to the natal den
(Thompson et al., 2010). Once dens were confirmed in the field their coordinates were
documented by a Garmin 60CSx GPS (estimated accuracy <10 m).

2.3 Ancillary data

Lidar data were collected using dual mounted Leica ALS50 Phase II laser

instruments at four returns per pulse (Kane et al., 2015). Approximately half of the Dinkey project data were acquired (24,012 ha) on October 16th 2010; the second data acquisition (25,171 ha) occurred on 21-27 November 2012. In the overlapping area between the two Dinkey lidar acquisitions (25171 ha), I used the 2012 data. In Yosemite National Park data were collected on 21 and 22 July 2010.

The metrics used to describe the fire histories of predicted den habitat in Yosemite were derived from the fire atlas assembled by Lutz et al. (2011). The fire atlas includes the burn boundaries and 30 m differenced normalized burn ratio (dNBR; a measure of burn severity) values for all fires ≥40 ha that occurred in the Yosemite study area between 1984 and 2010.

2.4 Modeling of fisher denning habitat

To determine if aspects of topography and forest structure could predict fisher den preference, I applied two modeling approaches: logistic regression with weights (glm function; R Core Team, 2018) and random forest (Breiman, 2001; Liaw and Wiener, 2002; randomForest package version 4.6-12). The logistic regression model is widely used in binary response habitat modeling studies (Manly et al., 2002), and the model coefficients and significance values allow for the effect of the variables on response prediction to be readily interpreted. The random forest machine-learning algorithm is a non-parametric classification technique that has been shown to produce high prediction accuracy in species distribution modeling and is well suited to handle non-linear predictor variables (Cutler et al., 2007). I applied both statistical methods on the same set of model variables and compared accuracy and relative variable importance to determine the

parsimonious set of variables most predictive of fisher den use. Individual fishers were weighted equally in the logistic regression models to address the range in the number of dens occupied by each animal (dens per animal ranged from 1 to 31) and to prevent individual idiosyncratic behavior from over-influencing model fit.

2.4.1 Model variables

The response variable was a binary used-available classifier, with fisher use observations composed of female den locations sampled from 2008 to 2015 within the Dinkey lidar acquisition layer. I randomly generated an equal number of available points (i.e., assumed unused) within an estimate of the female population home range (hereafter, den study area). To delineate the den study area (Fig. 3.1), I buffered all den sites to reflect the average kernel utilization distribution (KUD) for the subset of the population with ≥20 locations (telemetry points, rest sites, and dens) and an estimated error polygon <5 m^2. The KUDs were calculated using the adehabitatHR package version 0.4.15 (Fig. B.1; Calenge, 2011). Randomly generated available points were excluded from pixels occupied by den sites.

The model predictor variables were a selection of lidar-derived forest structure metrics and relevant landscape features hypothesized to influence den selection (Table 3.1). I calculated the minimum Euclidean distance to a road or water source using a comprehensive roads layer from the US Forest Service and the water sources provided by the National Hydrology Database. Slope and solar incidence were calculated with the 2013 USGS 1/3 arc second (10 m) digital elevation model (DEM). I used the solar radiation toolset in ArcGIS version 10.5.1 (ESRI, 2011) and the USGS DEM to calculate

Table 3.1

Predictors for models developed with random forest and logistic regression. The model response was a binary classification of fisher den used or available sites. The abiotic model variables were derived from the US Forest Service Roads layer, the US Geological Survey 10 m digital elevation model (DEM), the National Hydrology Database (NHD). The model predictors relating to forest structure were developed with lidar data collected and processed by Kane et al., (2018).

Variable	Description	Units	Source
Abiotic factors			
Distance to road	Minimum distance to road	Meters	USFS
Distance to water	Minimum distance to water source	Meters	NHD
Slope	Steepness of terrain	Degrees	DEM
Solar radiation	Total amount of solar energy hitting pixel surface	WH/m^2	DEM
Biotic factors			
Average elevation	Average tree height	Meters	Kane et al., 2018
Canopy rumple	Crown surface roughness	Ratio	Kane et al., 2018
Cover >2 m	Cover of lidar returns greater than 2 m in height	Percent	Kane et al., 2018
Cover 2-16 m	Cover occupied by vegetation 2-16 m in height	Percent	Kane et al., 2018
Cover 16-32 m	Cover occupied by vegetation 16-32 m in height	Percent	Kane et al., 2018
Cover >32 m	Cover occupied by vegetation >32 m in height	Percent	Kane et al., 2018
P25 height	25th percentile height, a measure of understory height	Meters	Kane et al., 2018
P95 height	95th percentile height, a measure of the tallest tree in the cell	Meters	Kane et al., 2018

solar incidence on the days the lidar data were acquired. Lidar data were processed as 30 m × 30 m pixels using Fusion software version 3.2 into three types of metrics: measure of vegetation height, cover, and canopy complexity. Stand height was calculated as an average pixel value, and as percentile heights (m) of first lidar returns. To determine cover, the lidar point cloud was divided into strata with breakpoints at 2, 4, 8, 16, 32, and >32 m; percent cover was then calculated by stratum as the percentage of returns over total returns (Kane et al., 2015). Rumple, a measure of variation in the height of the canopy, was generated with 1-m cell maximum return heights.

To assess den habitat preferences at multiple scales, I developed models at three scales: 30 m, 90 m, and 150 m. Model predictors at the 30-m scale were extracted from the pixel occupied by the den or random points. Predictors at the 90-m and 150-m scales were calculated as the average value of the 9-cell and 25-cell neighborhoods, respectively, surrounding and including the focal pixel.

2.4.2 Model selection and accuracy

I developed two sets of predictor variables to avoid collinearity and overfitting. The "height set" included all variables in Table 3.1 except for cover 2-8 m, cover 8-16 m, cover 16-32 m, and cover >32 m; the "cover set" omitted average height and 25th percentile height. I compared the global model of both sets, using Akaike's information criterion (AIC) for the logistic regression models and the out-of-bag (OOB) error rate for random forest and selected the height set to proceed with model selection.

To select the parsimonious logistic regression predictor set I developed 21 *a priori* candidate models based on variable importance suggested by exploratory analyses and known associations from the fisher habitat literature (Burnham and Anderson, 2002). I used logistic regression without weights to compare candidate models, as the use of weights required a quasi-likelihood framework (therefore I could not compute AIC); coefficient values, variable significance, and accuracy metrics (listed in Table 3.2) were very similar with or without the application of weights. I selected the model with the least number of variables and an AIC difference from the lowest AIC (ΔAIC) of $\leq$4.

I computed accuracy metrics by resubstitution and 10-fold cross validation for all models. The accuracy metrics used were: percent of rows correctly classified (PCC),

sensitivity (true positive rate), specificity (true negative rate), kappa (a measure that accounts for the correct classification rate expected by chance), and the area under the curve (AUC; a threshold-independent combined measure of sensitivity and specificity). Kappa has been critiqued for its dependence on species prevalence (Allouche et al., 2006), therefore I calculated an equivalent measure independent of prevalence, the true skill statistic (TSS), but did not report it as all TSS values were identical to kappa. The threshold for classification of model predictions was based on the distribution of predicted values (optimal.thresholds function; Freeman and Moisen, 2008).

2.5 Relating fisher den preferences to fire metrics

For each burned 30 m pixel in the Yosemite study area (*n*=85805) I calculated the most recent dNBR value, the number of years since fire, and the number of fires that occurred between 1984 and 2010. For each pixel I extracted values for the three forest structure metrics found to be most predictive of fisher dens: cover >2 m, 95th percentile height, and 25th percentile height. To ensure that lidar-derived metrics reflected surface conditions, I dropped all pixels that burned in 2010 from the analysis.

I examined individual lidar layers, as well as a composite measure of the layers identified by the logistic regression model I selected, in relation to fire metrics. The composite measure was derived by using the parsimonious model object (Table 3.3) to predict probability of presence values for the same combination of predictors in Yosemite ('predict' function in R, R Core Team, 2018). I used a threshold of 0.5 to categorize areas by low or high probability of den presence. For figures with panels featuring different groups (e.g., low and high probability, periods of years since fire), I analyzed random

subsets with an equal total number of observations in order to visualize relative differences in data distribution and to avoid overplotting. To test for significance in the time since fire between areas with high and low den probabilities, I used a linear regression model with time since fire as the response ('glm' function; R Core Team, 2018).

2.5.1 Fire and configuration of lidar-derived structure classes

To assess the importance of variable configuration and connectivity in the habitat suitability of burned forest, I examined the relationship between den probability and the proportion of neighboring pixels occupied by a composite forest structure variable within 90 m and 150 m forest neighborhoods in Yosemite. I developed 8 structure classes from the predictors selected in the parsimonious logistic regression model using hierarchical cluster analysis of a random sample of 30,000 cells in the Dinkey and Yosemite study areas. My methods followed those described in North et al., 2018. I used logistic regression to identify the structure classes with a positive association ($P < 0.05$) with fisher dens in Dinkey, and to calculate the predicted probability of fisher den presence in Yosemite. The model predictor variables were the proportion of the 9-cell and 25-cell neighborhoods surrounding a den or random point occupied by each structure class. I selected individual structure classes to examine in more detail based on model variable significance, and the number of non-zero observations in burned areas in Yosemite with a high probability of den presence. I used a general linearized model to assess the relationship between den probability and structure class proportion (glm function, R Core Team 2018).

3. Results

There were 261 dens within the footprint of the Dinkey lidar acquisition, occupied by 40 individual females. There were 30 females with ≥20 locations, with an average KUD size of 18.6 km^2 (Fig. B.1). There were 23 dens that occurred in previously burned forest, 18 of which were established in the 2006 SOS6 fire footprint. Between 1984 and 2016, 16.2% (6980.4 ha) of the Dinkey study area had burned, the majority in <400 ha prescribed burns. From 1984 to 2010, 82.5% (9223.8 ha) of the Yosemite study area burned at least once, predominantly in >400 ha wildfires.

3.1 Structural characteristics predictive of fisher dens

There were slight increases in model accuracy as the scale of the predictor variables increased from 30 m, to 90 m and 150 m (Table 3.2). The scales that included neighboring pixels surrounding the focal pixel (90 m, 150 m) had higher kappa and AUC relative to the 30 m models (increases of 0.02-0.06), as well as higher overall correct classification rates. Because differences were slight and variable importance was consistent across scales (Table B.1), I will present den habitat modeling results for the 30-m scale, as this best aligns with the scale at which the lidar, DEM, and Landsat-derived burn severity datasets were processed.

Logistic regression identified four variables that had a significant ($P<0.05$) association with fisher den presence (ordered by relative effect size): cover >2 m, 95th percentile height, 25th percentile height, and slope (Table 3.3). The parsimonious model I selected omitted slope and had no appreciable difference in accuracy metrics relative to the full model (Table 3.3). The full model correctly classified 69.5% of observations as

Table 3.2
Accuracy metrics for the logistic regression and random forest models at three scales: 30 m, 90 m, and 150 m. To assess model accuracy, metrics were computed by resubstitution ("Resub") and 10-fold cross-validation ("X-val"). Percent Correct Classification (PCC) is the percent of rows correctly predicted by the model, while sensitivity and specificity examine the percent of presence and absence responses correctly predicted, respectively. Cohen's kappa is a measure of overall model accuracy corrected for the accuracy of predictions expected by random chance. The area under the curve (AUC), a threshold-independent measure of predictive accuracy, is the area under the ROC specificity and sensitivity curve.

| | Model scale | | | | | |
| | 30 m | | 90 m | | 150 m | |
Accuracy metric	Resub	X-val	Resub	X-val	Resub	X-val
Logistic regression						
PCC	70.9	69.5	73.0	71.7	73.0	72.2
Sensitivity	75.1	79.3	84.3	90.4	84.3	83.1
Specificity	66.7	59.8	61.7	52.9	61.7	61.3
Kappa	0.42	0.39	0.46	0.43	0.46	0.44
AUC	0.77	0.75	0.79	0.78	0.79	0.78
Random forest						
PCC	73.6	74.3	76.2	76.1	78.2	76.3
Sensitivity	71.3	72.4	85.8	86.6	85.8	82.8
Specificity	75.9	76.3	66.7	65.5	70.5	69.7
Kappa	0.47	0.49	0.52	0.52	0.56	0.52
AUC	0.80	0.80	0.82	0.82	0.83	0.83

dens (AUC: 0.75), and was more skilled at predicting true positives (sensitivity: 79.3%) than true negatives (specificity 59.8%). Kappa indicated fair agreement (k: 0.39), suggesting some correctly classified rows may be due to chance.

Cover >2 m, 95th percentile height, and 25th percentile height ranked highest in random forest variable importance plots as well, but tended to include canopy rumple amongst the four most important variables rather than slope (Fig. B.3). Model accuracy was higher relative to the logistic regression model, with 74.3% of observations correctly classified, equal skill with true positives and negatives (sensitivity: 72.%, specificity: 76.3%), an AUC of 0.8, and moderate agreement suggested by kappa (k: 0.49). I draw

Table 3.3
Coefficients and *P*-values for two sets of logistic regression models at the 30-m scale.
The full model includes all variables from the height group (see methods for variable
grouping). The parsimonious model contains the three most predictive variables from the
full model, and represents the least number of variables with little appreciable change in
AIC (ΔAIC ≤4) or accuracy metrics. All continuous variables were standardized before
model fit, therefore coefficients may be interpreted as ranked by relative effect size. *P*-
values ≤0.05 are bolded.

| Full model | | | | | |
Variable	Coefficient	*P*-value	Accuracy metric	Resub	X-val
β_0	-0.0644	0.541	PCC	70.9	69.5
Cover >2 m	0.9405	**<0.001**	Sensitivity	75.1	79.3
Canopy rumple	0.1447	0.350	Specificity	66.7	59.8
P95 height	0.7034	**<0.001**	Kappa	0.42	0.39
P25 height	-0.4581	**0.001**	AUC	0.77	0.75
Slope	0.2801	**0.013**			
Solar	-0.1842	0.097			
Stream dist.	-0.1256	0.246			
Road dist.	-0.2162	0.078			

| Parsimonious model | | | | | |
Variable	Coefficient	*P*-value	Accuracy metric	Resub	X-val
β_0	-0.05998	0.548	PCC	69.9	68.8
Cover >2 m	0.97463	**<0.001**	Sensitivity	76.2	71.7
P95 height	0.78115	**<0.001**	Specificity	63.6	65.9
P25 height	-0.41460	**0.001**	Kappa	0.40	0.38
			AUC	0.76	0.75

two main points from the partial dependence plots of the top variables (Fig. 3.2). First,

the plots indicate thresholds at which the predicted probability of den presence exceeds

50%. Fisher den probability is high (≥0.5) when cover >2 m is greater than 60%, 95th

percentile tree height is greater than 32 m, 25th percentile heights are between 4 m and 14

m, and canopy rumple is between 2.75 and 5.1. Second, the plots suggest that while cover

>2 m and 95th percentile height have an approximately linear relationship with den

probability, 25th percentile height and canopy rumple are somewhat non-linear. The

random forest algorithm does not assume linearity between the predictor and the response
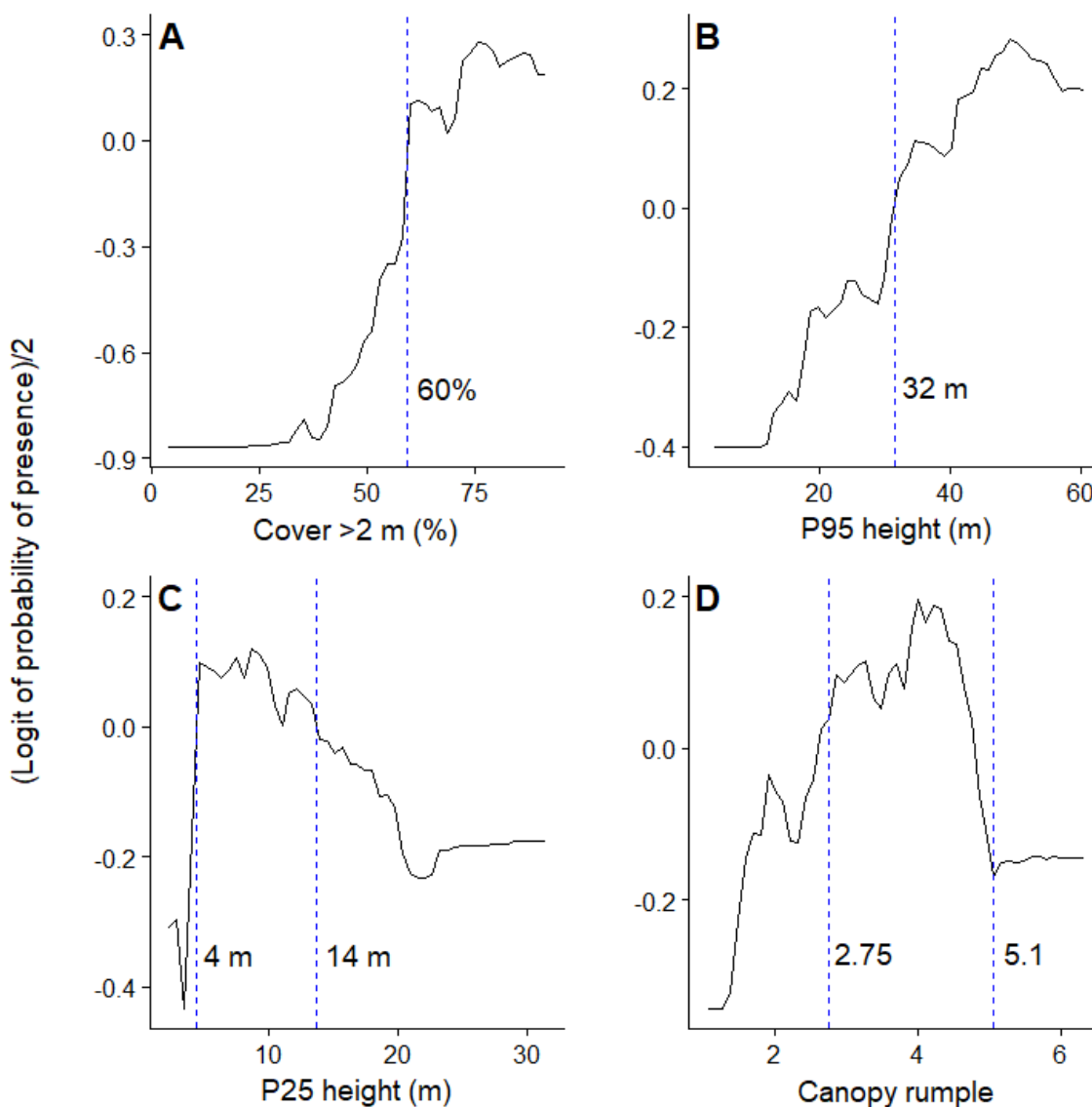
Fig. 3.2. Partial dependence plots for the most influential variables in the 30 m random forest model. Partial dependence plots help to visualize the relationship between a particular variable and the probability of response presence. Cover >2 m (A) is the proportion of a pixel occupied by vegetation taller than 2 m. P95 height (B) and P25 height (C) are the 95th and 25th percentile heights of first lidar returns, and can be interpreted as a measure of dominant tree height and understory height. Canopy rumple (D) is a measure of crown surface complexity. The y-axis is half the logit of the probability of presence, where values of -3 and 3 represent a 0% to 100% probability of den presence. The dashed vertical lines indicate predictor variable threshold values that contribute to >50% probability of den presence.

variables, which may explain the slight gains in model accuracy.

3.2.1 Preferred den structure and fire metrics at the 30-m scale

Of the burned pixels in the Yosemite study, 57.0% consisted of forest structure with a low predicted probability of den presence (probability <0.5), and 43.0% of pixels had a high predicted probability (probability ≥0.5; Fig. 3.3). Pixels with a high den probability largely burned at low severity, with a mean dNBR value of 128.4 and 1st and

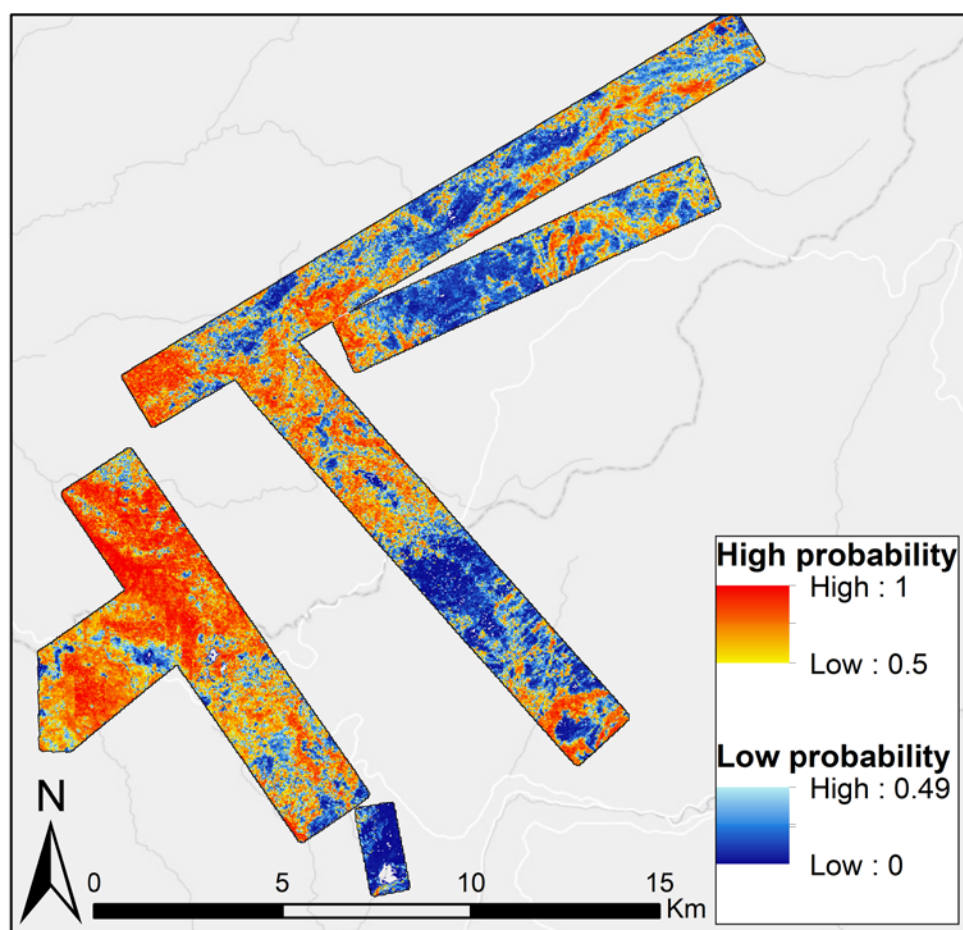**Fig. 3.3.** The footprint of the lidar acquisition in the Yosemite study area, colored by the predicted probability of fisher den presence. Areas with a high probability of den presence (≥0.5) are represented by shades of red, and shades of blue correspond to low den probability. Probabilities were derived from logistic regression models using the predictors: cover >2 m, 95th percentile height, and 25th percentile height.

3rd quantiles at 52.7 and 175.2. Areas with a low den probability largely burned at moderate severity, with a mean dNBR value of 250.0 and 1st and 3rd quantiles at 85.5 and 356.6. The dNBR distributions between high and low probability areas differed in two key ways (Figs. 3.4A, 3.4B). First, the low probability histogram was right-skewed by more high severity fire. High severity values (dNBR >366; Miller and Thode, 2007) constituted 23.8% of low probability areas but only 4.2% of high probability areas. Second, the proportion of lower severity fire in high probability areas was 57.7% greater than that of low probability areas. Low and unchanged fire severity values (dNBR <177; Miller and Thode, 2007) constituted 75.2% and 47.7% of high and low probability areas, respectively.

The distribution of years since fire for high and low probability areas largely overlapped (Fig. 3.4C, 3.4D), with diverging peaks that roughly reflect the occurrence of large fires. The most prominent low probability peaks occurred at 7 years and 20 years since fire, a result of the 2003 Kibbie Complex and 1990 A-Rock wildfires, both of which contained large high severity patches. The average time since the last fire was 10.6 years in high probability areas (n=36,916), and 11.2 years in low probability areas (n=48,889). The small difference in average time since fire was highly significant (P<0.001), though this was likely an effect of the large sample sizes.

Burned areas with a high predicted probability of den presence included a range of canopy cover and height values (Table 3.4). Cover >2 m, an estimate of canopy cover, had a mean of 59.7% and a median 60.3%, with 1st and 3rd quantiles at 51.7% and 68.6%.
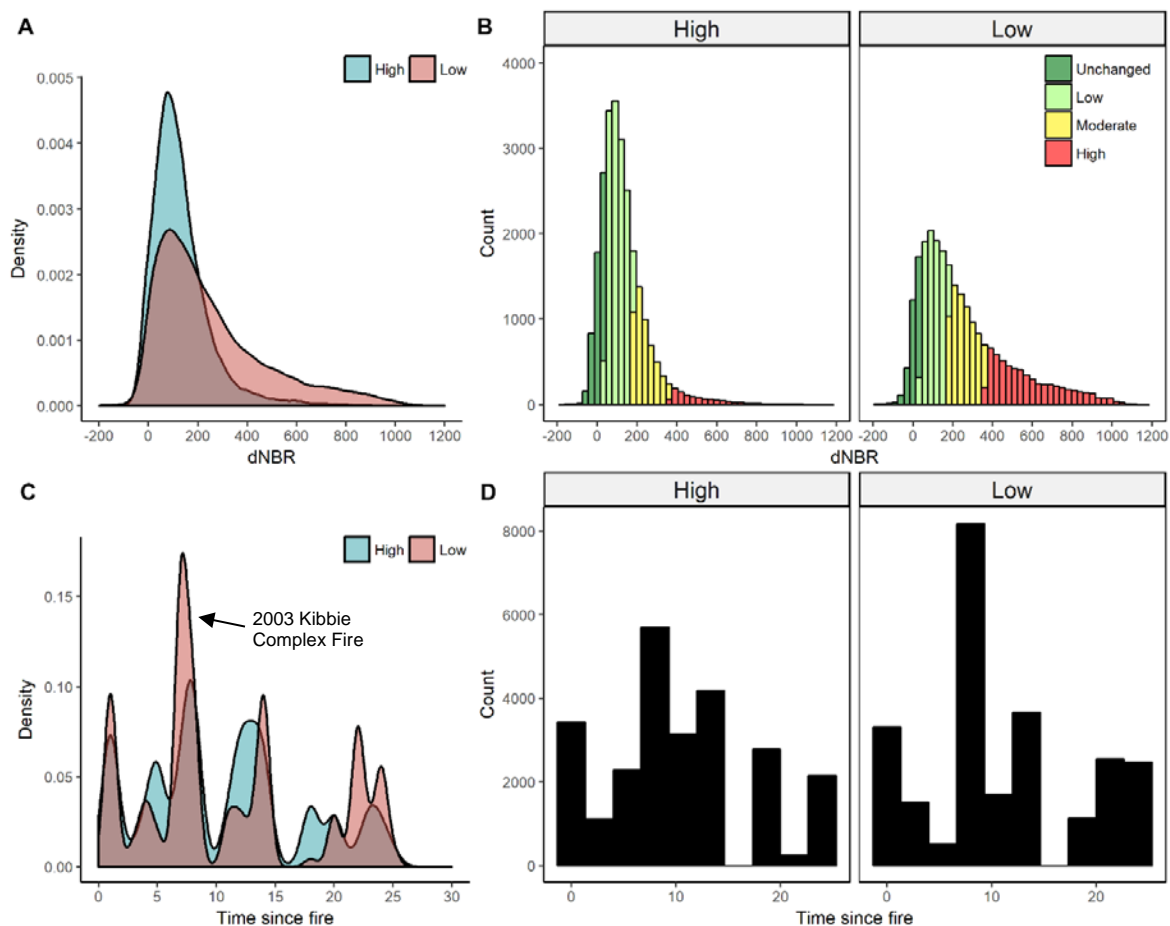
Fig. 3.4. Density plots (A,C) and histograms (B,D) of the portions of the Yosemite lidar acquisition that burned at least once between 1984 and 2010. Panel B compares the distribution of differenced normalized burn ratio (dNBR) pixels by predicted probability of den presence (High: ≥0.5, Low: <0.5). Pixels with forest structure predictive of fisher dens tended to burn at low severity (1st quantile: 52.6, 3rd quantile: 174.6), while pixels with a low predicted probability of presence tended to burn from low to high severity (1st quantile: 85.5, 3rd quantile: 353.6). Burn severity categories are based on thresholds from Miller and Thode (2007): unchanged, ≤40; low, 41-176; moderate, 177-366; high, ≥ 367. Panel D compares the distribution of years since fire for observations categorized as either high or low predicted probability of den presence, where each value represents the number of years since 2010 (e.g. 5 years since fire refers to fires that occurred in 2005). The time since fire density plot can roughly be interpreted as the timelines of low and high severity fires over the 25-year period, as forest structure predictive of den habitat tends to occur under lower severity conditions. For example, the peak at 7 years since fire refers to the 2003 Kibbie Complex Tuolumne fire, a wildfire with some large high severity patches.

Table 3.4
Summary metrics for burned pixels in the Yosemite study area with a high predicted probability of den presence. Each measure of forest structure (cover >2 m, 95th percentile height, 25th percentile height) is summarized for the study area, and by burn severity category represented by binned differenced normalized burn ratio (dNBR) values. Burn severity categories are based on thresholds from Miller and Thode (2007): unchanged, ≤40; low, 41-176; moderate, 177-366; high, ≥ 367.

	All burned areas	Burn severity (dNBR)			
		Unchanged	Low	Moderate	High
Cover >2 m (%)					
Mean	59.7	65.2	60.7	54.8	45.4
Min	3.3	20.4	19.4	10.9	3.3
25th percentile	51.7	57.1	53.1	47.4	36.5
50th percentile	60.3	66.1	61.2	55.2	47.4
75th percentile	68.6	74.2	68.8	63.0	56.1
Max	100.0	100.0	100.0	90.7	80.3
Standard dev.	12.3	11.6	11.1	11.5	14.5
95th percentile height (m)					
Mean	42.9	40.7	43.0	43.7	46.8
Min	5.1	12.7	9.6	5.1	10.6
25th percentile	36.7	34.3	37.1	37.7	41.3
50th percentile	43.4	40.6	43.6	44.7	47.7
75th percentile	49.4	46.9	49.4	50.5	53.4
Max	75.0	75	74.2	67.3	70.7
Standard dev.	8.9	8.7	8.6	9.1	9.5
25th percentile height (m)					
Mean	15.2	13.4	15.8	15.7	13.8
Min	2.2	2.3	2.3	2.2	2.2
25th percentile	10.7	9.3	11.6	10.8	5.3
50th percentile	14.8	12.6	15.4	15.2	14.0
75th percentile	15.2	16.7	19.6	20.0	19.9
Max	55.1	39.7	55.1	41.9	43.5
Standard dev.	6.2	5.3	5.9	6.8	8.5

The 95th percentile height, roughly the dominant tree height, had mean and median values of 42.9 m and 43.4 m, with 1st and 3rd quantiles at 36.7 m and 49.4 m. The 25th percentile height, an approximation of understory height, had a mean of 15.2 m, a median of 14.8 m, and 1st and 3rd quantiles of 10.7 m and 19.1 m.

3.2.2 Configuration of preferred structure classes at 90-m and 150-m scales

Hierarchical cluster analysis of 30,000 random samples separated cover >2 m, 95th percentile height, and 25th percentile height into 8 structure classes. Cover >2 m had a positive relationship with structure class (mean$_{SC1}$: 12.0%, mean$_{SC8}$: 73.0%), while 95th and 25th percentile heights varied by structure class (Fig. 3.5). Logistic regression
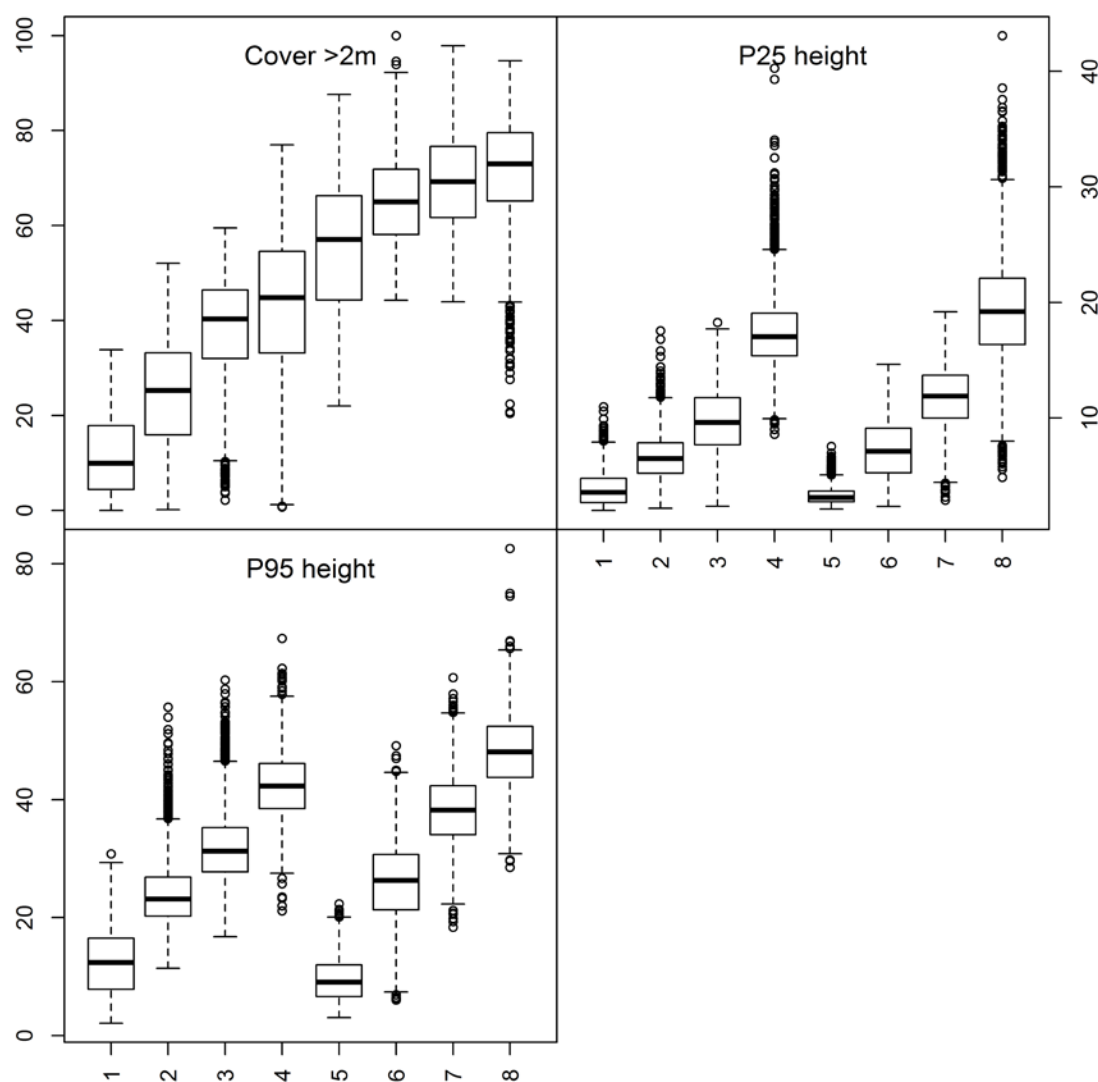

Fig. 3.5. Box plots of the 8 lidar-derived forest structure classes separated with hierarchical cluster analysis. Each forest structure class represents different ranges of cover >2 m, 95th percentile height, and 25th percentile height.

models built with structure classes had comparable but slightly lower accuracy relative to the models with continuous predictors (Table B.2). The 90-m and 150-m models had similar correct classification rates (70.7% and 71.3% of observations, respectively) and AUC values (90-m: 0.76, 150-m: 0.78), but differed in sensitivity (90-m: 90.8%, 150-m: 67.8%) and specificity (90-m: 50.6%, 150-m: 74.7%). Structure classes 6, 7, and 8 had positive associations ($P < 0.05$) with fisher dens at both scales.

Forest structure classes 7 and 8 constituted the majority of burned areas with a high probability of fisher den presence, most often representing a high proportion of each 9-pixel or 25-pixel unit (Fig. 3.6). Structure classes 7 and 8 describe forests in later stages of development, with mean cover, 95th percentile height, and 25th percentile height values above or within the suitable den habitat thresholds identified with random forest models (Fig. 3.2, Fig. 3.6). At the 90-m scale, 88.2% of the 9-pixel units contained a non-zero proportion of structure class 7, and 80.1% contained structure class 8. The other classes with the highest representation were structure classes 4 and 6, which occurred in 46.1% and 43.7% of observations. At the 150-m scale, 95.6% of high probability 25-pixel units contained structure class 7, 88.3% included structure class 8, and 71.2% contained structure class 4. Den probability was correlated with the proportion of structure classes 7 or 8 at both scales (90-m: $P < 0.001$, 150-m: $P < 0.01$). At the 90-m scale, pixel units composed of 75-100% structure classes 7 or 8 constituted 70.3% of high probability (≥ 0.5) observations, and 94.1% of pixel units with the highest den probabilities (≥ 0.75). At the 150-m scale, pixel units with 75-100% structure classes 7 or 8 constituted 59.6% of observations with ≥ 0.5 den probability and 83.1% of observations with ≥ 0.75 den probability.
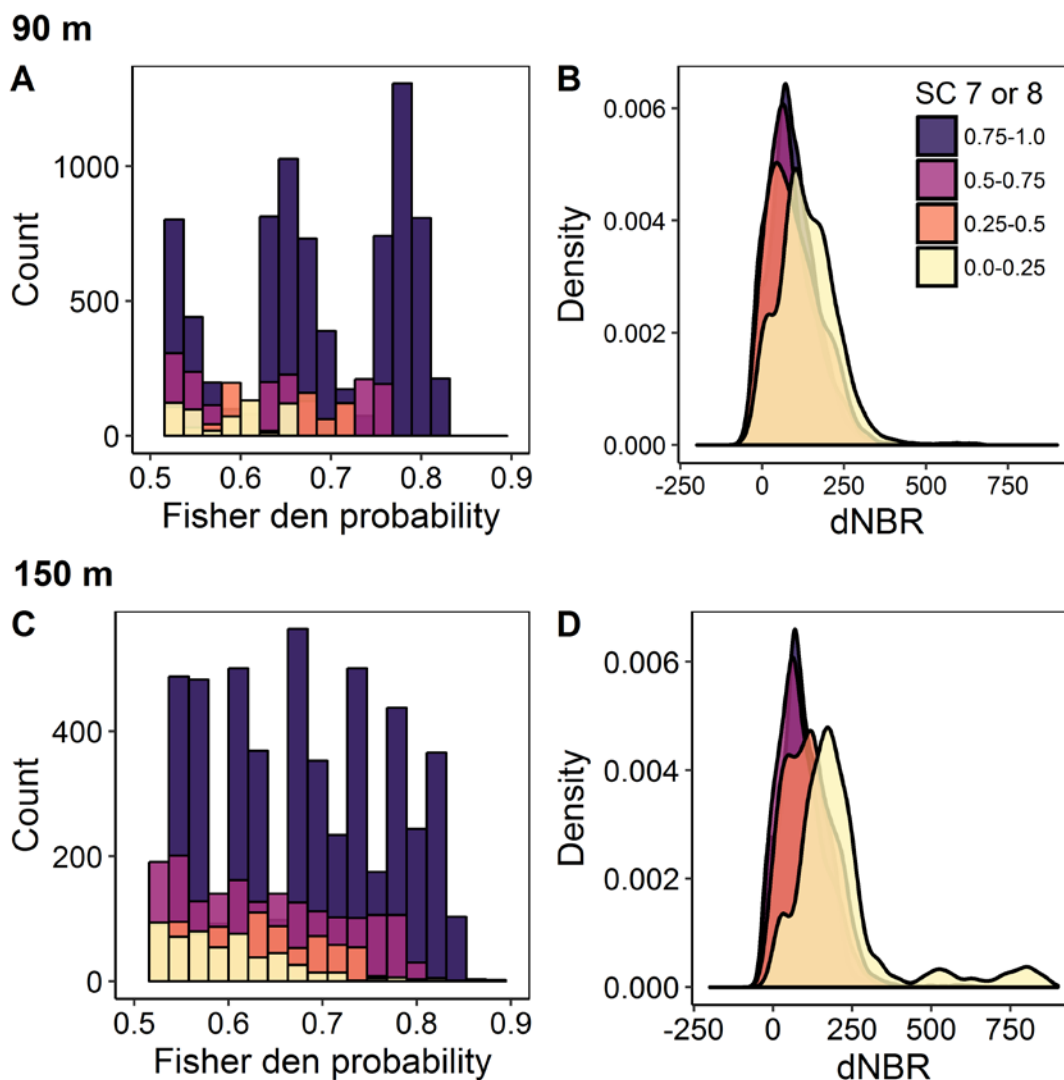
Fig. 3.6. Histograms (A, C) and density plots (B, D) of the 90-m and 150-m pixel neighborhoods in the burned portions of the Yosemite lidar acquisition with a high predicted probability of fisher den presence ≥0.5. The colors correspond with the proportion of the pixel neighborhood occupied by the lidar-derived forest structure classes 7 and 8, which had the most non-zero observations in high den probability areas and had positive associations ($P < 0.05$) with fisher den presence at both scales. Panels A and C compare the fisher den probability distributions of 4 classes of pixel neighborhood configuration (proportion of structure classes 7 or 8= 0-0.25%, 0.25-0.50%, 0.50-0.75%, 0.75-1.0%) at the 90-m and 150-m scales. At both scales, high fisher den probability occurs most often with high proportions of structure classes 7 or 8 (A, C), suggesting that connectivity of similar forest structure is an important component of forest neighborhood suitability. Panels B and D compare the differenced normalized burn ratio (dNBR) distributions of the same 4 classes of pixel neighborhood configuration at the 90-m and 150-m scales. At both scales, the presence of structure classes 7 or 8 (in all classes of neighborhood proportion) occurred predominantly under low-severity fire conditions.

High den probability areas occurred under low severity fire conditions at the 90-m and 150-m scales (Fig. 3.6), with lower average dNBR values than found at the 30-m scale. The average dNBR value was 95.4 (1st quartile: 42.4, 3rd quartile: 139.1) at the 90-m scale, and 104.0 (1st quartile: 47.1, 3rd quartile: 149.7) at the 150-m scale.

4. Discussion

Our results suggest that the aspects of forest structure fishers appear to consider when selecting suitable den habitat at the intermediate, within-home range scale are maintained in burned forests, chiefly under low-severity conditions. Cover >2 m, 95th percentile height, and 25th percentile height predict fisher den presence with comparable accuracy to the full model (Table 3.3). In selecting a den site, fishers seek forested areas that meet minimum thresholds of cover, dominant tree height, and understory height (Fig. 3.2). Suitable thresholds of forest cover and tree height exist in burned areas in Yosemite, within a range of fire severities and years since the most recent fire, and particularly in low-severity fire conditions (Fig. 3.4).

4.1 Structural characteristics predictive of fisher dens

Model accuracy was slightly higher when the neighboring pixels were analyzed in addition to the focal pixel (Table 3.2), on the whole, however, accuracy was comparable and the most important variables were consistent between scales. I offer two explanations that may be at play. First, in selecting a forested area with appropriate microsite conditions suitable for a den, fishers consider the broader forest neighborhood for suitability; a 30 m patch of forest that meets minimum cover and height requirements may be bordered by less desirable habitat (e.g., a meadow or road). Second, the fact that

there is little difference between scales suggests either that 30 m adequately encompasses the forest neighborhood surrounding a potential den site, or that bordering pixels in Dinkey often share similar structural characteristics.

The variables in the most parsimonious logistic regression model—cover >2 m, 95th percentile tree height, and 25th percentile tree height (Table 3.3)—and their minimum thresholds (Fig. 3.2) are well supported by previous research on fisher habitat. Fishers are closely associated with old-growth forests, characterized by high canopy cover and a diversity of tree sizes including tall trees (Ruggiero et al., 1994; Zielinski et al., 2004a; Purcell et al., 2009). High cover areas with tall trees are associated with the dead wood components (e.g., snags, logs, dead or decayed portions of hardwood stems) that fishers use for denning structures (Ruggiero et al., 1994). A distinct understory layer, suggested by the 25th percentile height thresholds, contributes to overall structural diversity and a variety in light gaps, which may support higher prey diversity and density (Zhao et al., 2012). Structural diversity is also measured by canopy rumple, which, while not significant in the logistic regression models (Table 3.2), was found to be important in random forest variable importance plots (Fig. B.3, Fig. 3.2).

I expect that some inaccuracy in model prediction is due to error associated with remote sensing. While the den coordinates were collected with high-precision instruments, interference from forest cover is known to reduce GPS accuracy (Pirti, 2008). Further, the lidar data and fisher den locations were collected at overlapping but slightly different time periods (lidar: 2010, 2012, dens: 2008 to 2015), thus in the event small-scale forest changes occurred some pixel values may not accurately represent conditions selected by a fisher. Another source of incorrect classification could be in the

use of randomly-generated points to compare with fisher den presence data; as I did not have field-based absence data, it is possible that some random points may reflect actually used but unsampled dens. Despite the errors associated with different types of remotely-sensed data, model accuracy was comparable to previous fisher habitat predictive modeling studies (Carroll et al., 1999; Zielinski et al., 2006).

For the scale of selection I examined, many forested in areas in Dinkey were identified as suitable den habitat, but dens only occupied a small fraction of suitable areas (Fig. B.7). I examined the immediate forest neighborhood appropriate for denning within the population home range. This is distinct from the decisions made by the population when establishing a home range (landscape scale), and from the activities of males which are known to have a much larger home range (Zielinski et al., 2004b). Den selection occurs at the microsite level (e.g., individual snags; Green, 2017); this study and those using remotely-sensed data are only able to examine intermediate scales that are suitable for further, hyper-local scales of selection such as microsite features. I expect that unused areas that occur in suitable habitat at the intermediate scale either do not contain necessary features at smaller scales (e.g., optimal proximity to water source, dead wood components), or are unoccupied due to territorial behavior or small population size.

4.2.1 Preferred den structure and fire metrics at the 30-m scale

The forest structural characteristics predictive of den presence exist in burned areas in Yosemite (Fig. 3.3), particularly in areas burned at low severity (Fig. 3.4). Suitable ranges of cover >2 m, 95th percentile height, and 25th percentile height are maintained under low severity fire (Figs. 3.7, 3.8), which includes unburned areas within

fire perimeters, surface burns, and fires that preserve the majority of overstory foliage (Sugihara et al., 2006; Kolden et al., 2012). Fisher dens are associated with tall trees (Table 3.3, Fig. 3.2), which are likely to have large stem diameters, thicker bark, and increased resistance to heat damage (VanderWeide and Harnett, 2011). Dominant, large-diameter trees often survive lower severity fires, and their large canopies contribute to overall forest cover. The lower threshold of understory heights associated with high den probability may be maintained by surface burns, while upper thresholds include medium-diameter trees with elevated canopies that can survive bole scorch and radiated heat. Patches of understory also survive in small to large fire refugia (Meddens et al., submitted), particularly in drainages which fishers are likely to use (Jones, 1991).

Though areas with a high predicted probability of den presence were most common after low-severity fire, they existed at a range of dNBR values (Table 3.4), including areas that have burned at moderate and high severity (Fig. 3.4). This is somewhat surprising, as higher fire severity reflects considerable changes in forest structure and high mortality of aboveground vegetation (Sugihara et al., 2006). Several explanations for a high probability of den presence in areas with higher burn severities are possible. First, there may be some cases where reduced cover and tree heights remain above minimum thresholds for fisher den suitability. These may be in areas containing some large-diameter trees capable of surviving higher-severity fire, with vegetation changes occurring mainly to small- and medium-diameter trees. Second, vegetation regrowth over the 25-year period likely restored some areas that had unsuitable post-fire structure, particularly in terms of overall canopy cover. Third, the majority of high den probability areas that experienced high- and moderate-severity fire burned in the 2009
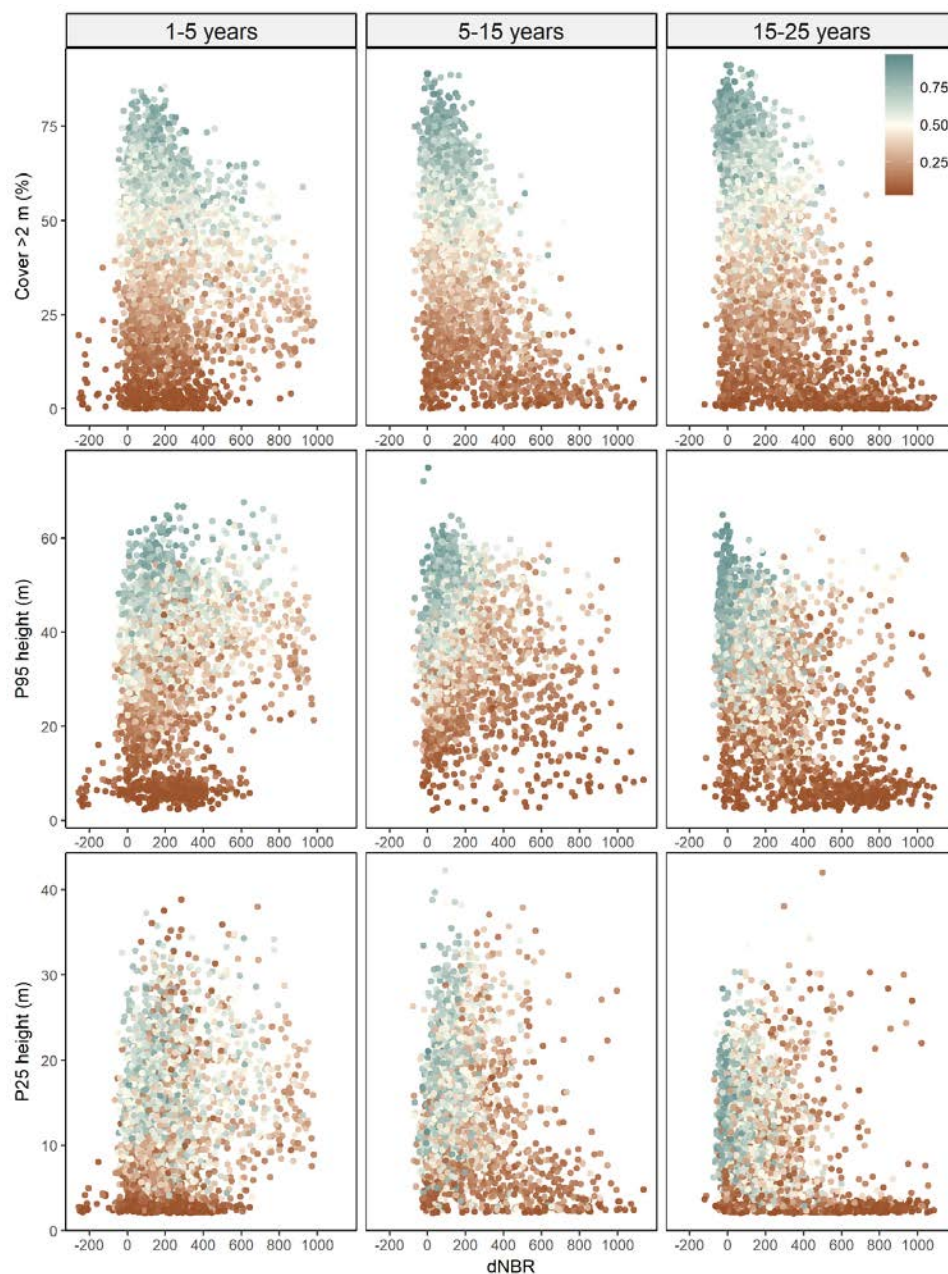
Fig. 3.7. The relationship between forest structure metrics and the differenced normalized burn ratio (dNBR, a measure of burn severity) over three periods of time since fire. In order to visualize relative differences in data distribution and avoid overplotting, each time series is built from a random subset of the data with an equal total number of observations (*n*=3000). The color of is each point represents the predicted probability of den occurrence, values from 0 to 1, where low probability areas (<0.5) are shades of brown and high probability areas (≥0.5) are shades of blue. Cover >2 m (%) is an estimate of tree canopy cover of the 30 m pixel. The 95th percentile and 25th percentile heights (P95, P25) of first lidar returns are approximations of the dominant tree and understory heights.
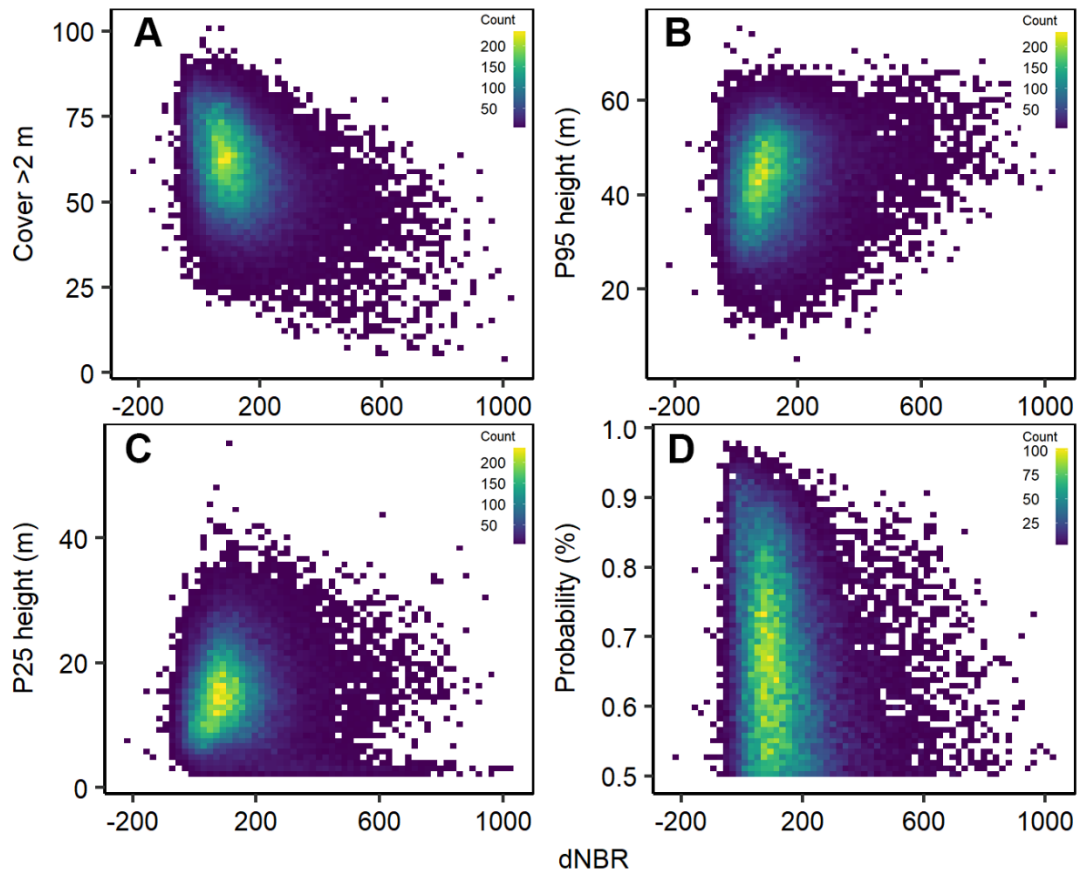
Fig. 3.8. Heat maps illustrating the relationship between the differenced normalized burn ratio (dNBR, a measure of burn severity) and forest structure metrics for areas with a high probability (logistic regression model predictions ≥0.5) of den presence (A, B, C). Each plot represents a grid of binned ranges of x- and y-axes, and the colors correspond to the number of cases in each bin. These plots highlight two main areas of interest: 1. the range in values of forest structure metrics (y-axes for A, B, and C) and dNBR (x-axes) associated with high predicted probability of fisher dens, illustrated by all colors in the heat maps, and 2. the narrower range of axis values associated the highest concentrations of cases, represented by shades of yellow and green. Cover >2 m (A) is an approximate measure of canopy cover. Dominant tree height and understory height are estimated by the 95th percentile (P95, B) and 25th percentile (P25, C) heights of lidar returns. Panel D relates the predicted probabilities to dNBR, where the greatest concentration of high probability pixels ranges between approximately 0 to 200 dNBR.

Big Meadow fire, one year before lidar data were collected. In the years immediately following a fire, relatively little structural change may be detected as snags and dying trees continue to provide relatively high cover. Den suitability was low in instances

where fire of any severity reduced cover >2m, and 95th and 25th percentile tree heights below minimum thresholds (Fig. 3.7).

I interpret no ecologically meaningful correlation between time since fire and predicted probability of den presence. High probability areas were associated with the full range of time since fire (Figs. 3.4, 3.7, B.6). I had expected to see a positive relationship between habitat suitability and time, but instead the distribution of time since fire for high and low probability areas (Fig. 3.4) followed the timeline of the largest fires that occurred in the 25-year study period. Research that controls for fire size and severity is needed to understand the relationship between time and suitable denning structure.

4.2.2 Configuration of preferred structure classes 90-m and 150-m scales

Previous work has highlighted the importance of continuous mature forest in fisher habitat selection (Sauder and Rachlow, 2014). The correlation between den probability and the proportion of late forest development structure classes found in this study adds support to the importance of connectivity of preferred forest structure to den habitat suitability. Burned areas with high den probabilities had high proportions (75-100%) of structure classes 7 and 8, suggesting preference for continuity of forest patches with suitable ranges of cover >2 m, 95th percentile height, and 25th percentile height (Fig. 3.5). Many high probability areas also had mixed representation of other structure classes, some with lower cover and shorter trees. Other studies have suggested that fishers also select for habitat heterogeneity, possibly to utilize different resources available at habitat edges (Sauder and Rachlow, 2015). Areas with high proportions of preferred forest structure classes were present in many burned areas in Yosemite, largely

after low-severity fire (Fig. 3.6).

5. Conclusion

5.1 Management applications and future research

Forest structural characteristics are predictive of fisher dens at the within-home range scale can exist in recently burned areas and are maximized in areas that burned at low severity. Measures of canopy cover and tree heights—cover >2 m, 95th percentile height, and 25th percentile height—consistently separated fisher den neighborhoods from randomly selected points. I suggest that managers utilize the forest structure thresholds associated with high den probability, particularly in the maintenance of tall and large-diameter trees that contribute considerably to high cover and canopy complexity. I found that suitable ranges of the predictors occurred most often in lower-severity fire (approx. dNBR < 250). This is promising for land managers that face the challenge of managing forests with the opposing objectives of reducing the risk of high-severity fire and conserving fisher habitat.

The lidar-derived metrics I utilized limited the scope of our research to the immediate forest neighborhood; thus, more research is needed to conclude whether suitable fisher habitat can exist in burned areas at all scales of selection and for all activities and demographics of the population. A central question that remains unanswered is whether the microsite features occupied by fishers for denning and resting activities (e.g., snags, dead stems, hardwood densities) are maintained after burning. Ground-based measurements of species composition and dead wood components measured in burned areas, such as those collected by the Forest Inventory and Analysis

(FIA) program, would provide critical insight toward fisher conservation in fire-prone forests.

References

Allouche, O., A. Tsoar, and R. Kadmon. 2006. Assessing the accuracy of species distribution models: prevalence, kappa and true skill statistic (TSS). Journal of Applied Ecology 43: 1223-1232.

Aubry, K. B., and J. C. Lewis. 2003. Extirpation and reintroduction of fishers (*Martes pennanti*) in Oregon: Implications for their conservation in the Pacific states. Biological Conservation 114: 79-90.

Breiman L. 2001. Random forests. Machine Learning 45: 5-32.

Burnham, K. P., and D. R. Anderson. 2002. Model selection and inference: a practical information-theoretic approach. Springer-Verlag, New York, New York, USA.

Buskirk, S. W., and R. A. Powell. 1994. Habitat ecology of fishers and American martens. Pages 283-296 in S.W. Buskirk, A.S. Harestad, M.G. Raphael, and R.A. Powell, editors. Martens, sables, and fishers: biology and conservation. Comstock Publishing Associates, Cornell University Press. Ithaca, New York.

Calenge, C. 2011. Home range estimation in R: the adehabitatHR package. http://cran.r-project.org/web/packages/adehabitatHR/vignettes/adehabitatHR.pdf.

California Department of Fish and Wildlife. 2015. Report to the Fish and Game Commission: A Status Review of the Fisher (*Pekania* [formerly *Martes*] *pennanti*) in California.

Carroll, C., W. J Zielinski, and R. F. Noss. 1999. Using presence–absence data to build

and test spatial habitat models for the fisher in the Klamath region, USA. Conservation Biology 13: 1344-1359.

Cutler D. R., T. C. Edwards, K. H. Beard, A. Cutler, K. T. Hess, J. Gibson, and J. J. Lawler. 2007. Random forests for classification in ecology. Ecology 88: 2783-2792.

ESRI. 2011. ArcGIS Desktop: Release 10.3. Environmental Systems Research Institute, Redlands, California, USA.

Fites-Kaufman, J., P. Rundel, N. Stephenson, and D. A. Weixelman. 2007. Montane and Subalpine Vegetation of the Sierra Nevada and Cascade Ranges. Pages 456-501 in M. G. Barbour, T. Keeler-Wolf, and A. A. Schoenherr, editors. Terrestrial vegetation of California. University of California Press, Berkeley, California, USA.

Franklin, A. B., D. R. Anderson, R. J. Gutierrez, and K. P. Burnham. 2000. Climate, habitat quality, and fitness in northern spotted owl populations in northwestern California. Ecological Monographs 70:539-590.

Freeman, E. A. and G. G. Moisen. 2008. A comparison of the performance of threshold criteria for binary classification in terms of predicted prevalence and kappa. Ecological Modeling 217: 48-58.

Green, R. E. 2017. Reproductive ecology of the fisher (*Pekania pennanti*) in the southern Sierra Nevada: an assessment of reproductive parameters and forest habitat used by denning females. Ph.D. dissertation, University of California, Davis.

Halofsky, J. E., D. C. Donato, D. E. Hibbs, J. L. Campbell, M. D. Cannon, J. B. Fontaine, J. R.Thompson, R. G. Anthony, B. T. Bormann, L. J. Kayes, B. E. Law, D. L.

Peterson, and T. A. Spies. 2011. Mixed-severity fire regimes: lessons and hypotheses from the Klamath-Siskiyou ecoregion. Ecosphere 2(4): 40.

Hanson, C. T. 2013. Habitat Use of Pacific Fishers in a Heterogeneous Post-Fire and Unburned Forest Landscape on the Kern Plateau, Sierra Nevada, California. Open Forest Science Journal 6: 24-30.

Jones, J. L. 1991. Habitat use of fisher in northcentral Idaho. Thesis, University of Idaho, Moscow, Idaho.

Kane, V. R., J. A. Lutz, S. L. Roberts, D. F. Smith, R. J. McGaughey, N. A. Povak, and M. L. Brooks. 2013. Landscape-scale effects of fire severity on mixed-conifer and red fir forest structure in Yosemite National Park. Forest Ecology and Management 287:17-31.

Kane, V. R., C. A. Cansler, N. A. Povak, J. T. Kane, R. J. McGaughey, J. A. Lutz, D. J. Churchill, and M. P. North. 2015. Mixed severity fire effects within the Rim fire: Relative importance of local climate, fire weather, topography, and forest structure. Forest Ecology and Management 358:62-79. University of Washington, Seattle.

Kane, J. T., V. R. Kane, J. A. Lutz, D. J. Churchill, and L. M. Moskal. 2018. Determining if managed wildfires and prescribed fires conserve critical habitat structure for fishers in the southern Sierra Nevada. Draft Report to the National Park Service. Task Agreement P14AC01558.

Keeler-Wolf, T., P. E. Moore, E. T. Reyes, J. M. Menke, D. N. Johnson, and D. L. Karavidas. 2012. Yosemite National Park Vegetation Classification and Mapping Project Report. Natural Resource Report NPS/YOSE/NRTR-2012/598. National

Park Service, Fort Collins, Colorado.

Kolden, C. A., J. A. Lutz, C. H. Key, J. T. Kane, and J. W. van Wagtendonk. 2012. Mapped versus actual burned area within wildfire perimeters: characterizing the unburned. Forest Ecology and Management 286:38-47.

Liaw, A., and M. Wiener. 2002. Classification and Regression by randomForest. R News 2:18-22.

Lutz, J. A., C. H. Key, C. A. Kolden, J. T. Kane, and J. W. van Wagtendonk. 2011. Fire frequency, area burned, and severity: a quantitative approach to defining a normal fire year. Fire Ecology 7(2):51-65.

Manly, B. F J., L. L. McDonald , D. A. Thomas , T. L. McDonald , and W. E. Erickson. 2002. Resource selection by animals, statistical design and analysis for field studies. Second edition. Kluwer Academic, Dordrecht, The Netherlands.

Mayer, K. E., and W. F. Laudenslayer. 1988. A guide to wildlife habitats of California. California Department of Forestry and Fire Protection, Sacramento, California, USA.

Miller, J. D., and A. E. Thode. 2007. Quantifying burn severity in a heterogeneous landscape with a relative version of the delta Normalized Burn Ratio (dNBR). Remote Sensing of Environment 109: 66-80.

Meddens, A. J. H., C. A. Kolden, J. A. Lutz, A. M. S. Smith, C. A. Cansler, J. Abatzoglou, G. Meigs, W. Downing, and M. Krawchuk. Submitted. Fire refugia: What are they and why do they matter for global change? Bioscience.

North, M. P., J. T Kane, V. R. Kane, G. P. Asner, W. Berigan, D. J. Churchill, and S. Whitmore. 2017. Cover of tall trees best predicts California spotted owl habitat.

Forest Ecology and Management 40: 166-178.

Parsons, D. J., and S. H. DeBenedetti. 1979. Impact of fire suppression on a mixed-conifer forest. Forest Ecology and Management 2: 21-33.

Pirti, A. 2008. Accuracy analysis of GPS positioning near the forest environment. Croatian Journal of Forest Engineering 29(2): 189-199.

Prism Climate Group. 2018. Climatological normals, 1981–2010. The PRISM Group, Oregon State University, Oregon, USA. http://prism.oregonstate.edu.

Purcell, K. L., A. K. Mazzoni, S. R. Mori, and B. B. Boroski. 2009. Resting structures and resting habitat of fishers in the southern Sierra Nevada, California. Forest Ecology and Management 258: 2696-2706.

Raley, C. M., E. C. Lofroth, R. L. Truex, J. S. Yaeger, and J. M. Higley. 2012. Habitat Ecology of Fishers in Western North Amercia: A New Synthesis. Pages 231-254 in K. B. Aubry, W. J. Zielinski, M.G. Raphael, G. Proulx, and S. W. Buskirk, editors. Biology and Conservation of Martens, Sables, and Fishers: A New Synthesis. Cornell University Press, Ithaca, New York.

R Core Team. 2018. R: A language and environment for statistical computing. Version 3.5.1 R Core Team, R Foundation for Statistical Computing, Vienna, Austria.

Roberts, S. L., D. A. Kelt, J.W. van Wagtendonk, A. K. Miles, and M. D. Meyer. 2015. Effects of fire on small mammal communities in frequent-fire forests in California. Journal of Mammology 96: 107-119.

Ruggiero, L. F., K. B. Aubry, S. W. Buskirk, L. J. Lyon, and W. J. Zielinksi. 1994. The Scientific Basis for Conserving Forest Carnivores: American Marten, Fisher, Lynx, and Wolverine in the United States. GTR RM-254. U.S. Department of

Agriculture, Forest Service, Rocky Mountain Forest and Range Experiment Station, Fort Collins, Colorado.

Sauder, J. D., and J. L. Rachlow. 2014. Both forest composition and configuration influence landscape-scale habitat selection by fishers (*Pekania pennanti*) in mixed-coniferous forests of the Northern Rocky Mountains. Forest Ecology and Management 314: 75-84.

Sauder, J. D., and J. L. Rachlow. 2015. Forest heterogeneity influences habitat selection by fishers (*Pekania pennanti*) within home ranges. Forest Ecology and Management 347: 49-56.

Spencer, W., H. Rustigian-Romsos, J. Strittholt, R. Scheller, W. Zielinski, and R. Truex. 2011. Using occupancy and population models to assess habitat conservation opportunities for an isolated carnivore population. Biological Conservation 144: 788-803.

Sugihara, N. G., J. W. Van Wagtendonk, and J. Fites-Kaufman. 2006. Fire as an ecological process. Pages 58–74 in N. G. Sugihara, J. W. Van Wagtendonk, K. E. Shaffer, J. Fites-Kaufman, and A. E. Thode, editors. Fire in California's ecosystems. University of California Press, Berkeley.

Thompson, C., K. Purcell, J. Garner, and R. Green. 2010. Kings River fisher project progress report 2007-2010. U.S. Department of Agriculture, Forest Service, Pacific Southwest Research Station, Fresno, California.

Truex, R. L., and W. J. Zielinski. 2013. Short-term effects of fuel treatments on fisher habitat in the Sierra Nevada, California. Forest Ecology and Management 293: 85-91.

U. S. Fish and Wildlife Service. 2016. Final species report: Fisher (*Pekania pennanti*), West Coast Population. https://www.fws.gov/klamathfallsfwo/news/Fisher/Final/ SpeciesRpt- FisherFinal-20160331.pdf

VanderWeide, B. L., and D. C Hartnett. 2011. Fire resistance of tree species explains historical gallery forest community composition. Forest Ecology and Management 261: 1530-1538.

Van Wagtendonk, J. W. 2007. The History and Evolution of Wildland Fire Use. Fire Ecology 3: 3-17.

Vierling, W. A. G., S. Martinuzzi, and R. M. Clawges. 2008. LiDAR: Shedding new light on habitat characterization and modeling. Frontiers in Ecology and the Environment 6: 90-98.

Weir, R. D., M. Phinney, and E.C. Lofroth. 2012. Big, sick, and rotting: Why tree size, damage, and decay are important to fisher reproductive habitat. Forest Ecology and Management 265: 230-240.

Williams, B. W., J. H. Gilbert, and P. A. Zollner. 2007. Historical perspective on the reintroduction of the fisher and American marten in Michigan and Wisconsin. U.S. Department of Agriculture Forest Service Northern Research Station, General Technical, Report, NRS-5, Newtown Square, Pennsylvania, USA.

Zhao, F., R. A. Sweitzer, Q. Guo, and M. Kelly. 2012. Characterizing habitats associated with fisher den structures in the Southern Sierra Nevada, California using discrete return lidar. Forest Ecology and Management 280: 112-119.

Zielinski W. J., R. L. Truex, G. A. Schmidt, F. V. Schlexer, K. N. Schmidt, and R. H. Barrett. 2004a. Resting habitat selection by fishers in California. Journal of

Wildlife Management 68: 475-492.

Zielinski, W. J., R. L. Truex, G. A. Schmidt, F. V. Schlexer, K. N. Schmidt, and R. H. Barrett. 2004b. Home range characteristics of fishers in California. Journal of Mammalogy 85(4) 694-657.

Zielinski, W. J., R. L. Truex, J. R. Dunk, and T. Gaman. 2006. Using forest inventory data to assess fisher resting habitat suitability in California. Ecological Applications 16: 1010-1025.

CHAPTER 4

CONCLUSION

The exclusion of fire from the historically frequent-fire forests of western North America since the late 19th century has caused changes in western forest structure and composition (Naficy et al., 2010, Collins et al., 2011). Rising temperatures and increased drought conditions, which have been well-documented in recent decades (Soloman et al., 2007, Diffenbaugh et al., 2015), interact with changes in western forest structure, giving rise to increased fuel loading and higher rates of tree mortality (Young et al., 2017). As a result, western forests are at increased risk of uncharacteristic, high-severity disturbance (Noss et al., 2006), which significantly alters forest structure for decades (Sugihara et al., 2006). It is critical, therefore, to manage the dry, fire-prone forests of the west with fire in order to maintain forest ecosystem function and resilience (Boisrame et al., 2017). In order to manage for the reintroduction of fire under a changing climate, land managers require science-based information on the interactions between fire and forest biota, particularly in vulnerable stands where fire has been excluded since European settlement. The two studies that constitute this thesis advance scientific understanding of biotic interactions with fire, and provide valuable recommendations for land management action.

My second chapter examined an aspect of the interactions between fire behavior and forest vegetation: fire refugia. Fire refugia are important, but understudied landscape elements that influence forest recovery and increase resilience to future disturbances (Kolden et al., 2012, Meddens et al., 2018). My study was the first to spatially

characterize small-scale fire refugia (1 m^2 to 1000 m^2); specific species are known to use and benefit from small unburned areas (Robinson et al., 2013) but refugia of this size are rarely studied because of limitations in identifying them with remote-sensing. I found that small fire refugia are abundant and occur in all classes of satellite-derived burned severity. I was able to predict the formation of fire refugia at this scale with some success, particularly unburned patches that formed in riparian areas or rocky outcroppings. Small fire refugia buffer the lethal effects of radiant and convective heat, and trees positioned within an unburned litter layer were more likely to survive, particularly small-diameters. Unburned areas were also found to have more diverse understory plant communities relative to burned areas, suggesting that small fire refugia are an important mechanism for the maintenance of post-fire understory communities. These findings fill critical knowledge gaps about fire refugia and provide data with which to start incorporating the maintenance of these important landscape elements into land management objectives.

The findings in my third chapter examined an aspect of the interaction between fire and wildlife, through the effects of fire severity on forest habitat. The need to reintroduce fire in the west is complicated by concerns of habitat loss, particularly in areas inhabited by threatened wildlife species. My study considered the effect of fire on Pacific fisher (*Pekania pennanti*) habitat of the last remaining fisher population in the central Sierra Nevada. I found that fisher dens could be predicted with moderate accuracy using lidar-derived metrics that characterized forest structure. Areas with a high predicted probability of fisher dens existed in burned forest, at a range of fire severities but particularly after low-severity fire. This study provides some promising first results for

land managers who need to balance the competing objectives of fire reintroduction and wildlife conservation.

LITERATURE CITED

Boisrame, G., S. Thompson, B. Collins, and S. Stephens. 2017. Managed wildfire effects on forest resilience and water in the Sierra Nevada. Ecosystems 20: 717-732.

Collins, B. M., R. G. Everett, and S. L. Stephens. 2011. Impacts of fire exclusion and recent managed fire on forest structure in old growth Sierra Nevada mixed-conifer forests. Ecosphere 2(4): article 51.

Diffenbaugh, N. S., D. L. Swain, and D. Touma. 2015. Anthropogenic warming has increased drought risk in California. Proceedings of the National Academy of Sciences 112: 3931-3936.

Kolden, C. A., J. A. Lutz, C. H. Key, J. T. Kane, and J. W. van Wagtendonk. 2012. Mapped versus actual burned area within wildfire perimeters: characterizing the unburned. Forest Ecology and Management 286: 38-47.

Meddens, A. J. H., C. A. Kolden, J. A. Lutz, A. M. S. Smith, C. A. Cansler, J. Abatzoglou, G. Meigs, W. Downing, and M. Krawchuk. 2018. Fire refugia: What are they and why do they matter for global change? Bioscience.

Naficy, C., A. Sala, E. G. Keeling, J. Graham, and T. H. DeLuca. 2010. Interactive effects of historical logging and fire exclusion on ponderosa pine forest structure in the northern Rockies. Ecological Applications 20: 1851-1864.

Noss R. F., J. F. Franklin, W. L. Baker, T. Schoennagel, and P. B. Moyle. 2006. Managing fire-prone forests in the western United States. Frontiers of Ecology

and the Environment 4: 481-7.

Robinson, N. M., S. W. J. Leonard, E. G. Ritchie, M. Bassett, E. K. Chia, S. Buckingham, H. Gibb, A. F. Bennett, and M. F. Clarke. 2013. Refuges for fauna in fire-prone landscapes: Their ecological function and importance. Journal of Applied Ecology 50: 1321-1329.

Solomon, S., D. Qin, M. Manning, Z. Chen, M. Marquis, K. B. Averyt, M. Tignor, and H. L. Miller. 2007. Climate Change 2007: The Physical Science Basis: Contribution of Working Group I to the Fourth Assessment Report of the Intergovernmental Panel on Climate Change. Intergovernmental Panel on Climate Change, Geneva, Switzerland.

Sugihara, N. G., J. W. Van Wagtendonk, and J. Fites-Kaufman. 2006. Fire as an ecological process. Pages 58–74 in N. G. Sugihara, J. W. Van Wagtendonk, K. E. Shaffer, J. Fites-Kaufman, and A. E. Thode, editors. Fire in California's ecosystems. University of California Press, Berkeley.

Young, D. J. N., J. T. Stevens, J. M. Earles, J. Moore, A. Ellis, A. L. Jirka, and A. M. Latimer. 2017. Long-term climate and competition explain forest mortality patterns under extreme drought. Ecology Letters 20: 78-86.

APPENDICES

APPENDIX A: Chapter 2 Supplemental Tables and Figures

Table A.1. Summary of vegetation cover (by species; total can be over 100%), mean seedling abundance per quadrat, and species richness for burned and unburned understory 1-m^2 quadrats measured in 2016.

	Early season		Late season		Overall	
	Burned	Unburned	Burned	Unburned	Burned	Unburned
Vegetation cover (%)						
Mean	11.8	21.4	14.5	22.1	13.1	21.8
Min	0	0	0	0	0	0
Max	112.7	86.8	150.8	104.5	150.8	104.5
Std	19.7	21.5	24.9	23.2	22.4	22.2
Seedlings						
Mean abundance	6.1	2.1	5.8	2.1	6.0	2.1
Species richness						
Mean	3.2	6.2	3.2	6.6	3.2	6.4
Min	0	1.0	0	0	0	0
Max	12.0	15.0	12.0	15.0	12.0	15.0
Std	3 .1	3.6	3.1	3.7	3.1	3.6
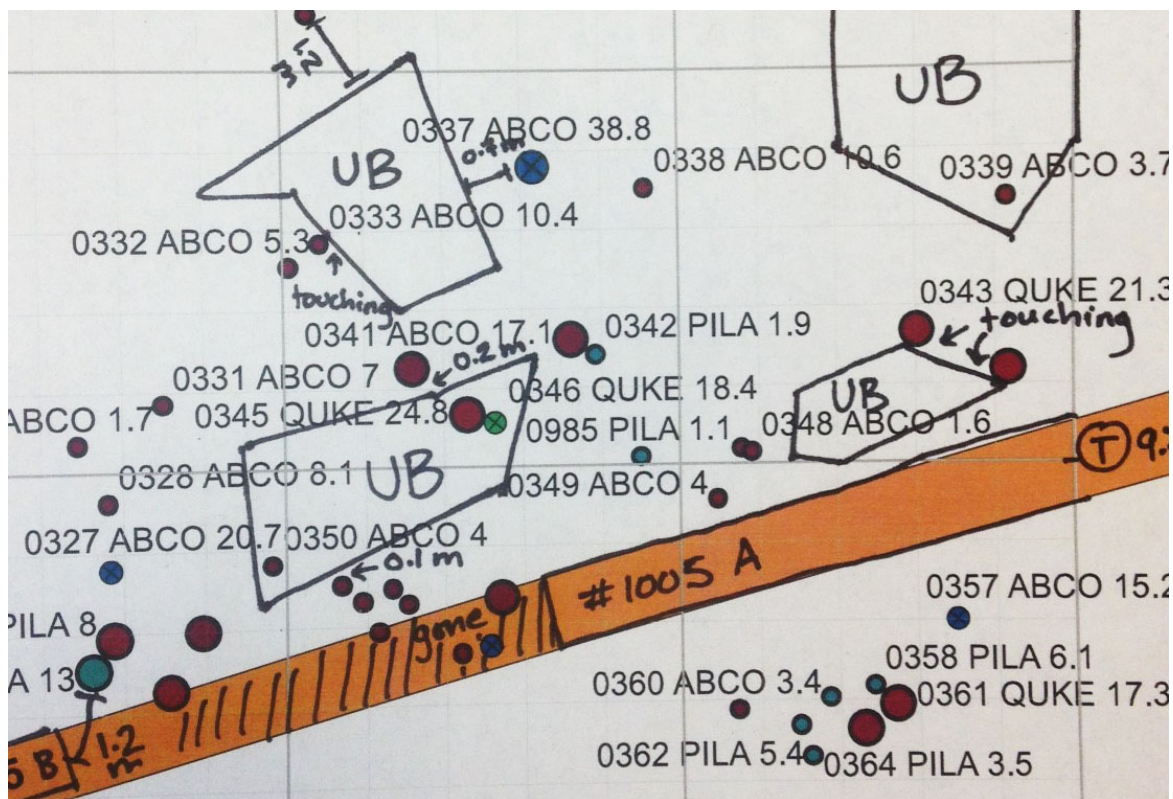
Figure A.1. A portion of a datasheet used to map unburned patches in the Yosemite Forest Dynamics Plot. Ocular estimation was used to delineate unburned patch vertices in relation to features on stem map (e.g. trees, grid corners). The unburned patches were measured using meter tapes and the datasheets included a 1-m grid to increase mapping accuracy. Nearby trees were traversed to confirm their position as either outside, intersecting, or within an unburned patch.
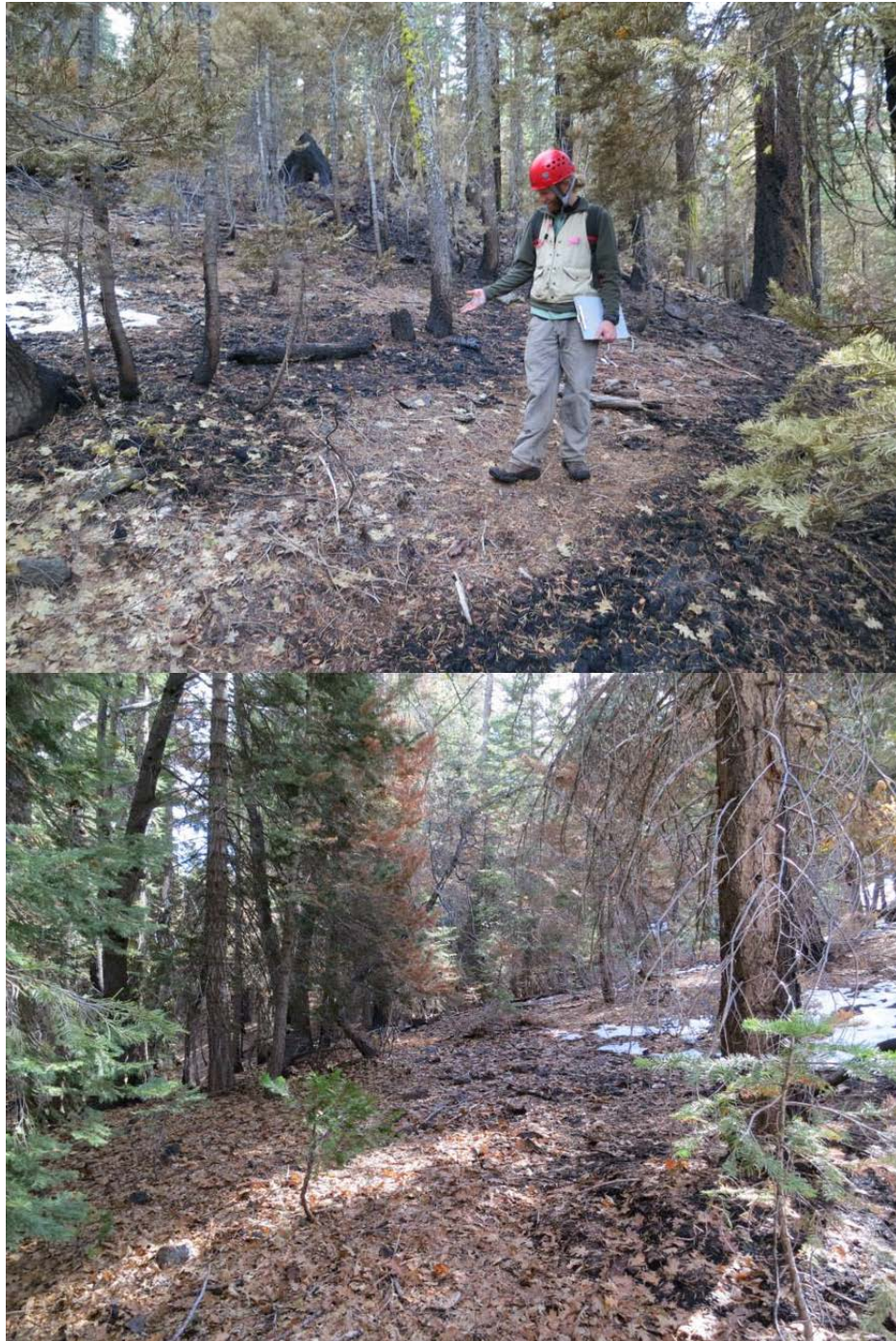
Figure A.2. The Yosemite Forest Dynamics Plot (YFDP) in November, 2013, two months after the Rim Fire. Unburned patches were delineated from burned areas based on the presence of ash or charcoal on the forest floor or on adjacent stems, and inspection of the substrate for intact litter and duff. Photo credit: James A. Lutz.
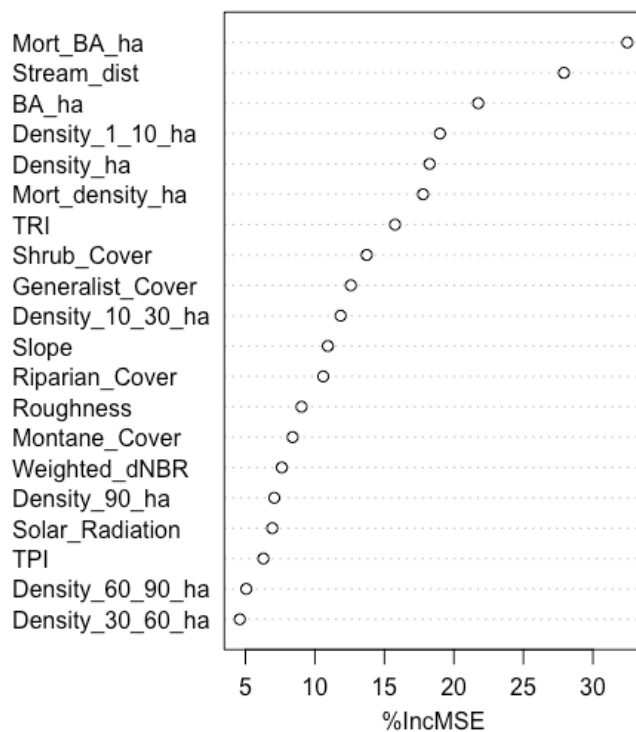
Figure A.3. Variable importance graphs for the random forest regression model predicting the response of proportion unburned. The metric %IncMSE calculates the mean decrease in prediction accuracy for each variable when it is removed from the model, with larger values indicating greater variable importance.
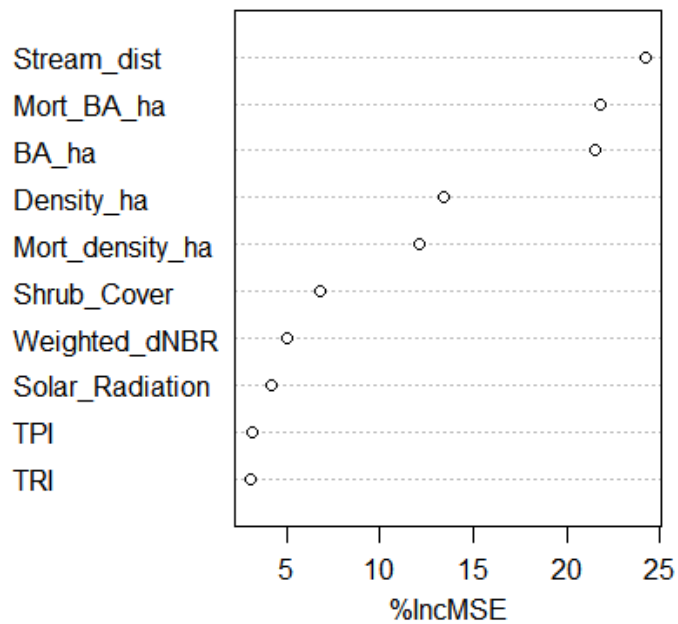
Figure A.4. Importance graphs for the top 10 variables in the random forest presence-only model predicting the response of proportion unburned.

APPENDIX B: Chapter 3 Supplemental Tables and Figures

Table B.1. Coefficients and *P*-values for the full logistic regression models at three scales: 30 m, 90 m, and 150 m. All continuous variables were standardized before model fit, therefore coefficients may be interpreted as ranked by relative effect size. *P*-values ≤0.05 are bolded.

	Model scale					
	30 m		90 m		150 m	
Variable	Coefficient	*P*-value	Coefficient	*P*-value	Coefficient	*P*-value
β_0	-0.0644	0.541	-0.1099	0.311	-0.1099	0.311
Cover >2 m	0.9405	**<0.001**	1.1069	**<0.001**	1.1069	**<0.001**
Canopy rumple	0.1447	0.350	0.1304	0.505	0.1304	0.505
P95 height	0.7034	**<0.001**	0.7539	**0.001**	0.7539	**0.001**
P25 height	-0.4581	**0.001**	-0.4583	**0.005**	-0.4583	**0.005**
Slope	0.2801	**0.013**	0.1973	0.087	0.1973	0.087
Solar	-0.1842	0.097	-0.1595	0.151	-0.1595	0.151
Stream dist.	-0.1256	0.246	-0.1656	0.137	-0.1656	0.137
Road dist.	-0.2162	0.078	-0.1070	0.377	-0.1070	0.377

Table B.2. Accuracy metrics for the logistic regression models using forest structure classes as predictor variables at three scales: 30 m, 90 m, and 150 m. To assess model accuracy, metrics were computed by resubstitution ("Resub") and 10-fold cross-validation ("X-val"). Percent Correct Classification (PCC) is the percent of rows correctly predicted by the model, while sensitivity and specificity examine the percent of presence and absence responses correctly predicted, respectively. Cohen's kappa is a measure of overall model accuracy corrected for the accuracy of predictions expected by random chance. The area under the curve (AUC), a threshold-independent measure of predictive accuracy, is the area under the ROC specificity and sensitivity curve.

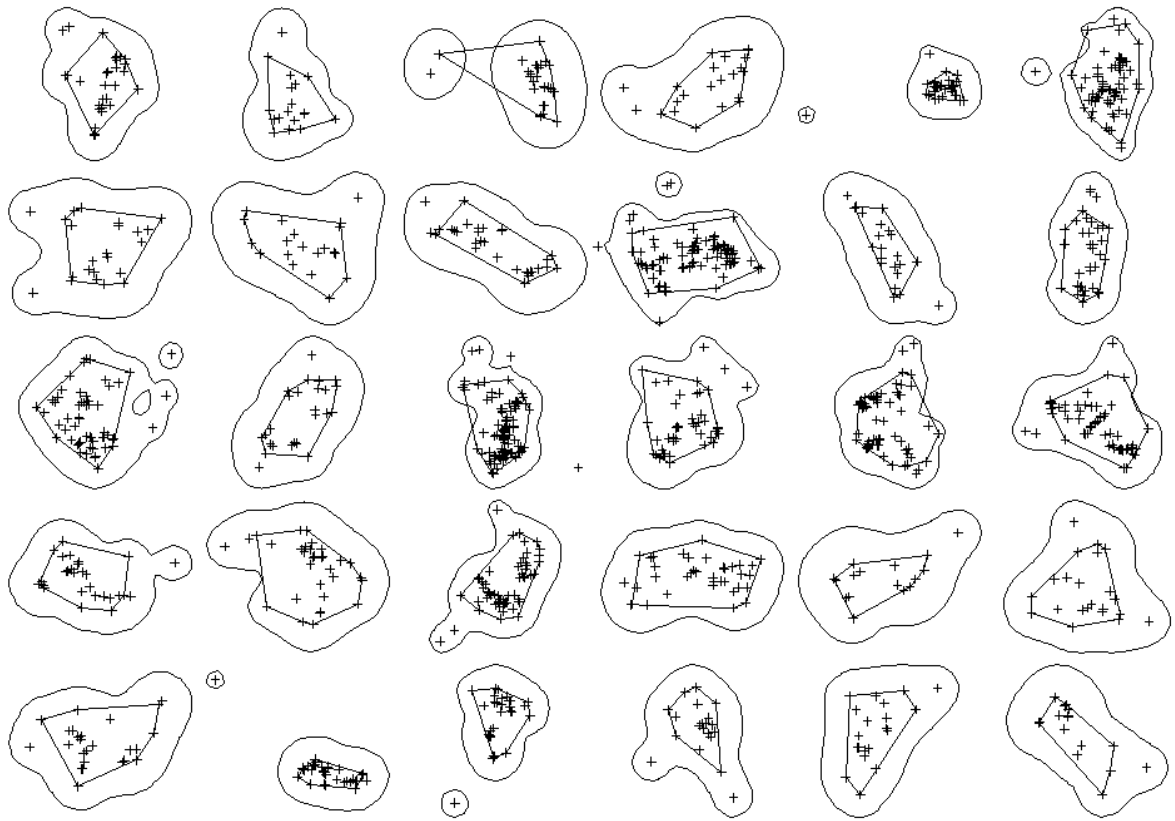| | Model scale | | | | | |
| | 30 m | | 90 m | | 150 m | |
Accuracy metric	Resub	X-val	Resub	X-val	Resub	X-val
PCC	67.6	67.6	71.5	70.7	71.5	71.3
Sensitivity	94.3	94.3	90.0	90.8	69.7	67.8
Specificity	40.1	41.0	52.9	50.6	73.2	74.7
Kappa	0.35	0.35	0.43	0.41	0.43	0.43
AUC	0.72	0.68	0.77	0.76	0.79	0.78

Figure B.1. Kernel Utilization Distributions (KUD) of the 30 female fishers with ≥ 20 locations (telemetry, rest sites, or dens) and an estimated error polygon of <5 m². The kernel method of UD uses known locations to estimate the range of points an individual animal has a minimum probability of being found. The resulting polygon is an estimate of an animal's home range. In order to estimate the home range of the female population, I buffered each den to reflect the average KUD size of 18.4 km (radius= 2.4 km).
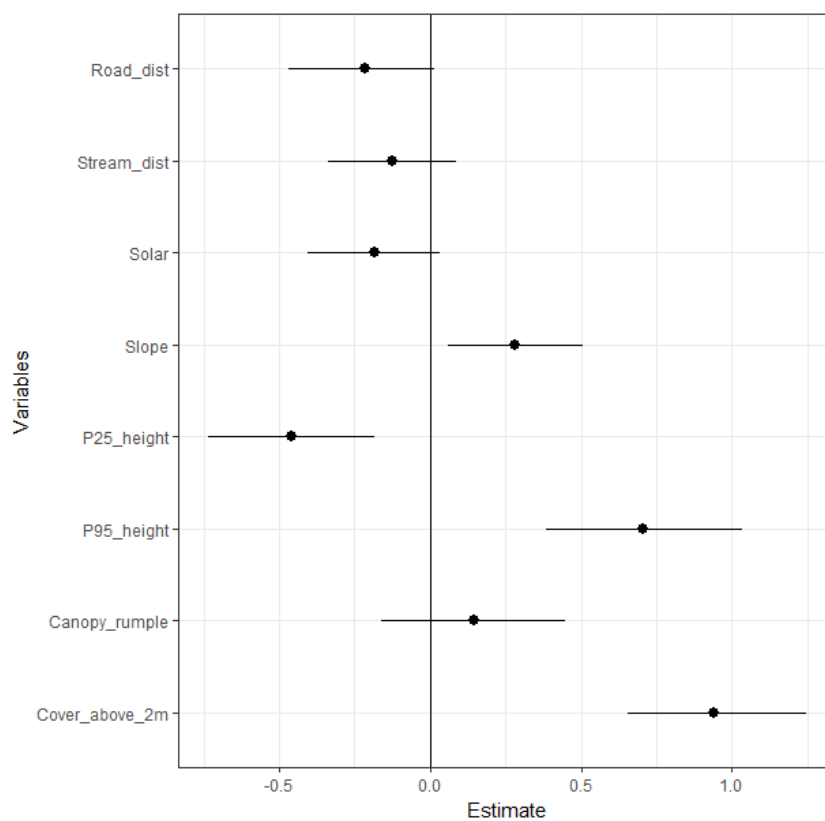
Figure B.2. A coefficient plot of the 30 m logistic regression model with all variables from the height group (see methods for variable grouping). The coefficients are standardized and may be interpreted as a relative effect size. The bars plotted with each coefficient represent confidence intervals, from 2.5% to 95%. Cover >2 m, 95th percentile height, and 25th percentile height have the largest impact on the likelihood of den presence.
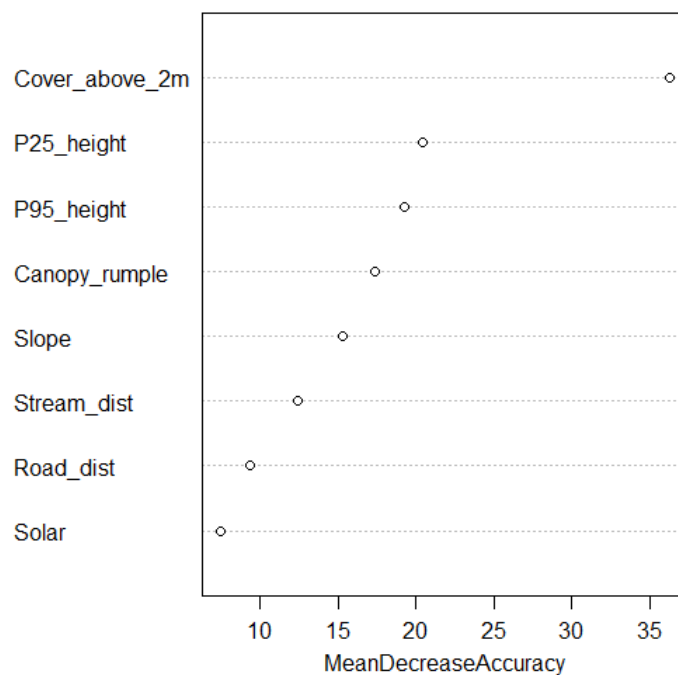
Figure B.3. Variable importance plot for the 30 m random forest model. The x-axis is the mean decrease in correct predictions when omitting a particular variable from the model, with higher values indicating increased importance to model accuracy. The y-axis lists all model predictor variables in order of importance.
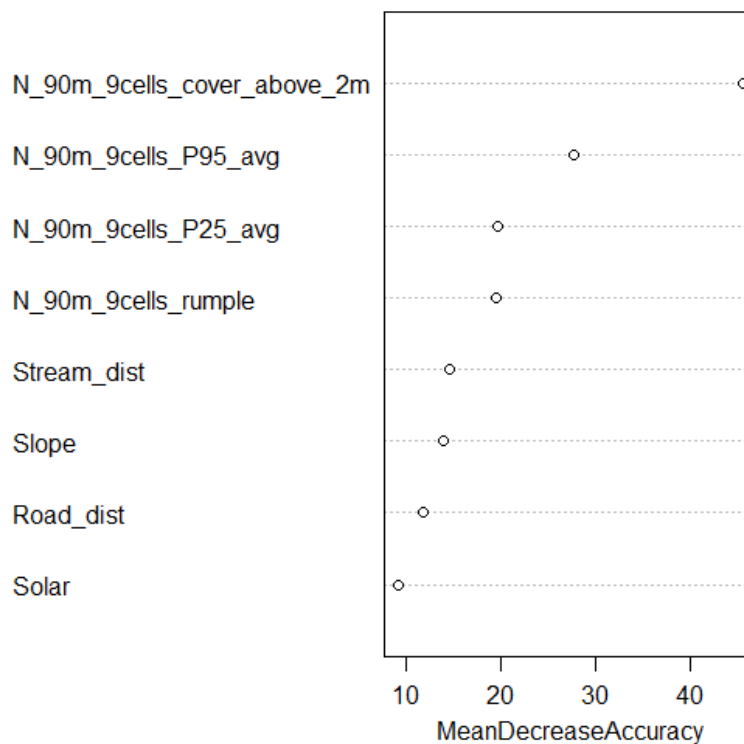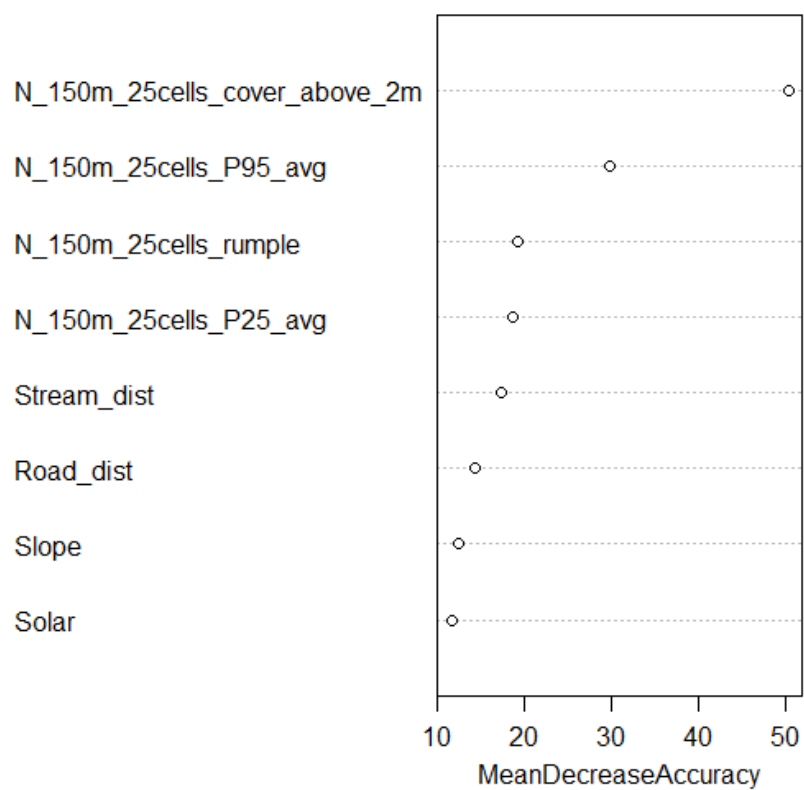
Figure B.4. Variable importance plot for the 90 m random forest model. The x-axis is the mean decrease in correct predictions when omitting a particular variable from the model, with higher values indicating increased importance to model accuracy. The y-axis lists all model predictor variables in order of importance.

Figure B.5. Variable importance plot for the 150 m random forest model. The x-axis is the mean decrease in correct predictions when omitting a particular variable from the model, with higher values indicating increased importance to model accuracy. The y-axis lists all model predictor variables in order of importance.
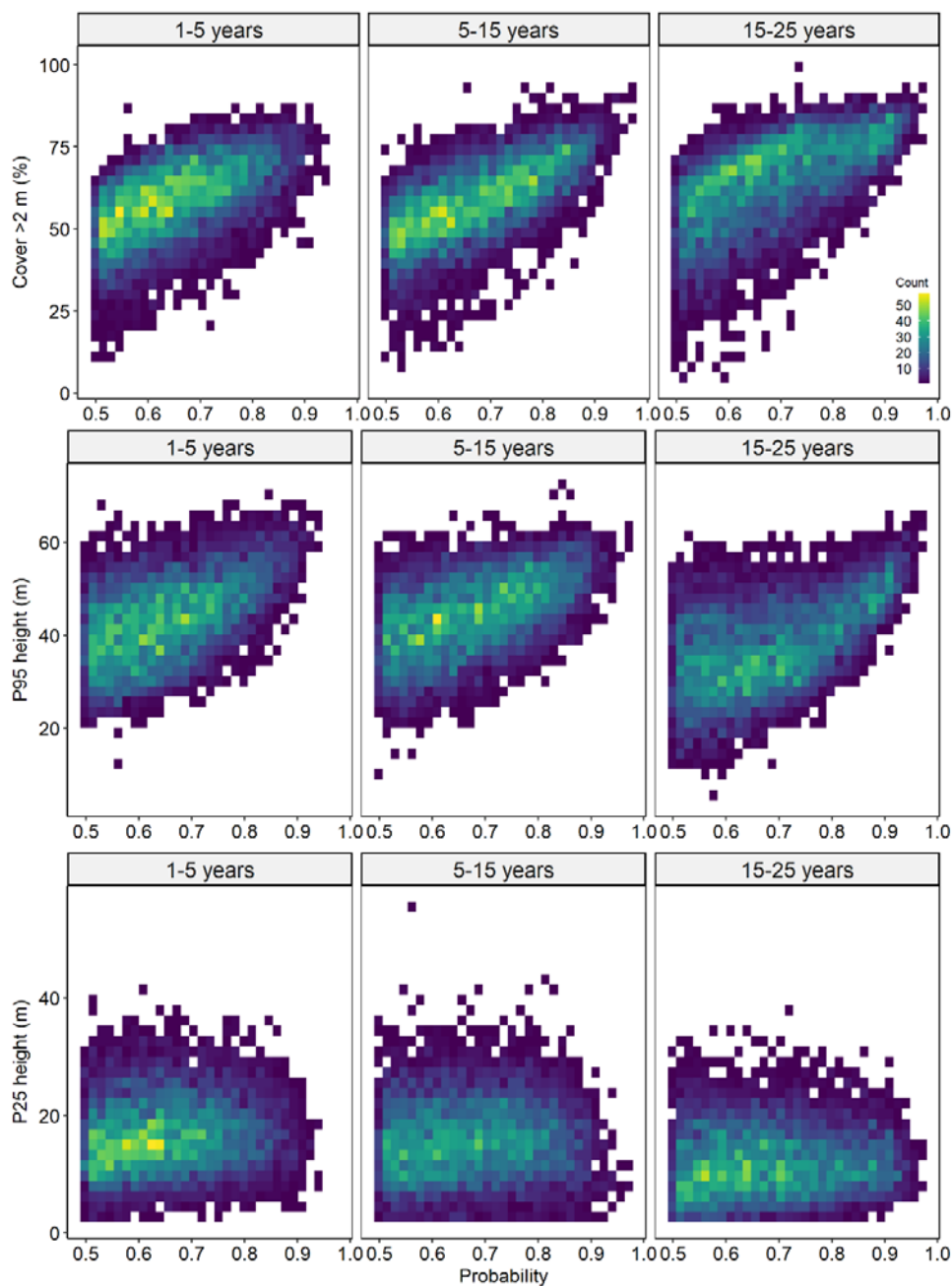
Figure B.6. Heat maps illustrating the relationship between forest structure metrics and probability of den presence ≥0.5. Each structure variable is shown in three time groups, where years represents the number of years since the last fire (until 2010; e.g., 5 years since fire corresponds to areas that burned in 2005). Each plot represents a grid of binned ranges of x- and y-axes, and the colors correspond to the number of cases in each bin. These plots highlight the range of forest structure values associated with increasing predicted probability, represented by all colors in the heat maps, as well as the areas where values are most concentrated, represented by yellow and green.
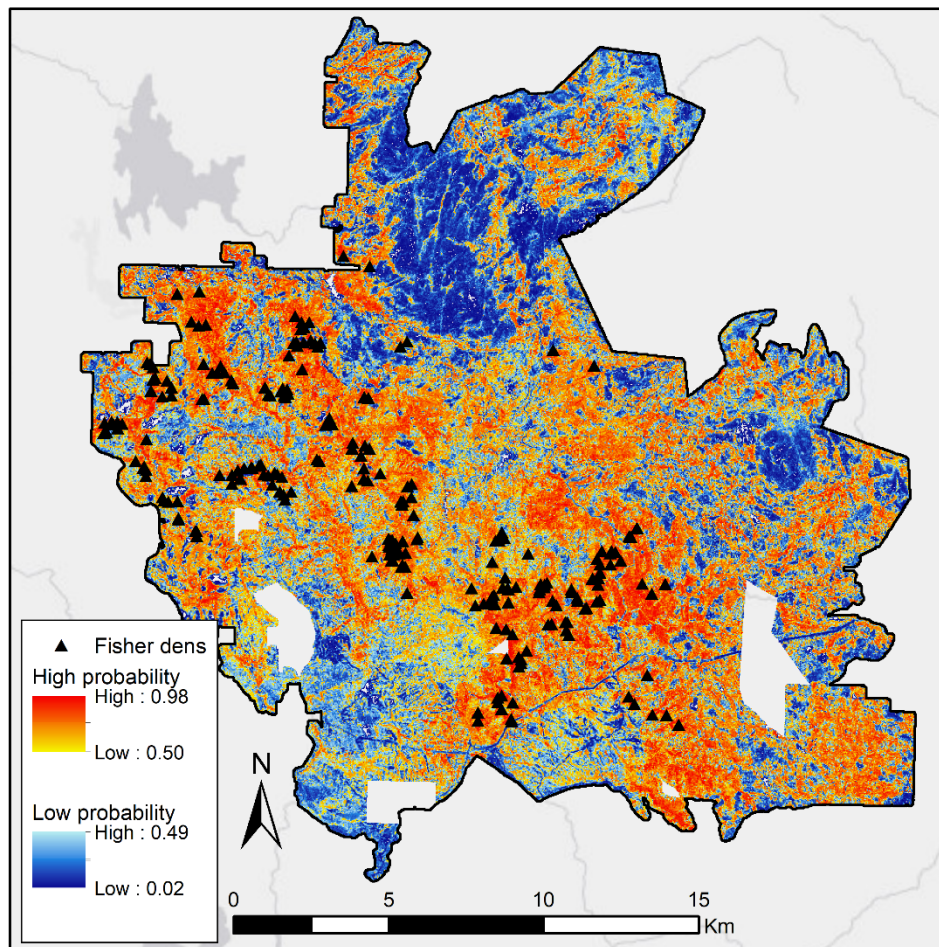
Figure B.7. Predicted probabilities of fisher den presence for the Dinkey study area. High probability of den presence (≥0.5) is represented by shades of red, and shades of blue correspond to low probability. Probabilities were derived from logistic regression models using the predictors: cover >2 m, 95th percentile height, and 25th percentile height. This map is meant as a tool to visualize model predictions with observed fisher locations.